



**EEEE3001**

**Final Year Individual Project Dissertation**

**Simulation Study of a STATCOM for Reactive Power  
and Harmonics Compensation**

**AUTHOR:** Yujian Cai

**ID NUMBER:** 20319967

**SUPERVISOR:** Dr Al Watson

**MODERATOR:** Dr. YingLi

**DATE:** May 8, 2024

This fourth year project Thesis is submitted in part fulfilment of the requirements of the degree of Master of Engineering.

# 1 CHAPTER1: Introduction

Modern power grids are facing congestion challenges due to new types of loads and a growing population. To address these issues without adding infrastructure, FACTS(Flexible AC Transmission System) devices have been developed to maximize the potential use of a transmission line by providing reactive power consumption loads locally rather than over the entire transmission line. By achieving this, it is possible to increase the actual (useful) power that can be transmitted before hitting thermal limits (for example) of the transmission cable.

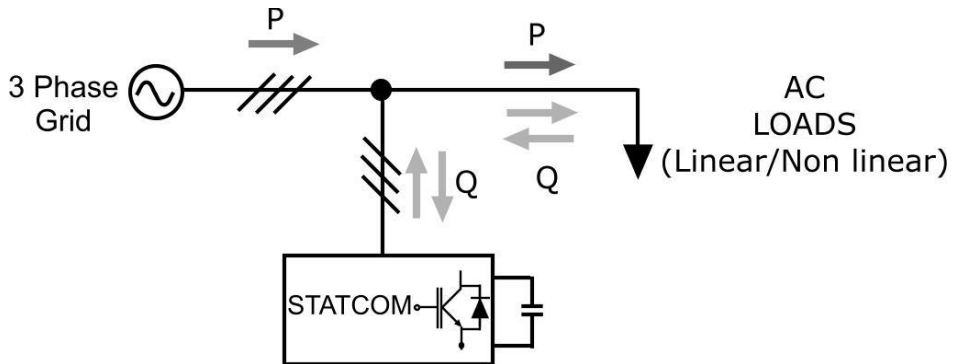


Figure 1: STATCOM being used to compensate reactive power in a load

FACTS devices include static VAr compensators such as the Thyristor-Controlled Reactor (TCR) or Thyristor-Switched Capacitor (TSC) as well as more flexible devices such as the STATIC Synchronous Compensator (STATCOM) [1]. *Figure 1* illustrates an example of a STATCOM application. In this scenario, a standard 2-level inverter is used to generate voltages which enable the reactive power to be supplied or absorbed locally by the STATCOM rather than through the three-phase grid.

This thesis will consider the use of a STATCOM as a reactive power compensation device for a grid supplying a reactive load. A simulation in the well-known PLECS platform will be developed. This will require the implementation of an algorithm to determine the required level of reactive power compensation. An example is the PQ theory, developed by Akagi in the 1980s [3,4]. Initially, the STATCOM power converter can be modelled using an ideal voltage source in order to develop the compensation algorithm. This voltage source will then be substituted with a power converter employing an appropriate Pulse Width Modulation (PWM) scheme [5].

## 1.1 Aim of this project

To explore the application of a 2-level converter based Static Synchronous Compensator (STATCOM) for the purpose of compensating reactive power in an electrical grid.

## **1.2 Objectives of the Projects**

The project consists of three objectives. Before building STATCOM, it is necessary to build a three-phase inverter to achieve the conversion of DC to three-phase power. The primary objective is to complete simulation of fully controlled 3 phase STATCOM with linear load, and the additional objective is to complete simulation of fully controlled 3 phase STATCOM with non-linear load.

### **1.2.1 Three phase inverter**

1. Understand the construction and principles of PWM modulation and full bridge converter.
2. Design a suitable filter to remove the HF components.
3. Design and verify the current controller and voltage controller.
4. Verification and analysis results after setting up a complete three phase inverter in PLECS

### **1.2.2 STATCOM with linear load**

1. Investigation into algorithms which are able to derive the required STATCOM voltage to compensate reactive power.
2. Implement algorithm in PLECS, modelling the STATCOM as an ideal voltage source.
3. Replace the ideal voltage source with a power converter and develop a DC side voltage controller
4. Complete simulation of fully controlled 3 phase STATCOM with linear load.

### **1.2.3 Stretch goal: STATCOM with non-linear load**

1. Replace the linear load by the non-linear load.
2. Update the algorithm in PLECS.
3. Design a fifth-order Butterworth filter, and redesign the controller.
4. Complete simulation of fully controlled 3 phase STATCOM with non-linear load.

## **2 CHAPTER2: Three phase inverter**

The main purpose of this chapter is to design and build three phase inverter, three phase inverter is an important part of STATCOM, it can regulate the DC current to three phase AC current, which is the basis to achieve reactive power and harmonic compensation. This chapter is mainly divided into three parts, filter and PWM design, current controller design, voltage controller design.

### **2.1 Full bridge converter and PWM modulation**

The whole switching model of three phase inverter consist of PWM modulator and full bridge converter. The design of full bridge converter is shown below:

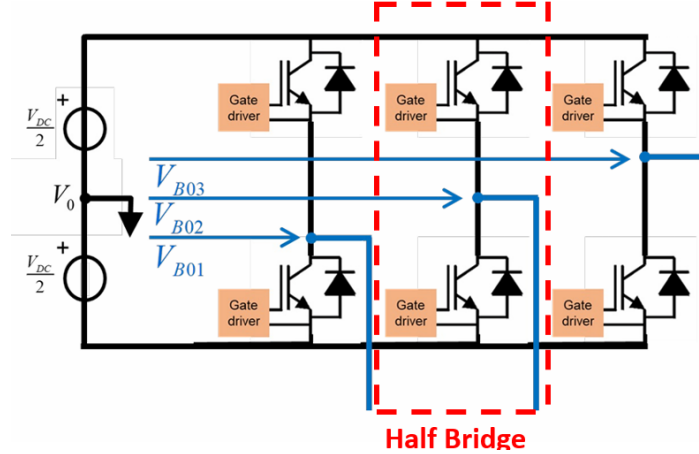


Figure 2.1. Design of full bridge converter [6]

As Figure 2.1 shown, the full bridge converter consists of three separate half bridges. The reasons for using a full bridge over a half bridge in a three-phase inverter primarily is the need for bidirectional energy flow and enhanced functionality. A full bridge allows bidirectional energy transfer, which is important for regenerative energy to be fed back into the DC source or the grid. [7]

In addition, the full bridge allows the use of a midpoint reference instead of a negative reference. This midpoint reference contributes to the ‘bidirectional’ of the inverter output, allowing a voltage greater than or less than zero to be generated. [7] Therefore, an AC waveform can be produced. Each of the three half-bridges is a fully controllable voltage source that can produce an AC voltage relative to the midpoint of the DC input in that range [-VDC/2, +VDC/2]. In contrast, half Bridges are limited to unidirectional output voltages. The PWM modulation for each phase is shown below:

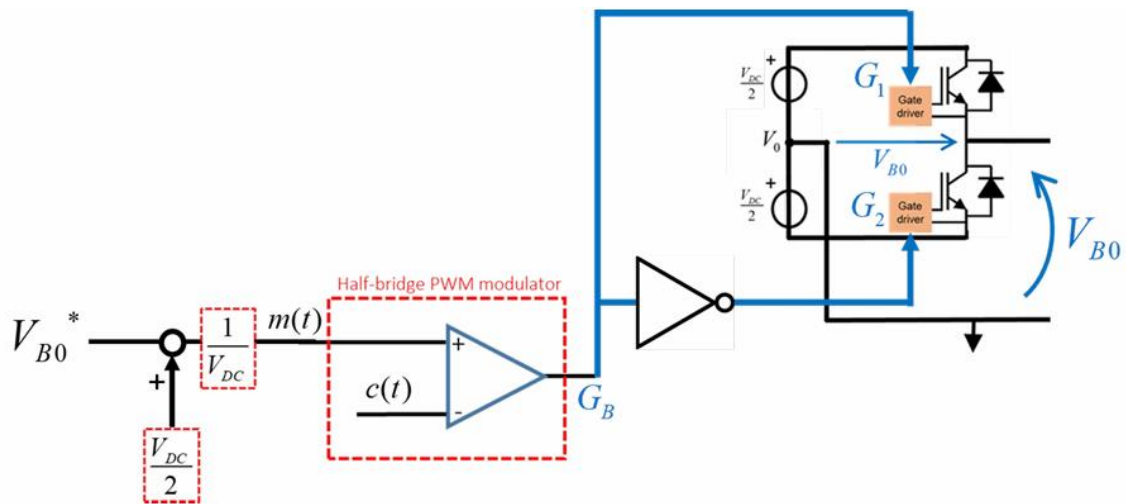
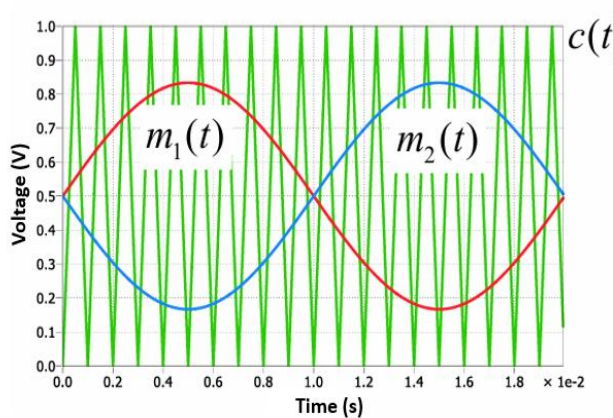


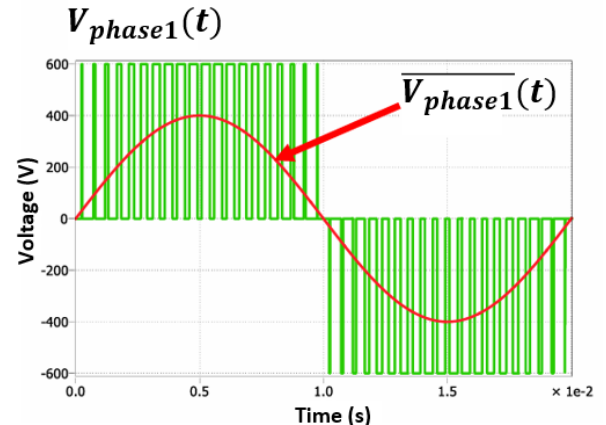
Figure 2.2. PWM modulation for each phase [6]

Pulse width modulation (PWM) is an electronic technique used to encode analogue information into digital signals. It involves changing the width of the pulses in a periodic waveform, where the width of each pulse represents the amplitude of the analogue signal at a specific point in time. [8]

In PWM modulation, a fixed-frequency square wave is generated, and the duty cycle of this waveform varies according to the desired analogue signal ( $m(t)$ ). The duty cycle is the ratio of the pulse width to the total period of the waveform. By adjusting the duty cycle, the average value of the waveform can be controlled, thus effectively controlling the analogue signal.



(a)



(b)

Figure 2.3. PWM modulation for each phase (a) Comparison between carrier signal and desired analogue signal (b) Average output voltage under different PWM demand [9]

Figure 2.3 is an example describing PWM modulation in each phase. Using a unity amplitude PWM carrier ( $C(t)$ ), the low-voltage component of the desired voltage is fed to the comparator to generate square wave with different widths. The average voltage of these square waves is the desired analogue signal ( $m(t)$ ). In the three phase inverter, three independent PWM modulators with the same carrier can be used.

## 2.2 Filter design

The three-phase inverter can be represented with a set of three independent voltage sources, which refer to the same point and are divided into low-frequency components and an high-frequency components. The purpose of filter is to remove the HF components.

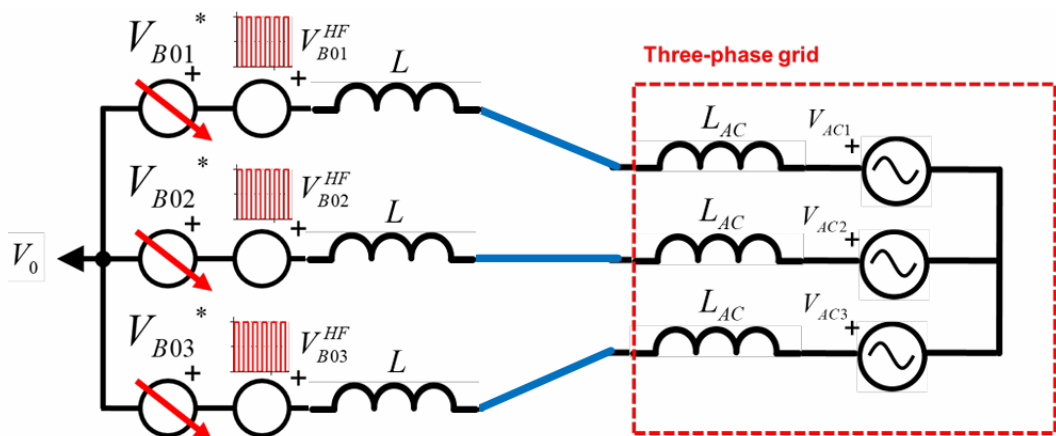


Figure 2.4. Design of full bridge converter [6]

The function of an inductor involves two key aspects. Firstly, it allows power transmission between the inverter and the grid. Secondly, it can filter the high-frequency component of the inverter voltage, thereby controlling the high-frequency component of the grid current. If the inductor is selected too small, the power transmission will be easy, but the filtering effect will be poor. The relation between AC current ripple and inductor is shown below [10]:

$$\Delta I = \frac{T_S V_{DC}}{8L} \quad \text{Eqn 2.1}$$

According to the equation above, when the inductance is too small, the AC current ripple in the circuit will be too large. On the other hand, if the inductor is selected too large, the filtering effect would be much good, but the power transmission would be hard. [10] In addition, larger inductors also cost more. In the three phase inverter, the phase diagram in each phase is shown below:

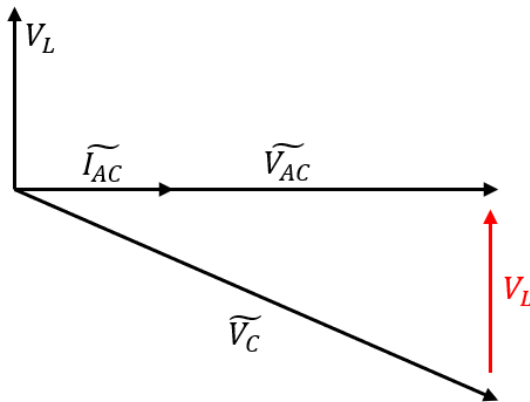


Figure 2.5. Phase diagram in each phase

The voltage across the inductor ( $V_L$ ) can be calculated as follows:

$$|V_L| = |I_{AC}| \omega L \quad \text{Eqn 2.2}$$

In the 2 level three phase converter,  $\widetilde{V}_C$  is limited to  $V_{DC}/2$  per phase. If the inductor is too large,  $V_L$  would be too large, limiting the PQ operation range of the converter, resulting in the system cannot work at large current. The power loss in inductor can be calculated as follows:

$$P_{LOSS} = (I_{AC})^2 * R \quad \text{Eqn 2.3}$$

According to the above formula, the greater the internal resistance of the inductor, the greater the power loss. Initially, the system design specifications are set as follows:

Table 2.1. System design specifications

Inductor ( $L_1, L_2, L_3$ )	Resistor ( $R_1, R_2, R_3$ )	Switching frequency ( $f_{SW}$ )	DC voltage ( $V_{DC}$ )
0.001H	0.1Ω	10KHz	850V

## 2.3 Current controller design

The main purpose of this section is to design the current controller and build the circuit in the PLCES. The current controller is an important part of the three phase inverter, which can regulate the output current to a desired level, ensuring that it meets the requirements of the connected load and maintains stable operation.

This section is divided into three parts. The first two parts are the derivation and verification of the transfer function, and the third part is the circuit construction and verification in PLCS.

### 2.3.1 Transfer function derivation

At each phase of the inverter, the simplified circuit diagram is shown below:

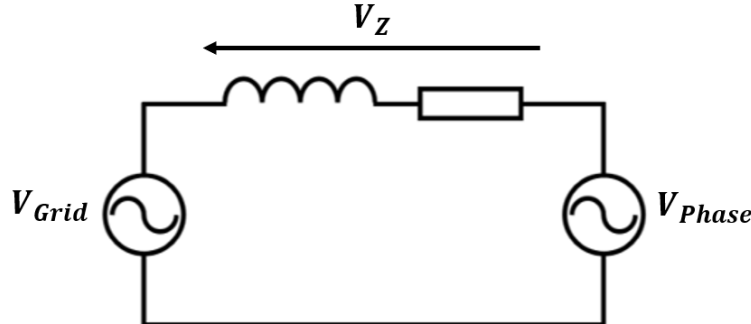


Figure 2.6. Simplified circuit in each phase

The relation between phase voltage, grid voltage and AC current can be derived as follows:

$$\widetilde{V_{Grid}} = \widetilde{V_{Phase}} + Z \widetilde{I_{AC}} \quad \text{Eqn 2.4}$$

In the inverter, it's crucial to regulate the AC output current ( $\widetilde{I_{AC}}$ ) in each phase to synchronize with the grid voltage ( $\widetilde{V_{Grid}}$ ) and adapt to changes in the phase voltage ( $\widetilde{V_{Phase}}$ ). Therefore, a mathematical model can be developed. This model uses the difference between the grid voltage and the phase voltage as input and the AC output current as output [11].

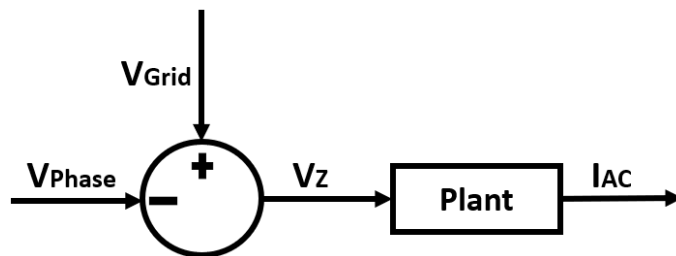


Figure 2.7. Plant block diagram

The plant transfer function ( $G_P$ ) can be derived as follows:

$$G_P(S) = \frac{\widetilde{I_{AC}}}{\widetilde{V_{Grid}} - \widetilde{V_{Phase}}} = \frac{1}{Z} = \frac{1}{LS + R} = \frac{1}{0.001s + 0.1} \quad \text{Eqn 2.5}$$

Based on the plant transfer function above, the overall block diagram can be drawn as follows:

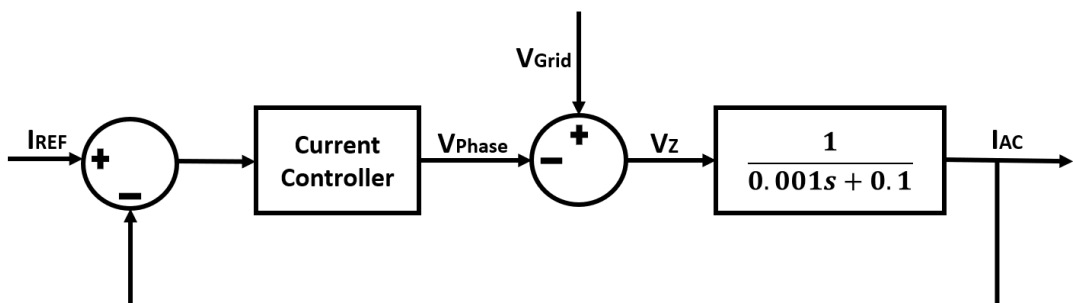


Figure 2.8. Plant block diagram

The role of the current controller in *Figure 2.8* is to reduce the error between the AC output current and the reference AC current to 0. [11] Since the plant transfer function in **Eqn 2.5** is first order, an PI controller can be applied as the current controller. The transfer function of PI controller is shown below:

$$G_c(s) = K_p + \frac{K_i}{s} \quad \text{Eqn 2.6}$$

Therefore, the open loop transfer function ( $G_{OPTF}(s)$ ) can be calculated in **Eqn 2.7**. Since the unity gain, the close loop transfer function ( $G_{CLTF}(s)$ ) can be derived in **Eqn 2.8**:

$$G_{OPTF}(s) = G_p(s) \cdot G_c(s) = \frac{K_p + \frac{K_i}{s}}{Ls + R} \quad \text{Eqn 2.7}$$

$$G_{CLTF}(s) = \frac{G_{OPTF}(s)}{G_{OPTF}(s) + 1} = \frac{\frac{K_p + \frac{K_i}{s}}{Ls + R}}{s^2 + \left(\frac{R+K_p}{L}\right)s + \frac{K_i}{L}} \quad \text{Eqn 2.8}$$

The denominator of the standard form transfer function for second-order system is shown below:

$$s^2 + 2\zeta\omega_0 s + \omega_0^2 \quad \text{Eqn 2.9}$$

Compare **Eqn 2.9** to the denominator in **Eqn 2.8**, the value of  $K_p$  and  $K_i$  can be calculated as follows:

$$\begin{cases} \frac{R+K_p}{L} = 2\zeta\omega_0 \\ \frac{K_i}{L} = \omega_0^2 \end{cases} \rightarrow \begin{cases} K_p = 2\zeta\omega_0 L - R \\ K_i = \omega_0^2 L \end{cases} \quad \text{Eqn 2.10}$$

In **Eqn 2.10**,  $\omega_0$  is natural frequency,  $\zeta$  is damping factor which is used to quantify the rate at which oscillations in a system decay over time. It is a measure of the system's damping or resistance to oscillation. [12]. In order to balance fast response and stability, the damping factor ( $\zeta$ ) is set as 0.707, which is also a common choice in engineering design across various applications. The settling time of inverter (time to reach 2% reference) can be calculated as follows:

$$t_S = \frac{4}{\omega_0 \cdot \zeta} \quad \text{Eqn 2.11}$$

In order to keep the settling time relatively small, the natural frequency is set to  $1000\pi\text{Hz}$ . Therefore, the values of  $K_p$  and  $K_i$  can be calculated below:

$$\begin{cases} K_p = 2\zeta\omega_0 L - R = 4.342 \\ K_i = \omega_0^2 L = 9869.6 \end{cases} \quad \text{Eqn 2.12}$$

Finally, the transfer function of the current controller is derived below:

$$G_c(s) = K_p + \frac{K_i}{s} = 4.342 + \frac{9869.6}{s} \quad \text{Eqn 2.13}$$

Based on the plant transfer function and current controller transfer function, the full block diagram can be drawn as follows:

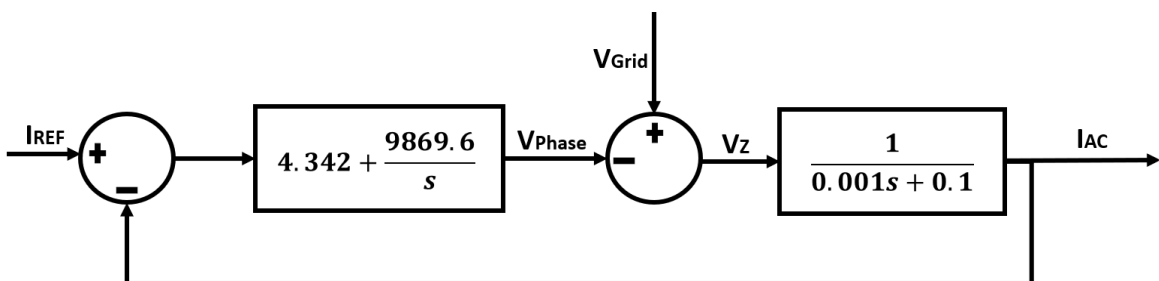


*Figure 2.9. Full block diagram*

### 2.3.2 Verification of the transfer function

The transfer function of current controller can be obtained using MATLAB's sisotool. The ‘sisotool’ is a powerful tool used for analysing and designing linear control systems. It provides a graphical interface for interactive design of single-input, single-output (SISO) feedback control systems.

In sisotool, the procedure for obtaining the current controller transfer function is as follows: Firstly, the plant transfer function derived in **Eqn 2.5** is set as the controlled object. Secondly, an integrator and a real zero are added into compensator editor to represent the PI controller. Thirdly, the natural frequency and damping factor are set to  $1000\pi$  and 0.707 respectively in the editor, and black polylines and arcs appear on the graph. Finally, adjust the size of the ellipse by dragging real zero, then drag the pole on the ellipse to the intersection of the arc and the polyline. The final root locus diagram that meets all the requirements is shown below:

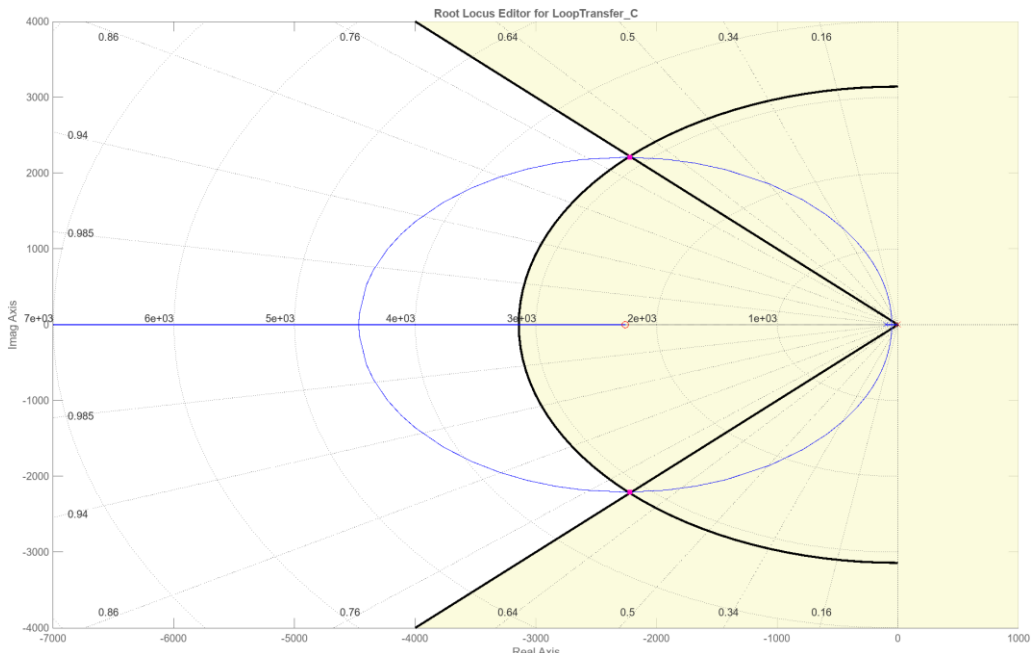


*Figure 2.10. Current controller root locus diagram*

In ‘sisotool’, the step response also can be drawn as follows:

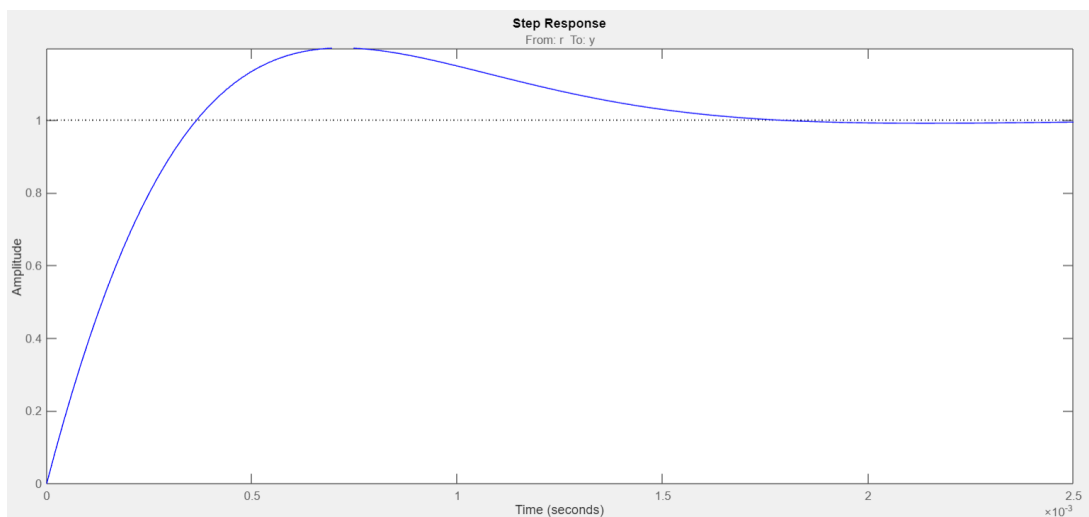


*Figure 2.11. Current controller step response*

As shown in Figure 2.11, with the increase of time, the amplitude gradually stabilizes around 1, indicating that the entire system will eventually stabilize. The settling time is about 1.6ms, which is also very short. The transfer function of the current controller obtained by sisotool is shown as follows:

$$G_c(s) = \frac{4.3335(s+2266)}{s} \quad \text{Eqn 2.14}$$

Compared **Eqn 2.14** to **Eqn 2.13**, the transfer function of the current controller obtained by MATLAB is almost consistent with the calculated value, which indicates that the calculated transfer function is correct. However, since the transfer function is determined by manually dragging poles and zeros in sisotool, there are errors, so the equation in **Eqn 2.13** is selected as the final transfer function to build the circuit in PLECS.

The transfer function can also be verified by PLECS. According to the block diagram in Figure 2.8, the circuit used to verify the current controller transfer function is constructed in PLECS as follows:

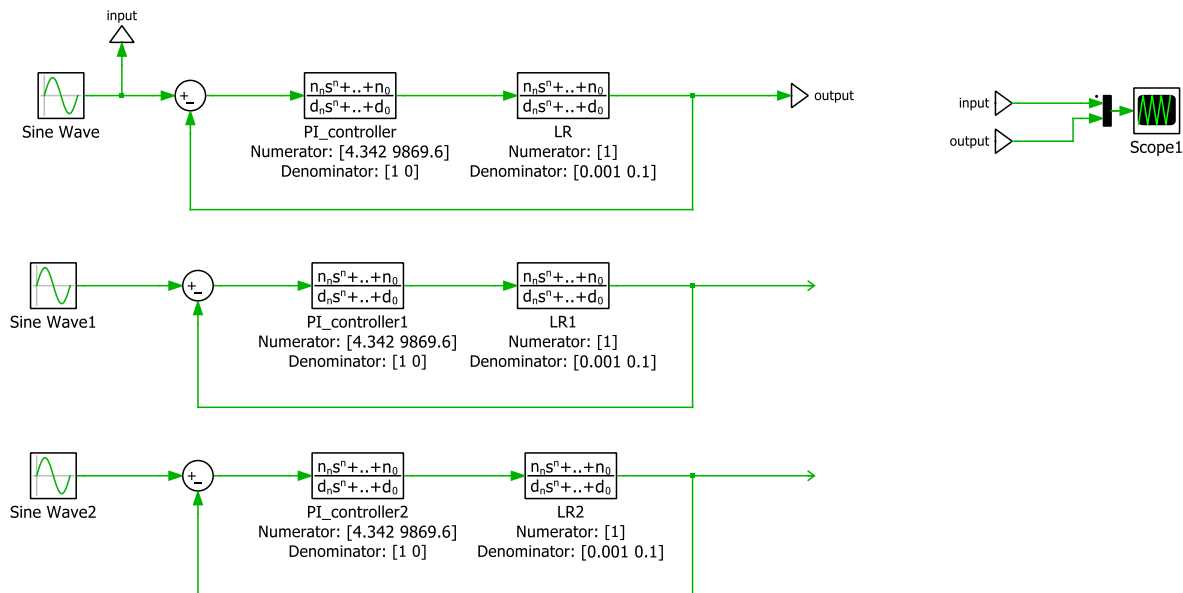


*Figure 2.12. The circuit used to verify the current controller transfer function*

In the scope, the reference current and output current are compared as follows:

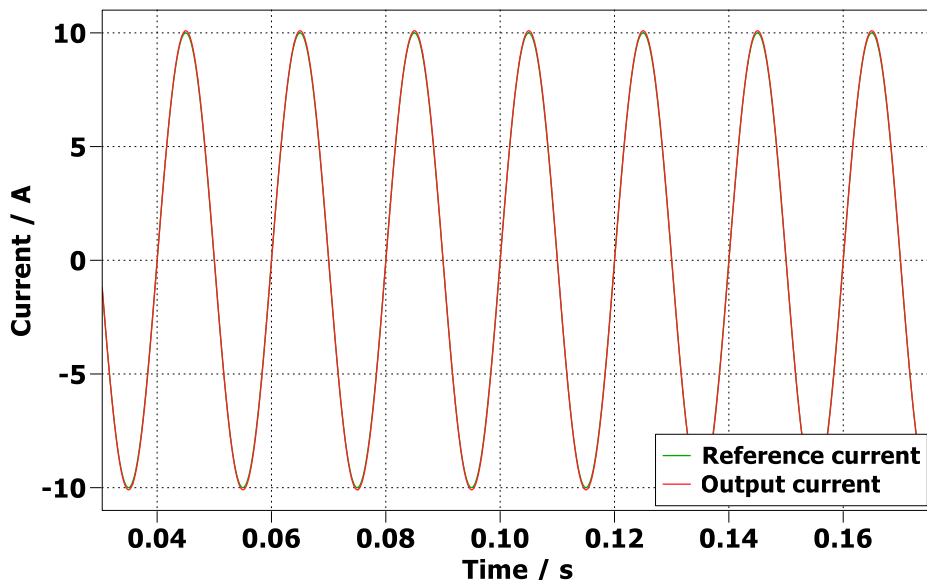


*Figure 2.13. Comparison of control system inputs and outputs*

As shown in Figure 2.13, the output signal is almost identical to the input signal, which indicates that the transfer function design of the current controller is correct

### 2.3.3 Switching model simulative verification

The main purpose of this section is to verify the current controller by building the circuit in the PLECS. PLECS (Piecewise Linear Electrical Circuit Simulation) is a specialized software tool commonly used for the simulation and analysis of power electronic systems. In this section, the grid current for each phase is measured in the same diagram and the grid current in each phase is compared to reference current. Furthermore, after changing the amplitude and direction of reference currents, these values are measured and compared again.

In PLECS, using the ideal DC voltage source, the switching model with the current controller is built as follows:

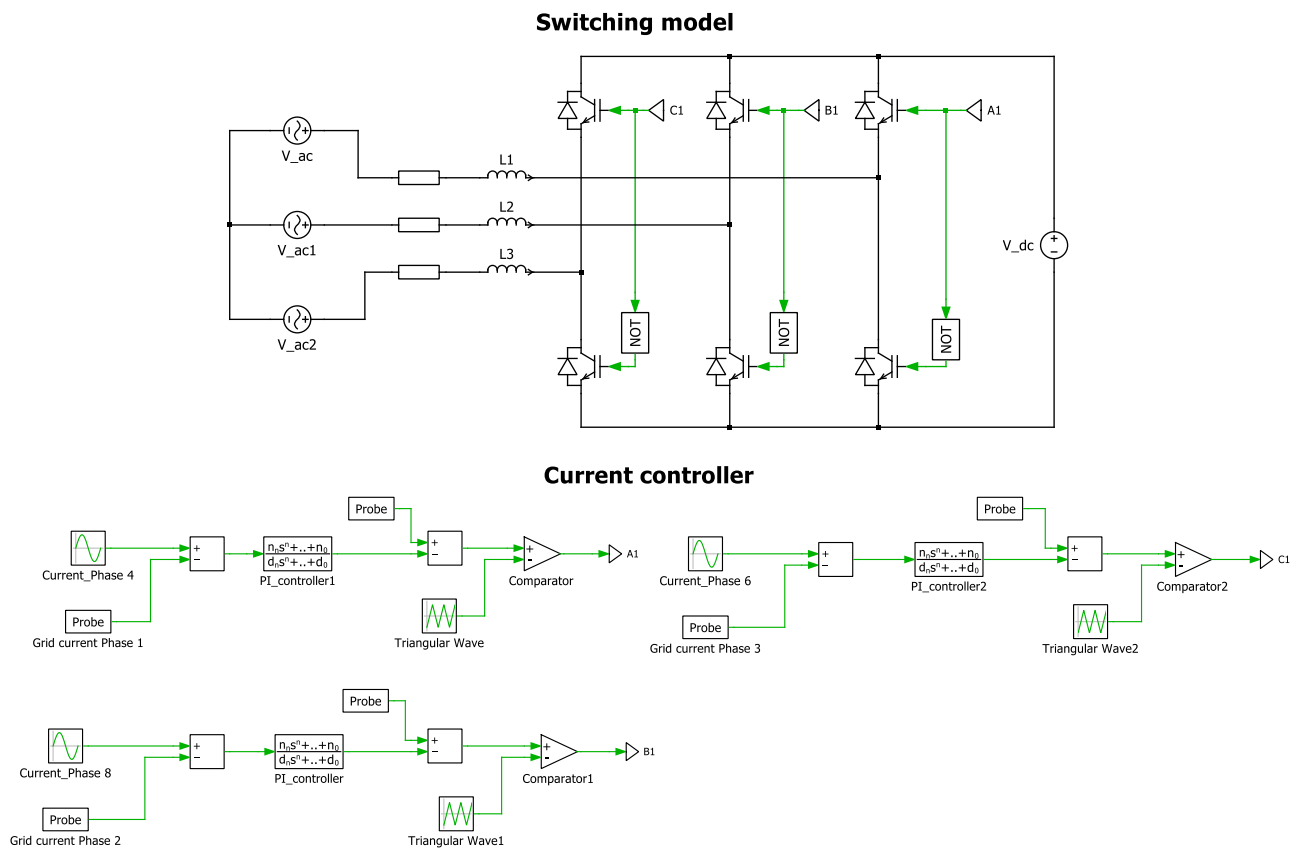


Figure 2.14. Three phase inverter with the current controller

In each PWM modulator, the magnitude of the reference current is set to  $10\sqrt{2}$  A and the phase difference in every two phases is set to 120 degree. The grid current in each phase and the can be measured as follows:

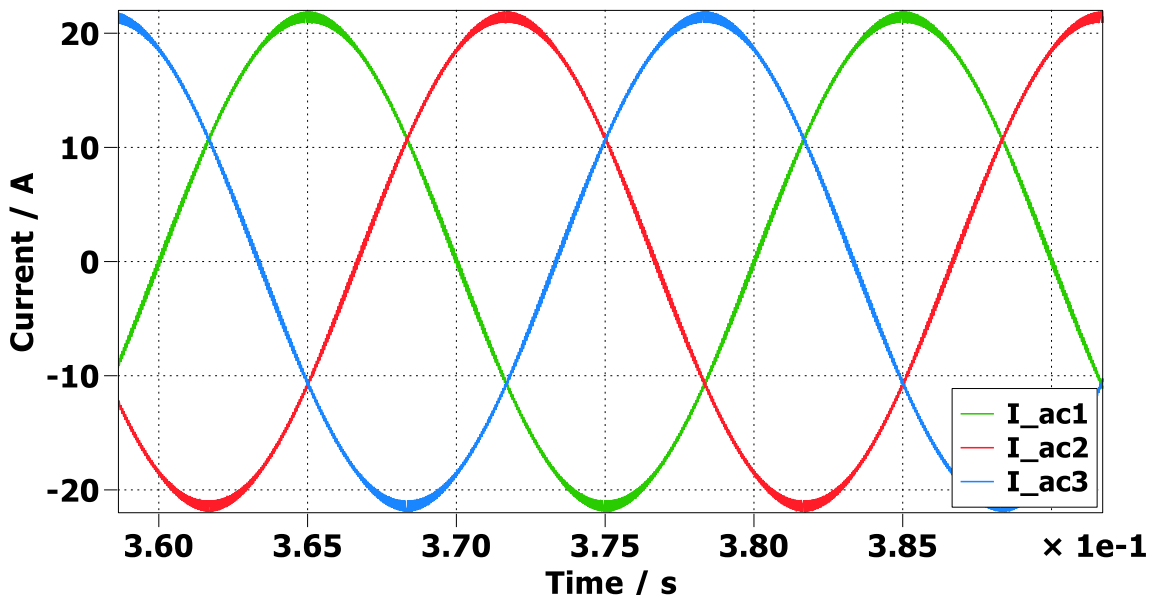


Figure 2.15. The grid current in three phase

In each phase, the grid current and reference current can be compared as follows:

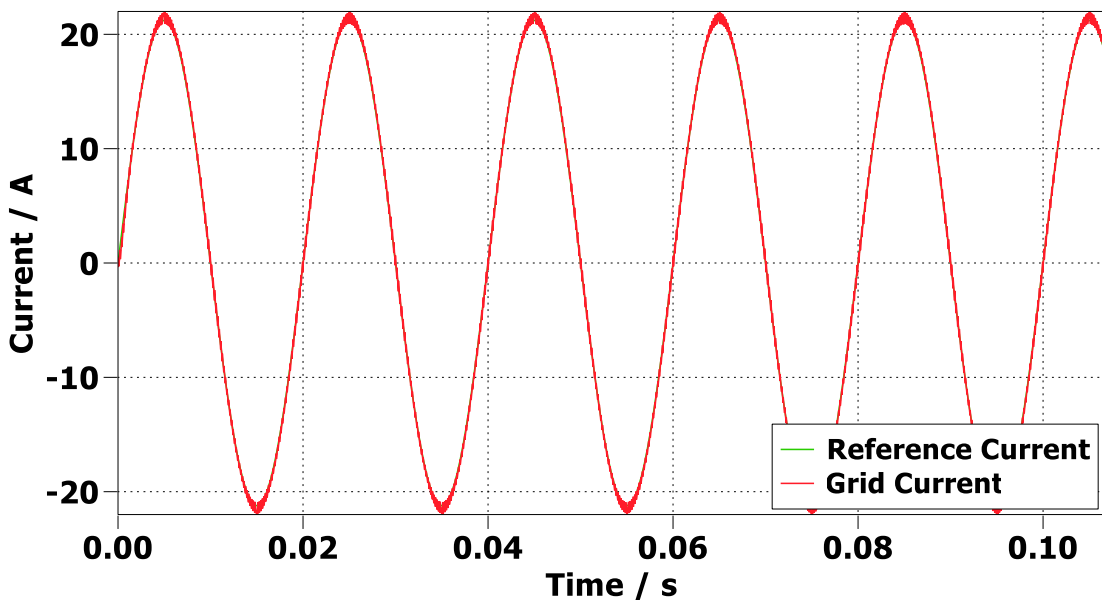


Figure 2.16. Comparison between reference current and grid current in each phase

As Figure 2.15 shown, although the current has some high frequency harmonics, the magnitude of the grid current for each phase is about  $10\sqrt{2}$ A, and the three phases currents are evenly distributed in the diagram. According to Figure 2.16, it can be proved that the reference current is almost identical to the grid current in each phase. Therefore, the current controller works as expected.

### 2.3.3.1 Different current and Bi-directional

In order to verify the current controller in different current, the PWM modulator in each phase is modified as follows:

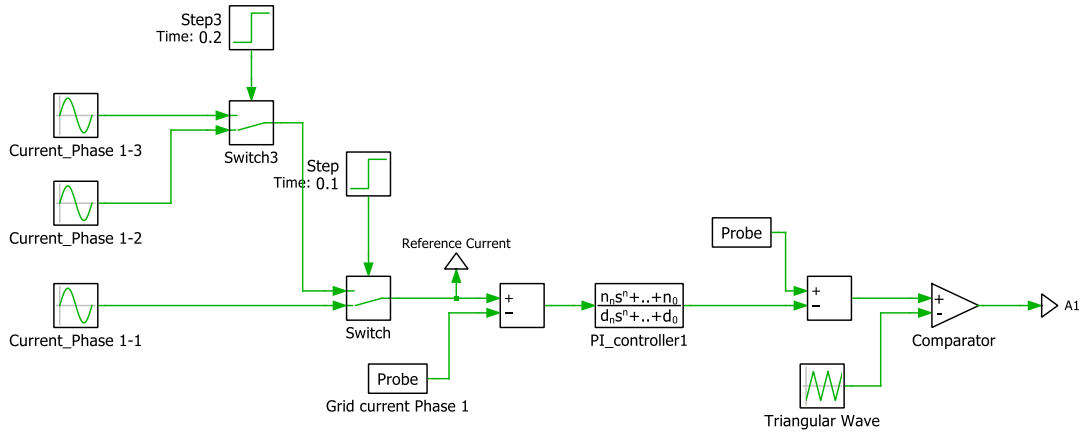


Figure2.17. Modified PWM modulator for each phase

Figure2.17 shows a certain phase as an example, the initial magnitude of the reference current is ‘Current\_phase 1-1’. It changes to ‘Current\_phase 1-2’ at 0.1 seconds and finally to ‘Current\_phase1-3’ at 0.2 seconds. It worth noting that the amplitude of reference current is limited by the DC voltage , which can be illustrated in Figure2.5. Phase diagram in each phase. To verify that the current controller can operate at different currents and that the converter can absorb and transmit power, the reference current can be set as follows:

Table2. The change of reference current

	Transmit power (Positive current)	Negative current (Negative power)
0-0.1s	$5\sqrt{2}A$	$-5\sqrt{2}A$
0.1s-0.2s	$10\sqrt{2}A$	$-10\sqrt{2}A$
0.2s-0.3s	$15\sqrt{2}A$	$-15\sqrt{2}A$

When the reference current is positive, the grid current in three phase is measured as follows:

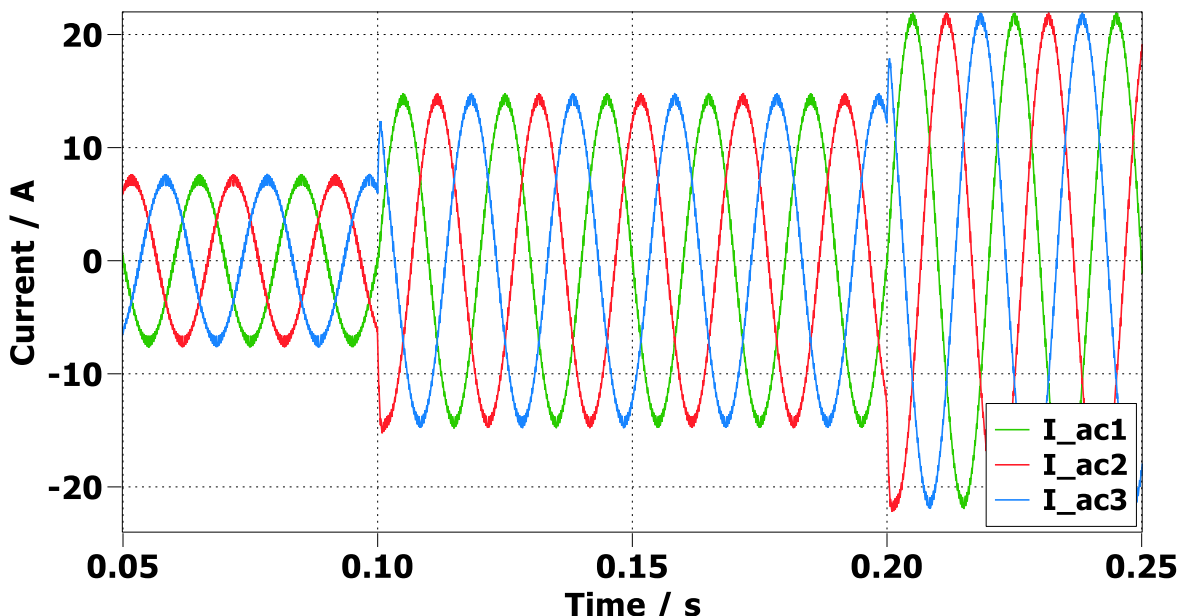


Figure2.18. The grid current in different positive reference current

When the reference current is negative, the grid current in three phase is measured as follows:

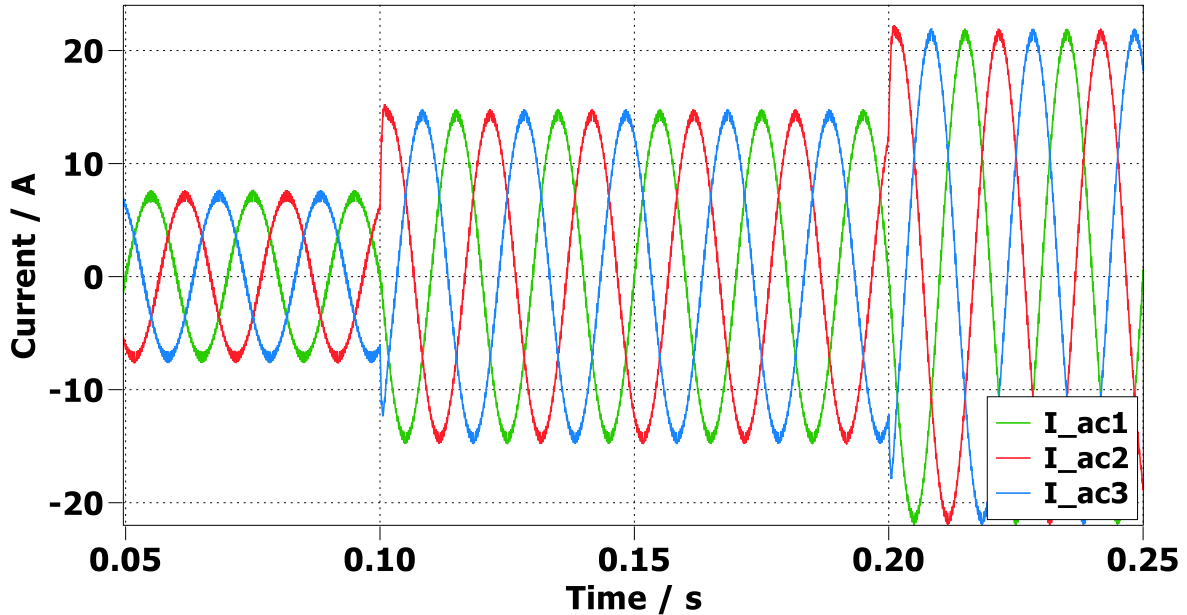


Figure 2.19. The grid current in different negative reference current

As Figure 2.18 and Figure 2.19 shown, with some high frequency harmonics, the magnitude of the grid current starts at  $5\sqrt{2}$  A, increases to  $10\sqrt{2}$  A at 0.1 seconds, and finally increases to  $15\sqrt{2}$  A at 0.2 seconds and the three phases currents are evenly distributed in the diagram. The grid current performance of positive and negative reference current is consistent.

In each phase, when the reference current is positive, the grid current is compared to the reference current as follows:

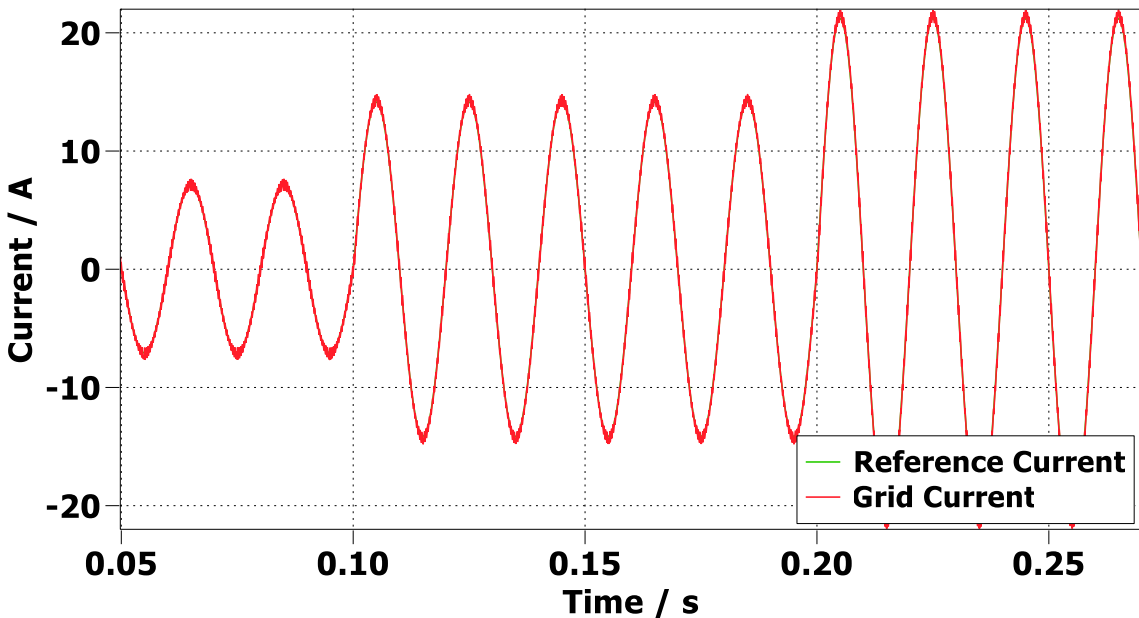


Figure 2.20. Comparison between reference current and grid current in different current

When the reference current is negative, the grid current is compared to the reference current as follows:

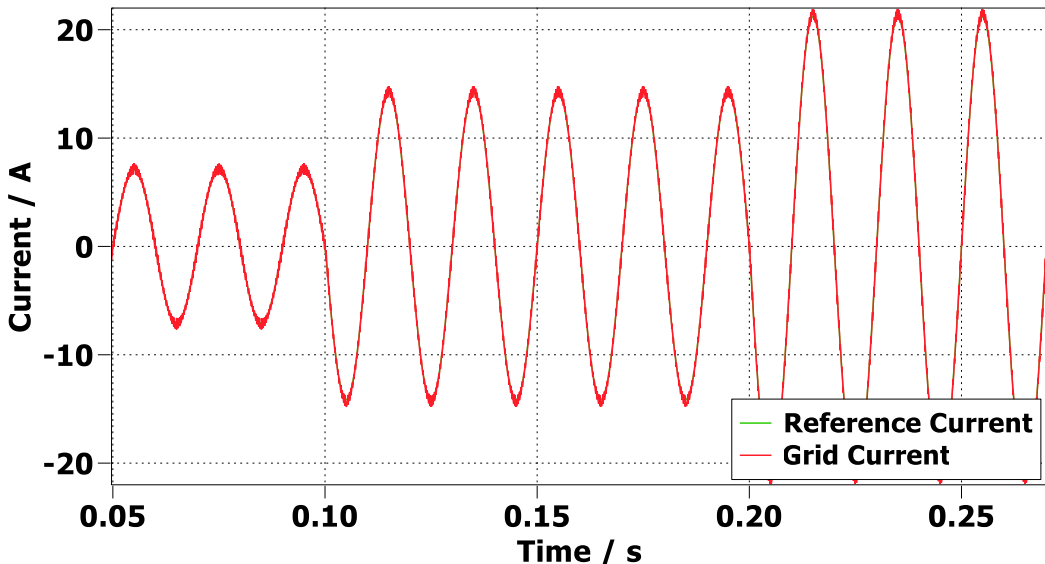


Figure 2.21. Comparison between reference current and grid current in different current

Both Figure 2.20 and Figure 2.21 shows that in each phase, the reference current is almost the same as the reference current at different currents amplitude. Therefore, the current controller works as expected. Comparing Figure 2.21 and Figure 2.20, when the reference current is negative, the corresponding grid current is the opposite of the grid current when the reference current is positive.

## 2.4 Voltage controller design

The main purpose of this section is to design the voltage controller and build the circuit in the PLCES. The voltage controller is an important part of the three phase inverter, which can regulate the output voltage to a desired level, ensuring that it meets the requirements of the connected load. [13] This section is divided into three parts. The first two parts are the derivation and verification of the transfer function, and the third part is the circuit construction and verification in PLCES.

### 2.4.1 Transfer function derivation

In the switching model containing the voltage controller, a capacitor is used instead of a DC voltage source to power the two-level inverter. The simplified switching model can be drawn as follows:

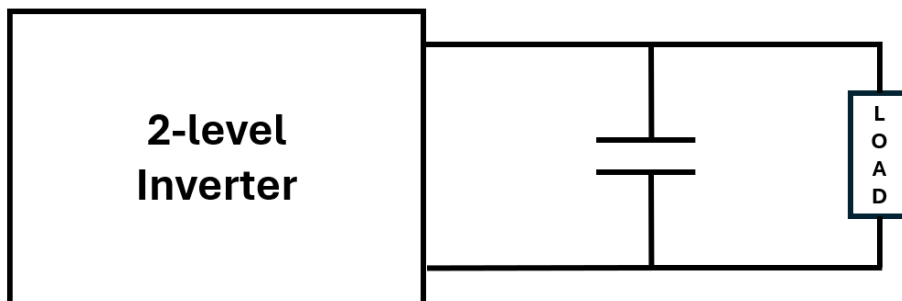


Figure 2.22. Simplified switching model with capacitor

By replacing the 2-level inverter with an ideal DC current source, the circuit can be further simplified as follows:

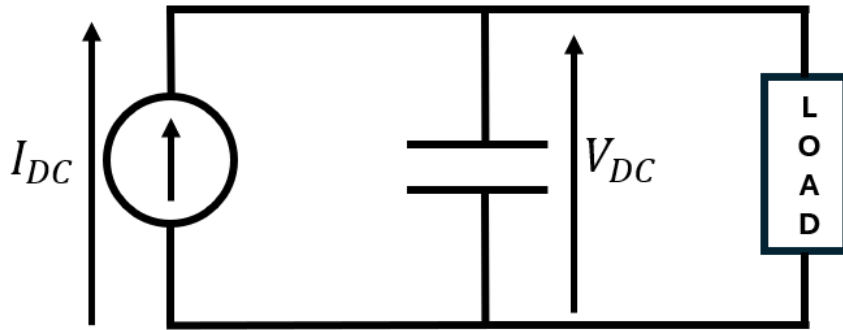


Figure 2.23. Simplified switching model with current source

Ignoring the influence of load, the Laplace transform relationship between the current  $I(t)$  flowing through a capacitor and the voltage  $V(t)$  across the capacitor can be approximated as follows:

$$V_{DC}(s) \approx \frac{1}{Cs} * I_{DC}(s) \quad \text{Eqn 2.15}$$

The capacitance of capacitor is set 0.001F, so the plant transfer function ( $G_P$ ) can be derived as follows:

$$G_P(s) = \frac{\widetilde{V}_{DC}}{\widetilde{I}_{DC}} = \frac{1}{Cs} = \frac{1}{0.01s} \quad \text{Eqn 2.16}$$

According to the Eqn 2.15, the block diagram can be drawn as follows:

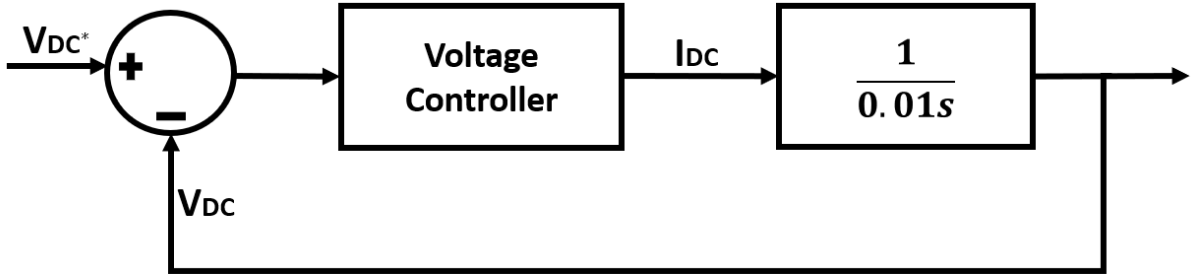


Figure 2.24. Preliminary block diagram

The role of the voltage controller in Figure 2.24 is to reduce the error between the DC voltage and the reference DC voltage to 0. [13] Same as current controller, since the plant is first order, an PI controller can be used as the voltage controller. The transfer function of PI controller is shown below:

$$G_c(s) = K_p + \frac{K_i}{s} \quad \text{Eqn 2.16}$$

Therefore, the open loop transfer function ( $G_{OPTF}(s)$ ) can be calculated in Eqn 2.17. Since the unity gain, the close loop transfer function ( $G_{CLTF}(s)$ ) can be derived in Eqn 2.18:

$$G_{OPTF}(s) = G_p(s) \cdot G_c(s) = \frac{K_p + \frac{K_i}{s}}{sC} \quad \text{Eqn 2.17}$$

$$G_{CLTF}(s) = \frac{G_{OPTF}(s)}{G_{OPTF}(s)+1} = \frac{\frac{K_p}{C}s + \frac{K_i}{C}}{s^2 + \frac{K_p}{C}s + \frac{K_i}{C}} \quad \text{Eqn 2.18}$$

The denominator of the standard form transfer function for second-order system is shown below:

$$s^2 + 2\zeta\omega_0 s + \omega_0^2 \quad \text{Eqn 2.19}$$

Compare **Eqn 2.19** to the denominator in **Eqn 2.18**, the value of  $K_p$  and  $K_i$  can be calculated as follows:

$$\begin{cases} \frac{K_p}{C} = 2\zeta\omega_0 \\ \frac{K_i}{C} = \omega_0^2 \end{cases} \rightarrow \begin{cases} K_p = 2\zeta\omega_0 C \\ K_i = \omega_0^2 C \end{cases} \quad \text{Eqn 2.20}$$

It worth noting that in the CASCADE design, the natural frequency of the internal controller(the current controller) should be at least 10 times greater than the natural frequency of external controller (voltage controller). Otherwise, the control effect will be unstable.[14] Therefore, the natural frequency of the voltage controller is set to  $10\pi\text{Hz}$ .

In addition, as in the current controller design, the damping factor ( $\zeta$ )is set to 0.707 to balance fast response and stability, which is also a common choice in engineering design across various applications. So, the values of  $K_p$  and  $K_i$  can be calculated below:

$$\begin{cases} K_p = 2\zeta\omega_0 C = 0.44 \\ K_i = \omega_0^2 C = 9.87 \end{cases} \quad \text{Eqn 2.21}$$

Finally, the transfer function of the voltage controller is shown below:

$$G_c(s) = K_p + \frac{K_i}{s} = 0.44 + \frac{9.87}{s} \quad \text{Eqn 2.22}$$

Based on the plant transfer function and voltage controller transfer function, the full block diagram can be drawn as follows:

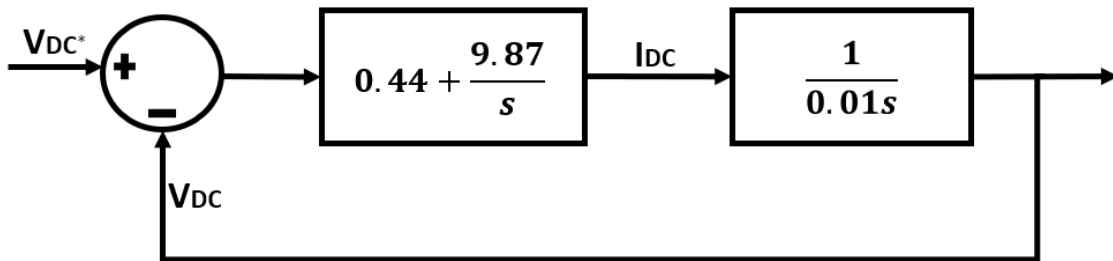


Figure2.25. Full block diagram

#### 2.4.2 Verification transfer function

Same as current controller, the transfer function of voltage controller also can be obtained using sisotool in MATLAB. The ‘sisotool’ is a powerful tool used for analysing and designing linear control systems. It provides a graphical interface for interactive design of single-input, single-output (SISO) feedback control systems.

In sisotool, the procedure for obtaining the voltage controller transfer function is as follows: Firstly, the plant transfer function derived in **Eqn 2.22** is set as the controlled object. Secondly, an integrator and a real zero are added into compensator editor to represent the PI controller. Thirdly, the natural frequency and damping factor are set to  $10\pi$  and 0.707 respectively in the editor. Accordingly, a black polyline and an arc appear on the figure. Finally, adjust the size of the ellipse by dragging real zero, then drag the pole on the ellipse to the

intersection of the arc and the polyline. The final root locus diagram that meets all the requirements is shown below:

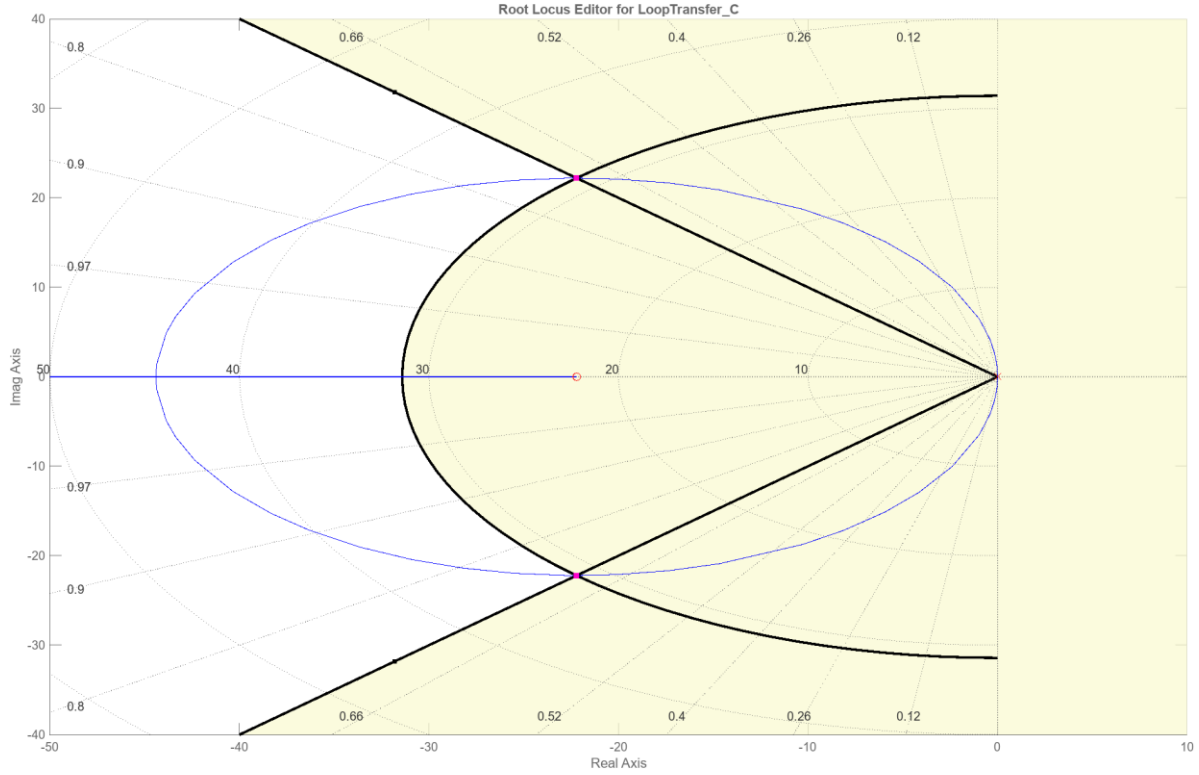


*Figure2.26. Voltage controller root locus diagram*

In ‘sisotool’, the step response also can be drawn as follows:

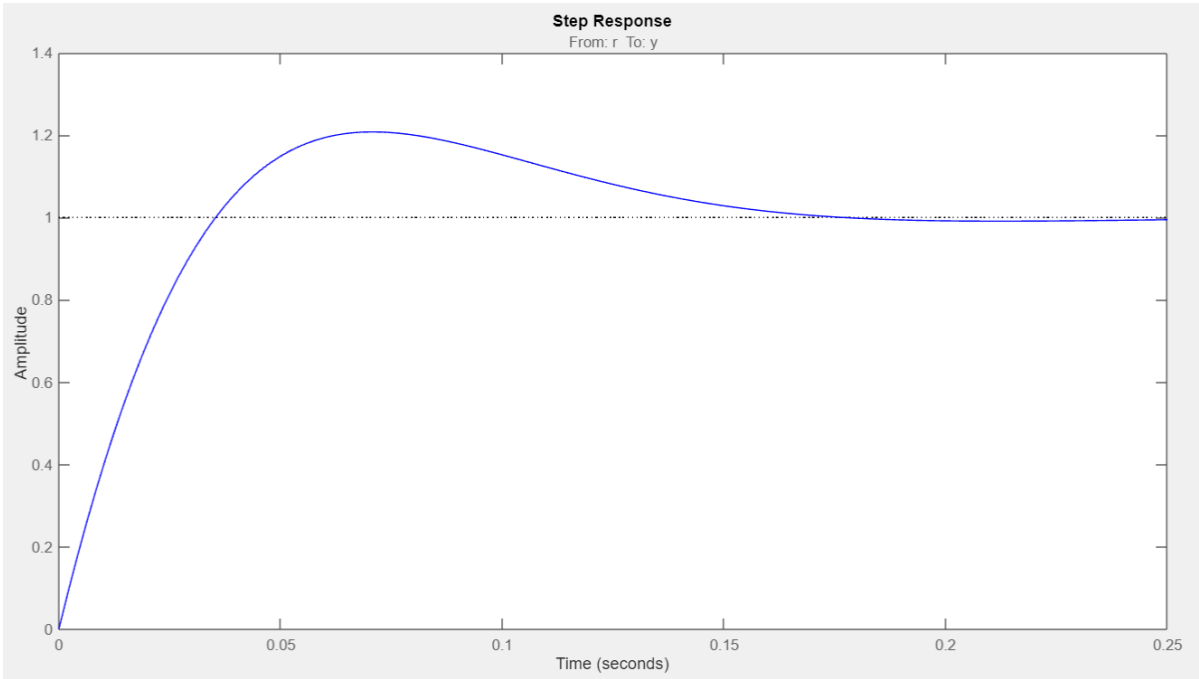


*Figure2.27. Voltage controller step response*

As shown in Figure 2.27, with the increase of time, the amplitude gradually stabilizes around 1, indicating that the entire system will eventually stabilize.

The settling time is about 1.6ms, which is about 100 times the setting time of the current controller.

According to **Eqn 2.11**, settling time is inversely proportional to the natural frequency. Therefore, the natural frequency of current controller is about 100 times greater than voltage controller which is as expected. The transfer function of the current controller obtained by ‘sisotool’ is shown as follows:

$$G_c(s) = \frac{9.868(1+0.045s)}{s} \quad \text{Eqn 2.23}$$

Compared **Eqn 2.23** to **Eqn 2.22**, the transfer function of the voltage controller obtained by MATLAB is almost consistent with the calculated value, which indicates that the calculated transfer function is correct. However, since the transfer function is determined by manually dragging the poles and zeros in the 'sisotool', there is an error. So the equation in **Eqn 2.22** is selected as the final transfer function to build the circuit in PLECS.

The transfer function can also be verified by PLECS. According to the block diagram in Figure 2.25, the circuit used to verify the voltage controller transfer function is constructed in PLECS as follows:

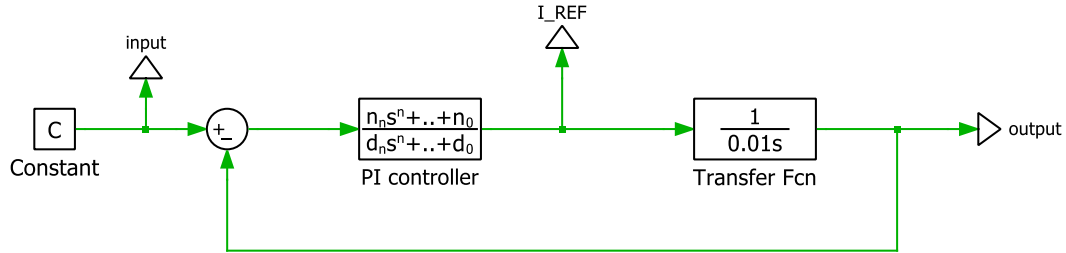


Figure 2.28. The circuit used to verify the current controller transfer function

In the scope, the reference voltage and output voltage are compared as follows:

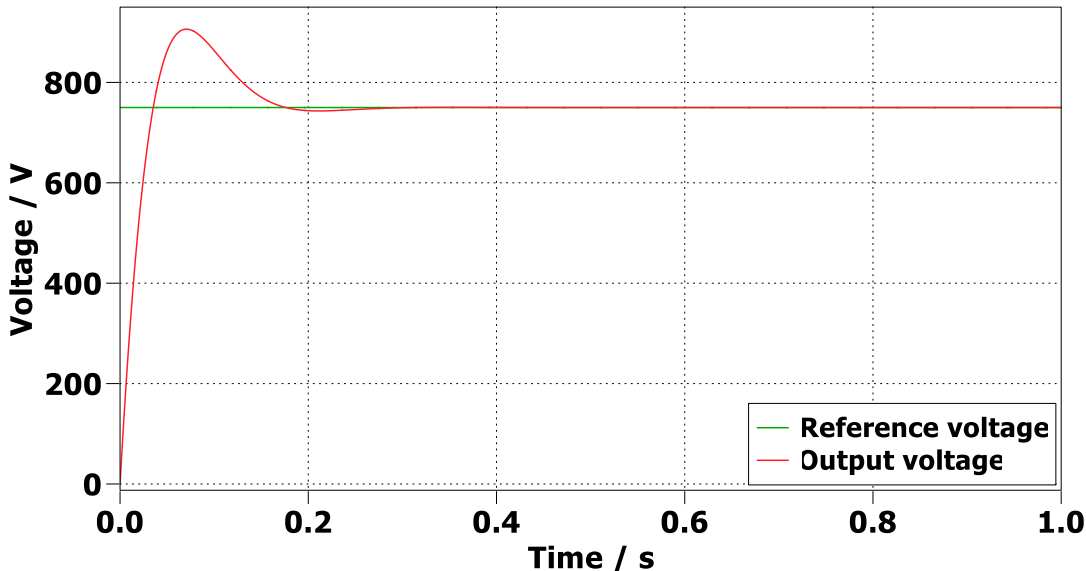


Figure 2.29. Comparison of control system inputs and outputs

As shown in Figure 2.29, after settling time of about 1.6 seconds, the output voltage and reference voltage almost matched. Therefore, the voltage controller works as expected.

## 2.5 Complete three-phase inverter analysis

After designing the current controller and voltage controller, a complete three-phase inverter can be built in the PLECS. In this section, a complete analysis of three inverters, including three-phase output current, DC voltage changes, will be performed.

### 2.5.1 Full block diagram

According to the block diagrams of current controller and voltage controller, the full block diagram of control system can be drawn as follows:

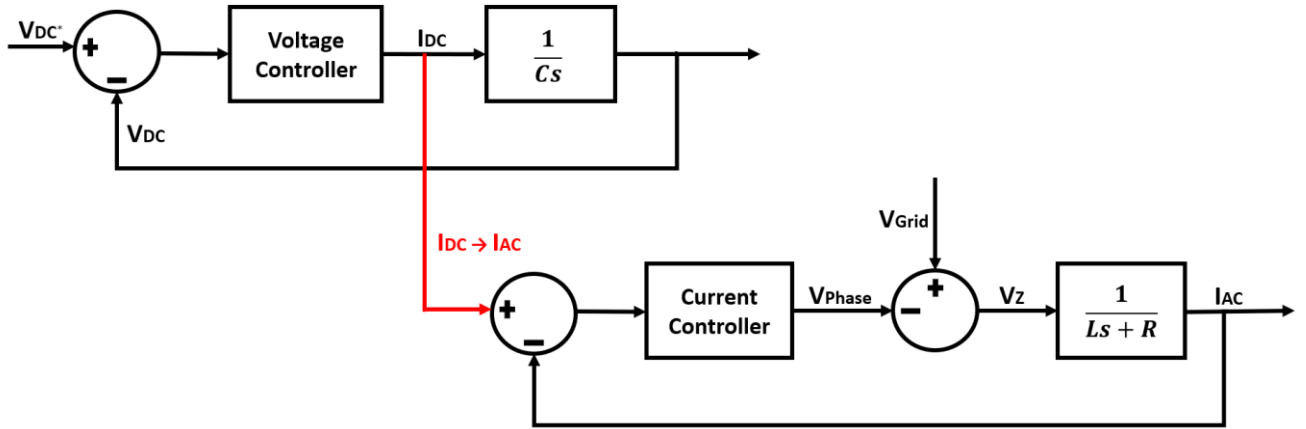


Figure 2.30. Full block diagram of control system in three phase inverter

Figure 2.30 shows the combination of a voltage controller and a current controller. The input signal of voltage controller is the difference between the DC reference voltage and capacitor voltage. And it is worth noting that the output of the voltage controller is DC current. After the DC current is converted into AC current, it can be used as the reference current of the current controller, which is also the input signal.

### 2.5.2 Specification

In the complete three phase inverter, the system design specifications are shown below:

Table 2.2. System design specifications

Term	Symbol	Value
Inductor	$L_1, L_2, L_3$	0.001H
Inductance internal resistance	$R_1, R_2, R_3$	50Ω
Capacitor	$C$	0.01F
Load	$R_{Load}$	5Ω
Fundamental frequency	$f_B$	50Hz
Inverter Switching Frequency	$f_{sw}$	20KHz
DC voltage	$V_{DC}$	850V
AC RMS voltage	$V_{AC}$	240.4V

### 2.5.3 The schematic of three phase inverter

According to the full block diagram and all the results above, a complete three phase inverter can be built in PLECS, the schematic is shown below:

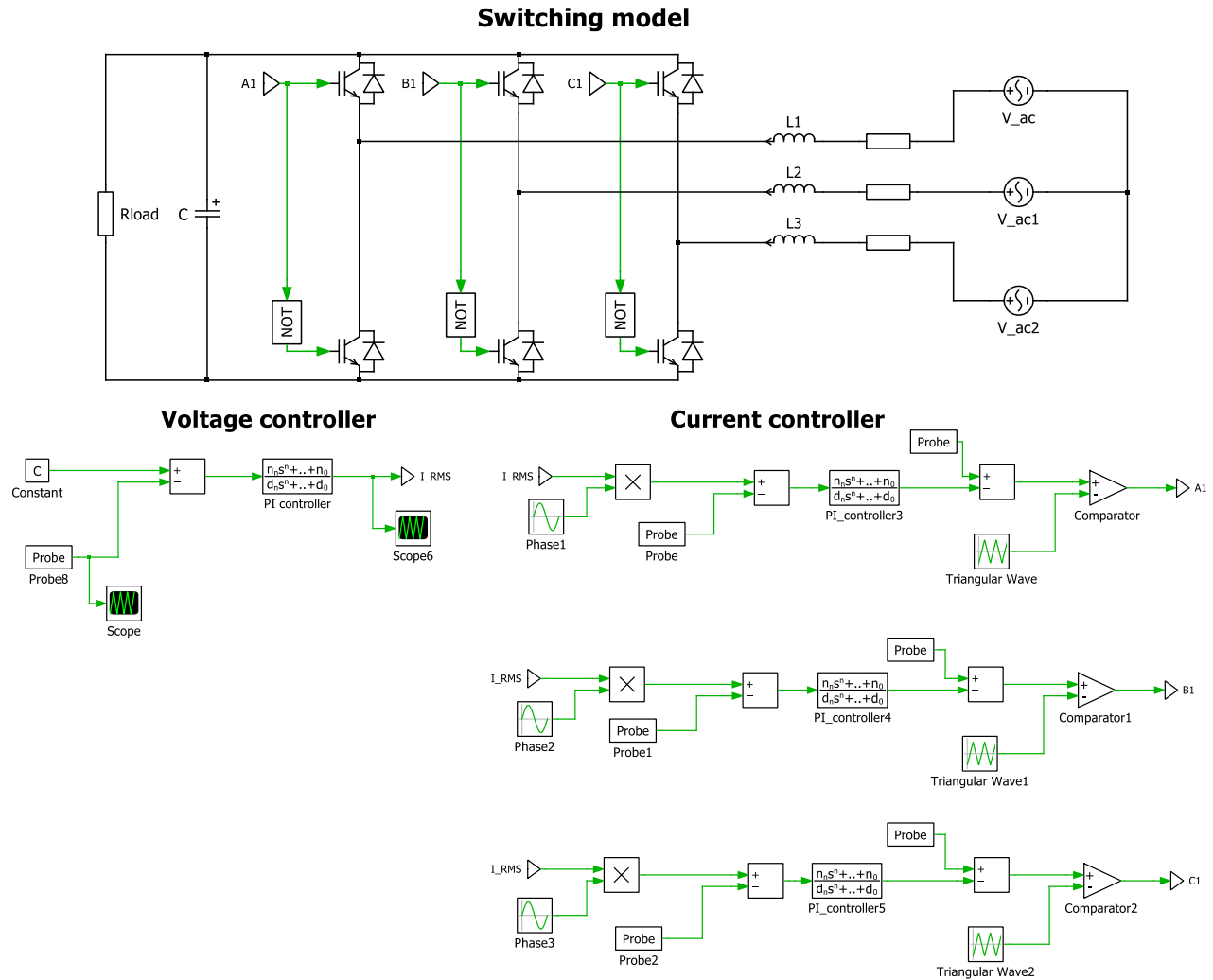


Figure 2.31. The schematic of three phase inverter

### 2.5.4 Results analysis

The Three-phase grid current and measured in real time as follows:

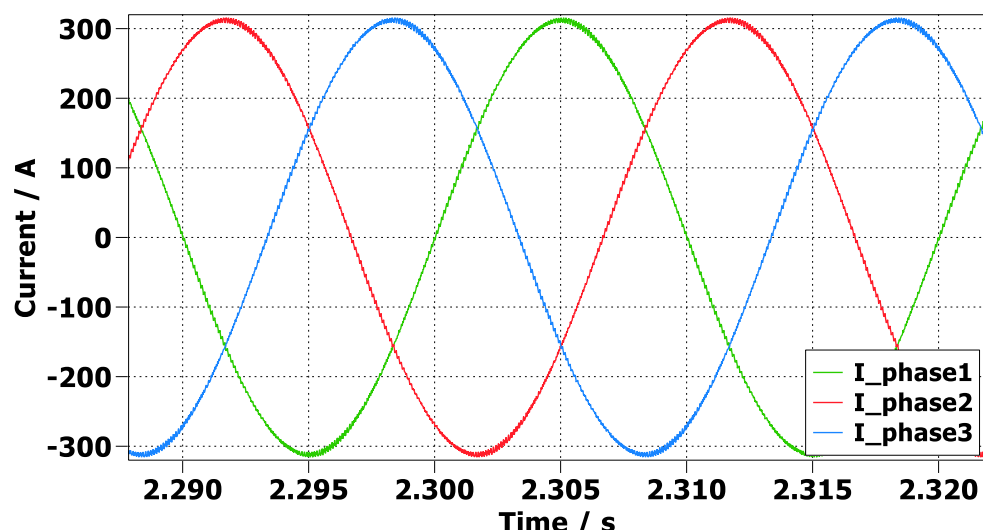


Figure 2.32. The grid current in three phase

The frequency spectrum of grid current is measured as follows:

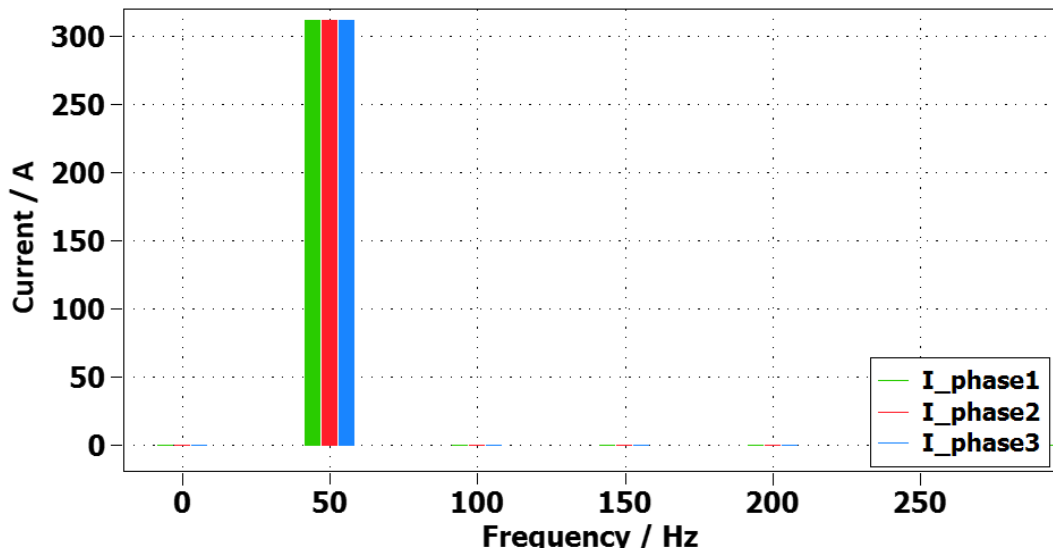


Figure 2.33. The frequency spectrum of grid current

As Figure 2.32 shown, although the current has some high frequency harmonics, the three-phase current is evenly distributed in the diagram. According to the frequency spectrum in Figure 2.33, all three phases of the grid current are concentrated at 50Hz, which is the fundamental frequency in the circuit.

Mathematically, based on the DC voltage, inductance of inductor and switching frequency, the AC current ripple can be calculated as follows [15]:

$$\Delta I = \frac{V_{DC}}{8Lf_{SW}} = \frac{600V}{8 \times 0.001H \times 10000Hz} = 7.5A \quad \text{Eqn 2.24}$$

In order to measure the maximum AC current ripple in the three phase inverter, the current ripple should be measured at point of maximum voltage change from the PWM.

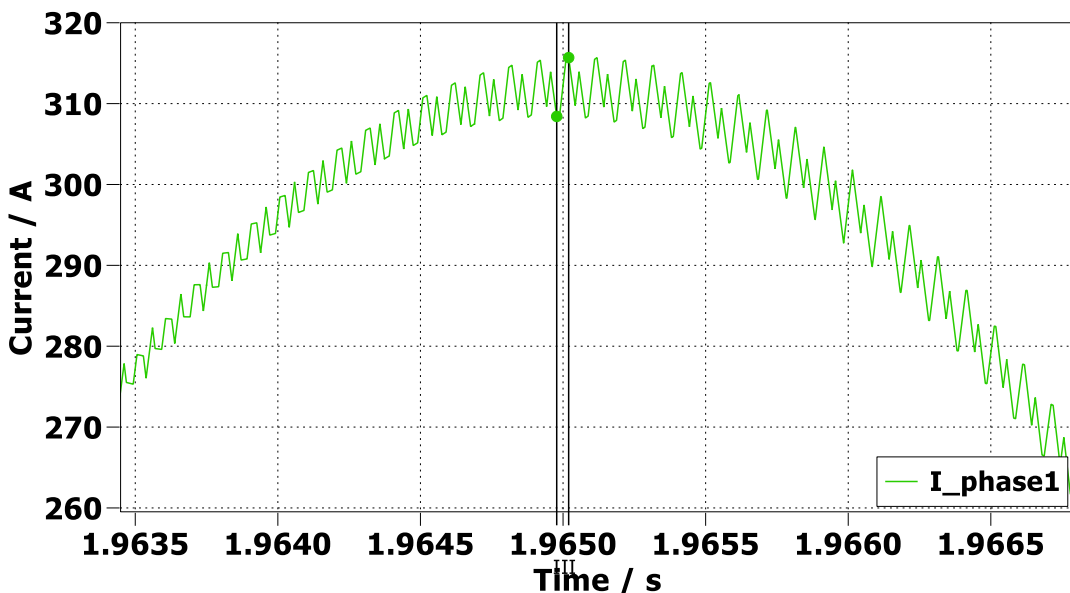


Figure 2.34. Maximum AC current ripple

In PLECS, cursors can be used to measure data. In Figure 2.34, the maximum AC current ripple can be calculated as 7.272A through the cursors, which is consistent with the calculated value in **Eqn 2.24**. The capacitor voltage are measured as follows:

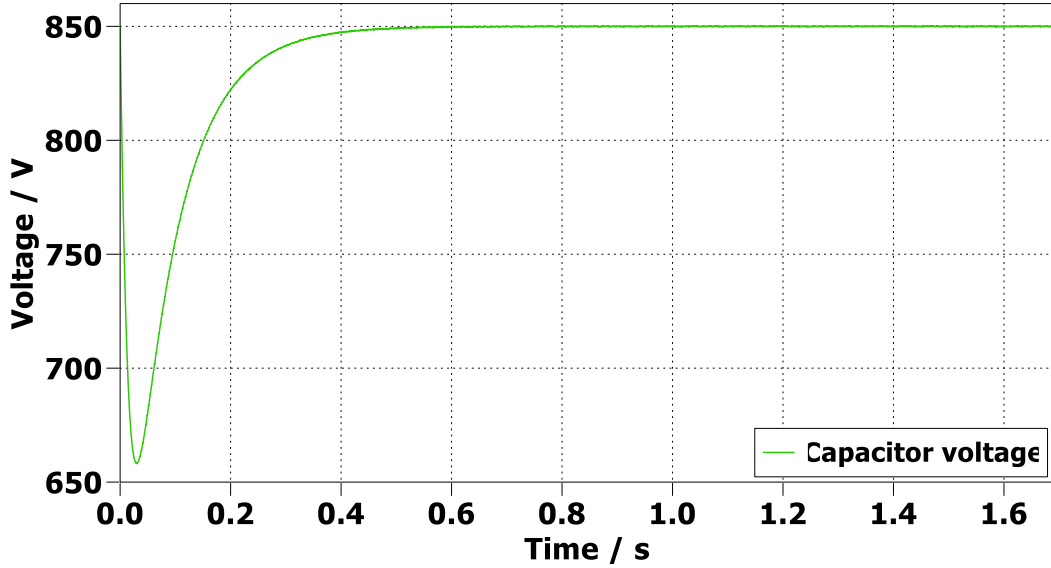


Figure 2.35. Capacitor voltage

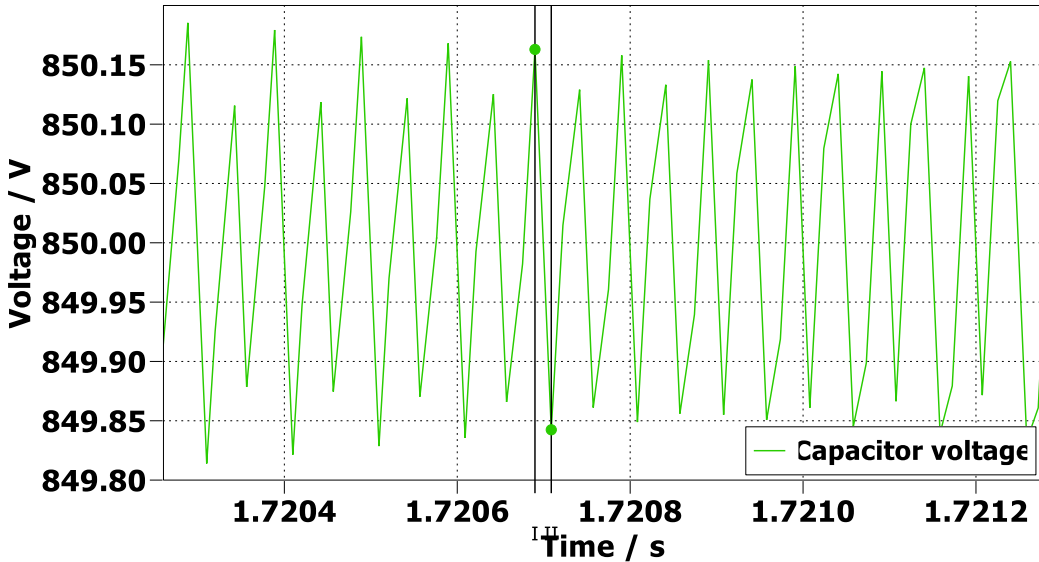


Figure 2.36. Ripple in capacitor voltage

Figure 2.35 shows that the capacitor voltage stabilizes at about 850V after 0.6 seconds, which is also the DC voltage in the specification. This proves that the voltage controller works as expected. According to the specifications and measured value, the DC voltage ripple can be calculated as follows [16]:

$$V_{DC}^{ripple} = \frac{\sqrt{2} \times 240.4V \times 315.6A}{4 \times 2\pi \times 50 \times 600V \times 10mF} = 1.423 \times 10^{-2}V \quad \text{Eqn 2.25}$$

According to the cursors in Figure 2.36, the DC voltage ripple are measured as 0.321V, which is slightly larger than the calculated value in **Eqn 2.25**. The reason may be that in the process of designing the voltage controller, the value of the load is not considered in the design in order to facilitate the calculation.

### 3 CHAPTER3: STATCOM with linear load

In the last chapter, a three phase inverter was built to achieve the conversion of DC to three-phase power. In this chapter, a well-designed three-phase inverter is connected in parallel between a three-phase grid and a linear load. The compensation of reactive power is realized by applying PQ theory in three-phase inverter. This whole system is also called STATCOM. This chapter is basically divided into three parts. The first part is the understanding and exploration of PQ theory. The first part is the understanding and exploration of PQ theory. On this basis, STATCOM is modelled as an ideal voltage source, and the circuit is constructed in PLECS. Finally, a DC voltage controller is developed by using a power converter instead of an ideal voltage source.

#### 3.1 Basis of the p-q Theory

The p-q theory is rooted in a collection of instantaneous powers defined within the time domain. This approach doesn't impose any limitations on the voltage or current waveforms, making it applicable to both three-phase systems, regardless of the presence of neutral lines, and adaptable to three-phase generic voltage and current waveforms. Therefore, it is effective not only in steady state, but also in steady state transients. Compared to traditional power concepts which define a three-phase system as three different single-phase circuits, The p-q theory initially converts voltages and currents from the abc to  $\alpha\beta0$  coordinates, subsequently defining instantaneous power within these coordinates. Therefore, this theory consistently treat the three-phase system as a cohesive unit, rather than just an aggregation or summation of three independent single-phase circuits. [17]

##### 3.1.1 Clark transform

The  $\alpha\beta0$  transformation, also known as the Clarke transformation converts the three-phase instantaneous voltage or current from the abc phases(a, b, c) into the corresponding instantaneous voltages on the  $\alpha\beta0$  axes ( $\alpha, \beta, 0$ ). In contrast, the inverse clark transform converts the coordinates on  $\alpha\beta0$  axes to abc. It worth noting that in a balanced three-phase system, where the loads are symmetrically distributed and the phases are identical in terms of impedance and connectivity, the zero-sequence current ( $I_0$ ) and voltage ( $V_0$ ) can be eliminated. Therefore, in a balanced three-phase system, the diagram which illustrate the Clark transform and inverse Clark transform is shown below [17]:

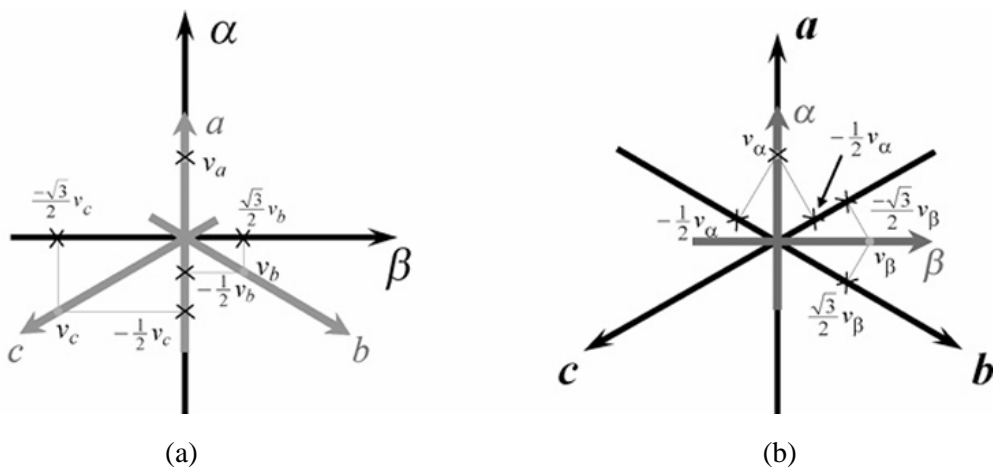


Figure 3.1 (a) Clark transform (b) inverse Clark transform [17]

### 3.1.2 The p-q theory in three-phase and three-wire systems

It worth noting that all the calculations in this section are derived from ‘*The Instantaneous Power Theory*’ in the book ‘*Instantaneous Power Theory and Applications to Power Conditioning*’ [17] In a balanced three-phase system, the zero-sequence current ( $I_0$ ) and voltage ( $V_0$ ) can be neglected. So, an instantaneous voltage vector and current vector can be defined from instantaneous  $\alpha$  and  $\beta$  components as follows :

$$e = v_\alpha + jv_\beta \quad \text{Eqn 3.1}$$

$$i = i_\alpha + ji_\beta \quad \text{Eqn 3.2}$$

A method of introducing the p-q theory of a three-phase three-wire system is shown below: Based on instantaneous voltage and current vectors defined in **Eqn 3.1** and **Eqn 3.2**, the instantaneous complex power ( $s$ ) can be defined as the multiplication of the voltage vector ( $e$ ) and the conjugate of the current vector ( $i^*$ ):

$$s = e \cdot i^* = (v_\alpha + jv_\beta)(i_\alpha - ji_\beta) = (v_\alpha i_\alpha + v_\beta i_\beta) + j(v_\beta i_\alpha - v_\alpha i_\beta) \quad \text{Eqn 3.3}$$

In the **Eqn 3.3**, the real power ( $p$ ) and imaginary power ( $q$ ) are defined as follows:

$$p = v_\alpha i_\alpha + v_\beta i_\beta \quad \text{Eqn 3.4}$$

$$q = v_\beta i_\alpha - v_\alpha i_\beta \quad \text{Eqn 3.5}$$

Given the utilization of instantaneous voltages and currents, there is no limit to instantaneous complex power. Therefore, it is applicable for both steady and transient states. The definition of  $p$  and  $q$  can also be expressed as a matrix of the following formula:

$$\begin{bmatrix} p \\ q \end{bmatrix} = \begin{bmatrix} v_\alpha & v_\beta \\ v_\beta & -v_\alpha \end{bmatrix} \begin{bmatrix} i_\alpha \\ i_\beta \end{bmatrix} \quad \text{Eqn 3.6}$$

In the forthcoming explanation, the  $\alpha\beta$  currents will be formulated as functions of voltages, real power ( $p$ ) and reactive power ( $q$ ). This method can better explain the physical definition of powers in p-q theory. Based on **Eqn 3.6**, the current can be expressed in matrix as follows:

$$\begin{bmatrix} i_\alpha \\ i_\beta \end{bmatrix} = \frac{1}{\sqrt{v_\alpha^2 + v_\beta^2}} \begin{bmatrix} v_\alpha & v_\beta \\ v_\beta & -v_\alpha \end{bmatrix} \begin{bmatrix} p \\ q \end{bmatrix} \quad \text{Eqn 3.7}$$

According to **Eqn 3.7**, the instantaneous reactive current on the  $\alpha$  axis  $i_{\alpha q}$  and on the  $\beta$  axis  $i_{\beta q}$  can be calculated as follows:

$$i_{\alpha q} = \frac{v_\beta}{\sqrt{v_\alpha^2 + v_\beta^2}} q \quad \text{Eqn 3.8}$$

$$i_{\beta q} = -\frac{v_\alpha}{\sqrt{v_\alpha^2 + v_\beta^2}} q \quad \text{Eqn 3.9}$$

### 3.1.3 Application of p-q theory in STATCOM

According to the results in **3.1.2**, the algorithm of STATCOM to realize reactive power compensation through p-q theory can be expressed as the following block diagram

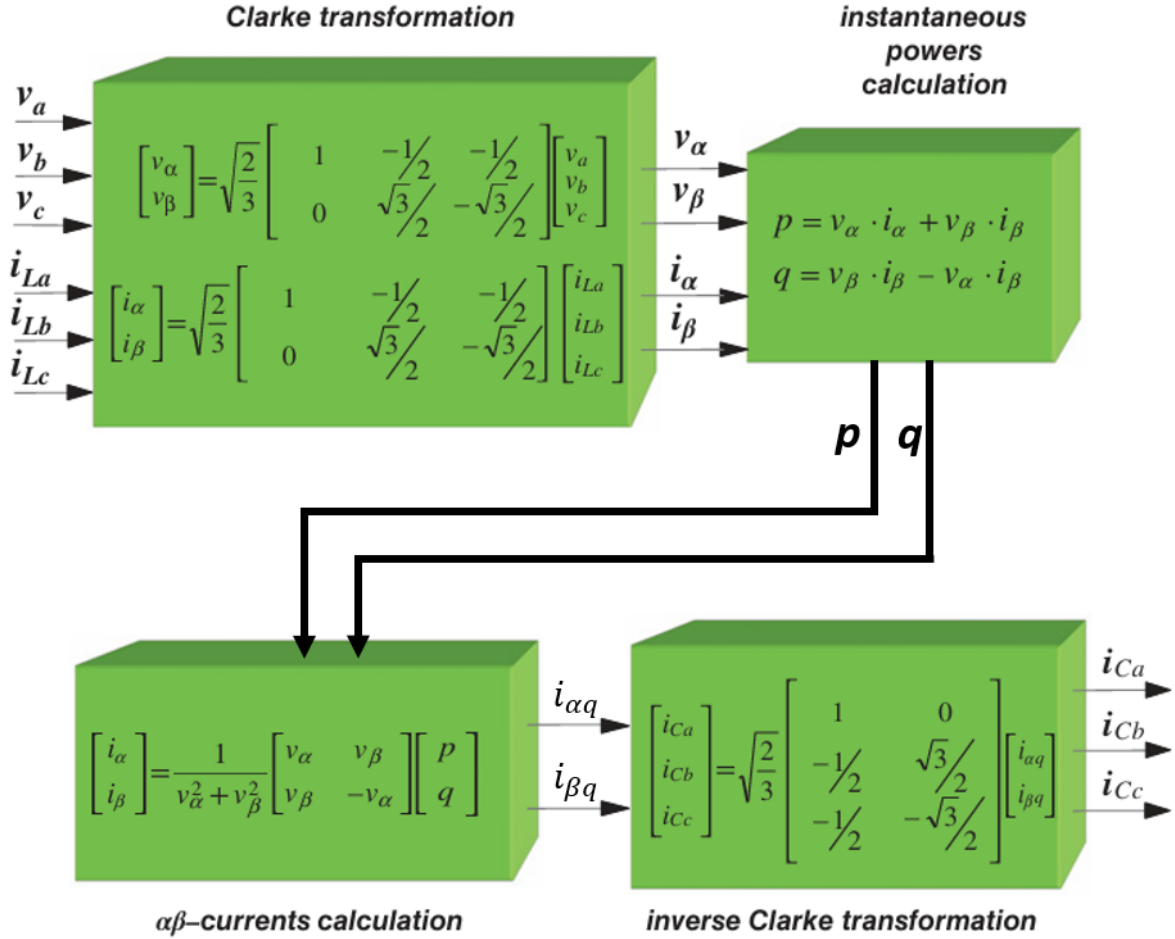


Figure 3.2 Block diagram of reactive power compensation in STATCOM [17]

Under linear load, STATCOM's reactive power compensation process is divided into four steps: Firstly, the three-phase voltage from the grid and the three-phase current from the load are measured and converted into instantaneous  $\alpha$  and  $\beta$  components by Clark transformation. It is worth noting that the detailed math expressions of Clark transformation and inverse Clark transformation are shown in the Figure 3.2, but in PLECS, the conversion between the abc and  $\alpha\beta$  coordinates can be implemented directly through the components. Therefore, this mathematical principle of Clark transformation and inverse Clark transformation are not explained in this thesis.

Secondly, based on Eqn 3.6, the real power ( $p$ ) and imaginary power ( $q$ ) can be calculated through  $v_\alpha, v_\beta, I_\alpha, I_\beta$  obtained in step1. The third step is about  $\alpha\beta$ -current calculation, the instantaneous reactive current on the  $\alpha$  axis ( $i_{\alpha q}$ ) and on the  $\beta$  axis ( $i_{\beta q}$ ) can be calculated based on the Eqn 3.8 and Eqn 3.9.

Finally, based on the inverse Clarke transformation, the  $i_{Ca}, i_{Cb}, i_{Cc}$  can be calculated from  $i_{\alpha q}$  and  $i_{\beta q}$  which are obtained in the step3. These three currents ( $i_{Ca}, i_{Cb}, i_{Cc}$ ) represent the reactive current of the three phases in the current controller.

## 3.2 STATCOM circuit modelled as an ideal voltage source

Before building a complete STATCOM circuit, STATCOM is first modelled as an ideal voltage source. According to the application of p-q theory in STATCOM in 3.1.3, the algorithm is implemented in PLECS. This section is roughly divided into two parts, the first part is to build and analyse the circuit in PLECS, the second part is to verify the circuit.

### 3.2.1 Schematic

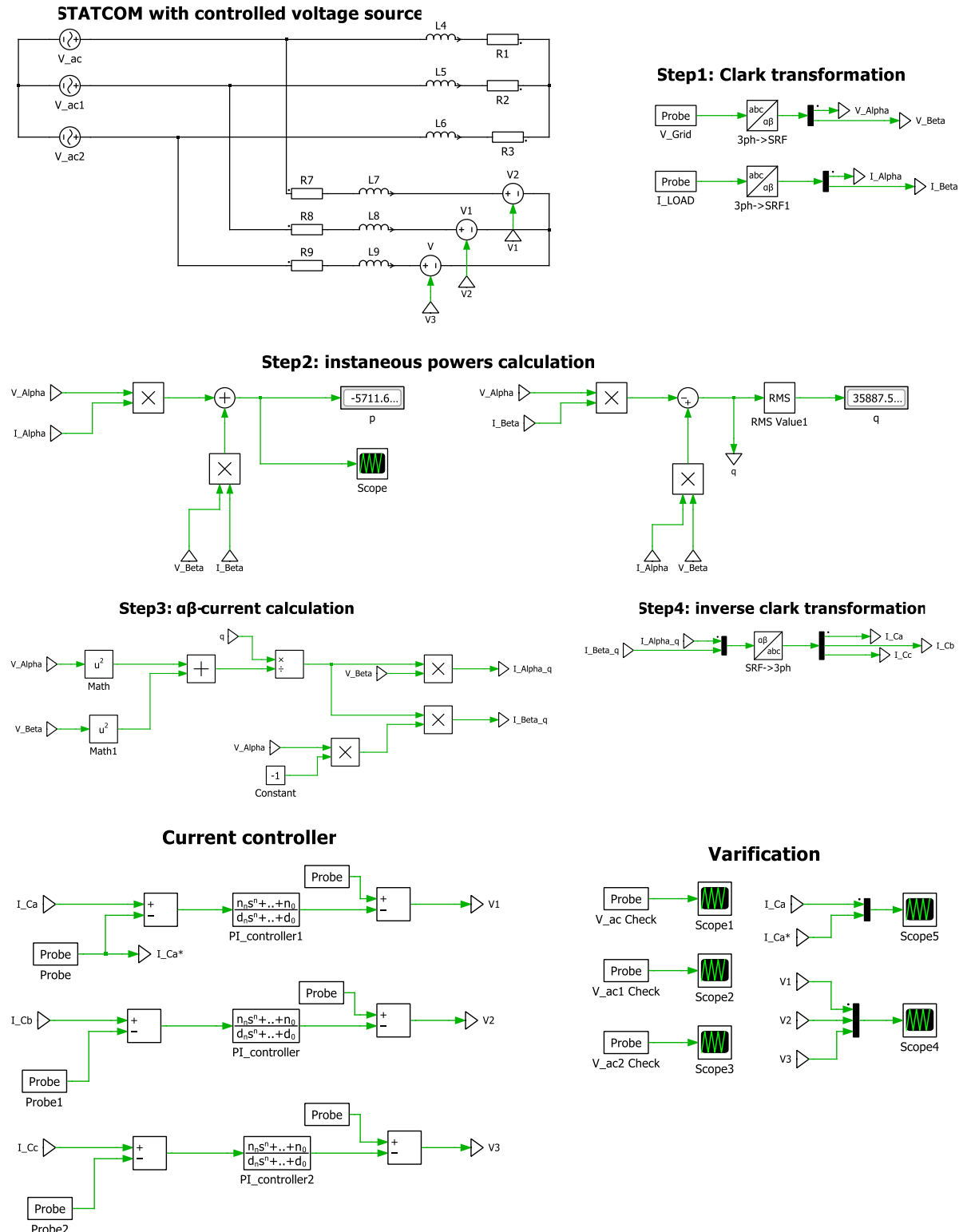


Figure 3.3 STATCOM with controlled voltage source

In the main circuit, three-phase grid is connected in series with linear load, which is represented by resistance and inductance in series. STATCOM is modelled as an ideal voltage source placed in parallel between three-phase grid and linear load.

STATCOM's reactive power compensation algorithm is divided into four steps: In the first step, the three-phase voltage from the grid and the three-phase current from the load are measured and converted into instantaneous  $\alpha$  and  $\beta$  components by Clark transformation. Secondly, the real power ( $p$ ) and imaginary power ( $q$ ) can be calculated through 'V\_Alpha', 'V\_Beta', which are obtained in step1. It worth noting that although the real power is calculated, it is not used in the reactive power compensation algorithm.

The third step is about  $\alpha\beta$ -current calculation. Based on the imaginary power ( $q$ ), 'V\_Alpha' and 'V\_Beta' obtained in step1 and step2, the instantaneous reactive current on the  $\alpha$  axis ( $I_{Alpha\_q}$ ) and on the  $\beta$  axis ( $I_{Beta\_q}$ ) can be calculated. In the last step, the ' $I_{Ca}$ ', ' $I_{Cb}$ ', ' $I_{Cc}$ ' can be calculated from ' $I_{Alpha\_q}$ ' and ' $I_{Beta\_q}$ ' through the inverse Clarke transformation. These three currents (' $I_{Ca}$ ', ' $I_{Cb}$ ', ' $I_{Cc}$ ') represent the reactive current of each phases in the current controller, which is designed in the **Chapter 2: Three phase inverter**.

### 3.2.2 Verification

In order to better verify the effect of STATCOM on the circuit, the switch block is added to the circuit. Therefore, the main circuit can be modified as follows:

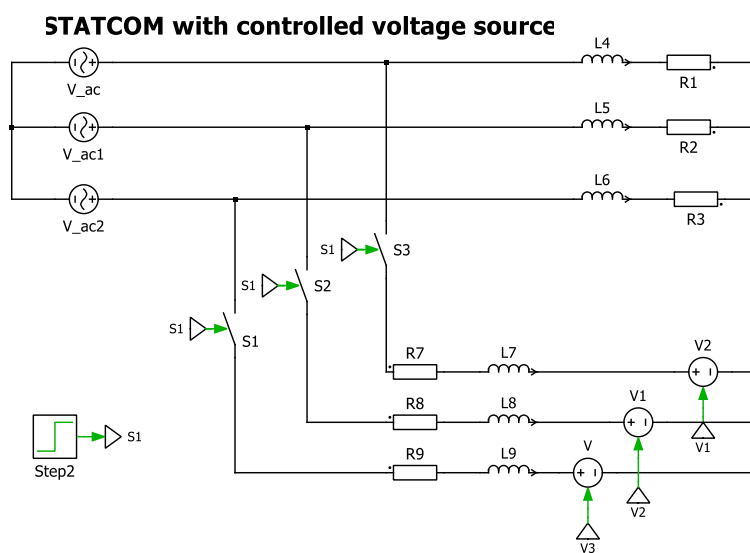
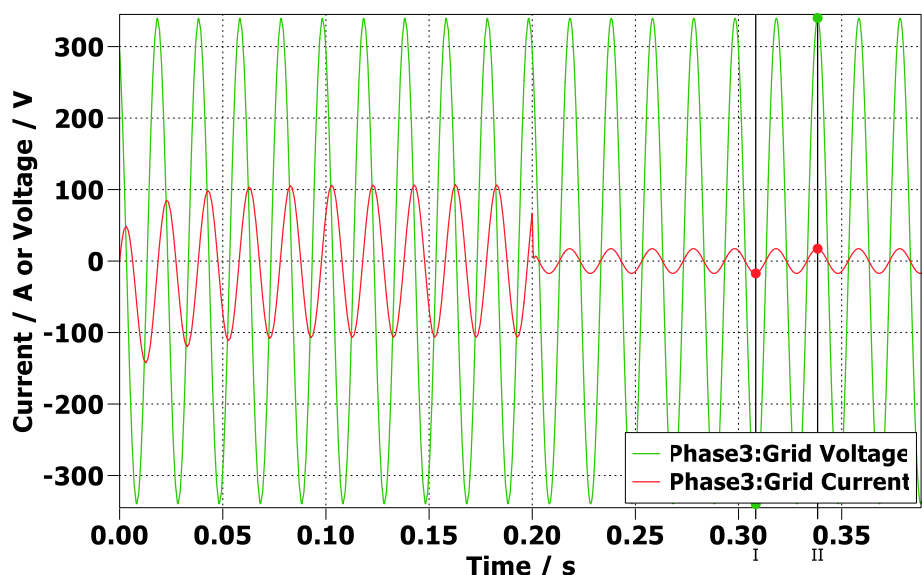
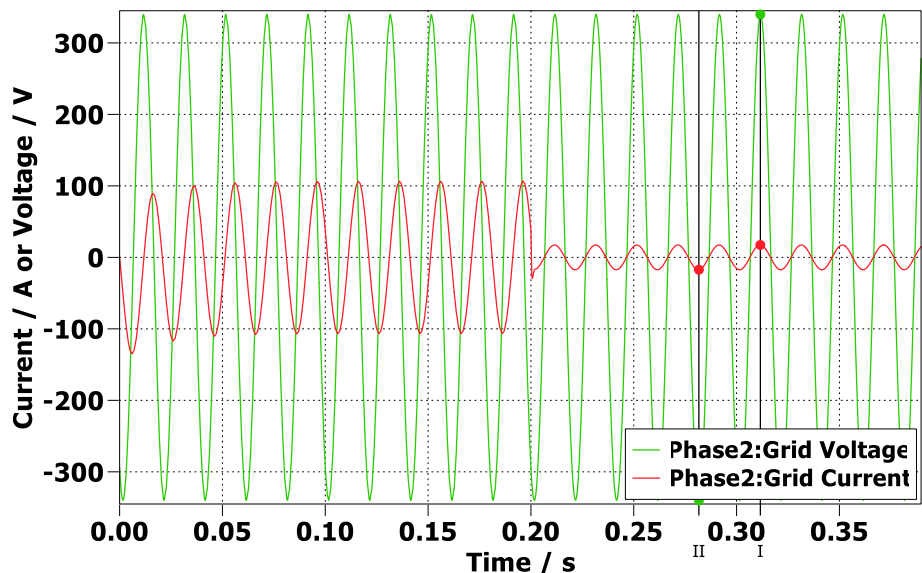
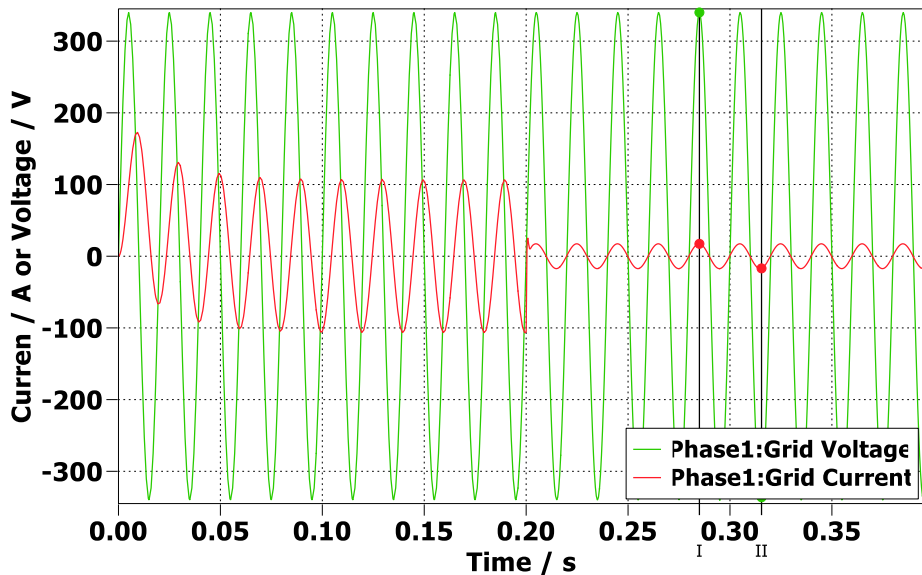


Figure3.4 Main circuit with switching model

In Figures 3.4, the step time of blocks" step2 'is set to 0.2s, which means that the STATCOM and current controller will connect to the circuit after 0.2 seconds.

#### 3.2.2.1 Reactive power compensation verification

In each phase, the grid voltage and grid current are compared as follows:



As shown in Figures 3.5, 3.6, and 3.7, at every phase before STATCOM is connected to the circuit, there is a phase difference between the grid voltage and the grid current. After STATCOM is connected to the circuit, as indicated by the cursor in the figure, the grid current and grid voltage reach the minimum and maximum values at the same time, which also means that the grid current and grid voltage are in the same phase state. Therefore, it can be proved that after STATCOM is connected to the circuit, the grid only provides active power, and the reactive power in the load is all provided by STATCOM.

### 3.2.2.2 Current controller verification

In order to better verify current controller on the circuit, the switch blocks are added to the current controller as well. The diagram is shown below:

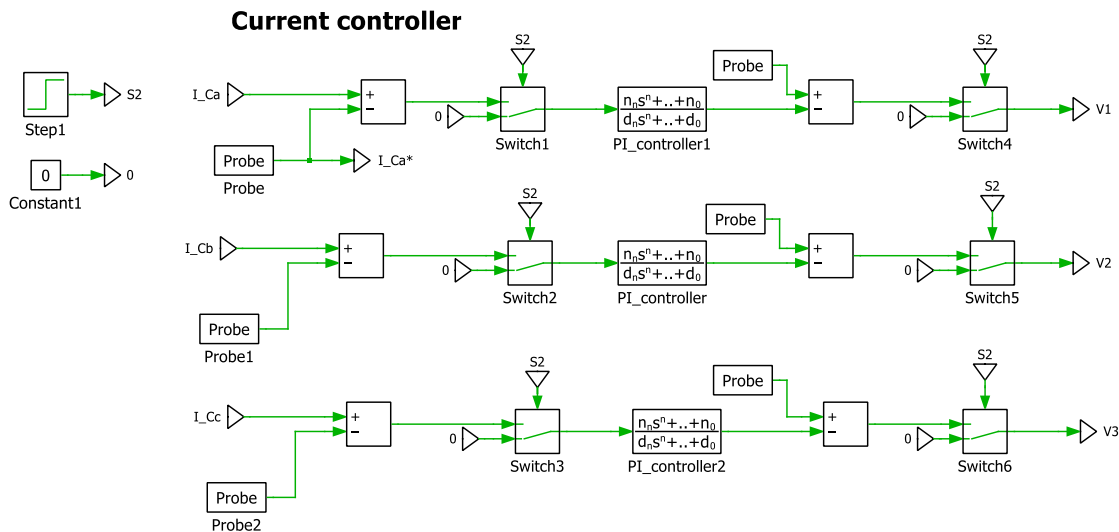


Figure 3.8 Current controller with switching model

In order to verify whether the current controller works properly, the connection time of the current controller to the circuit is also set to 0.5s. The current controller's inputs in a certain phase are compared as follows:

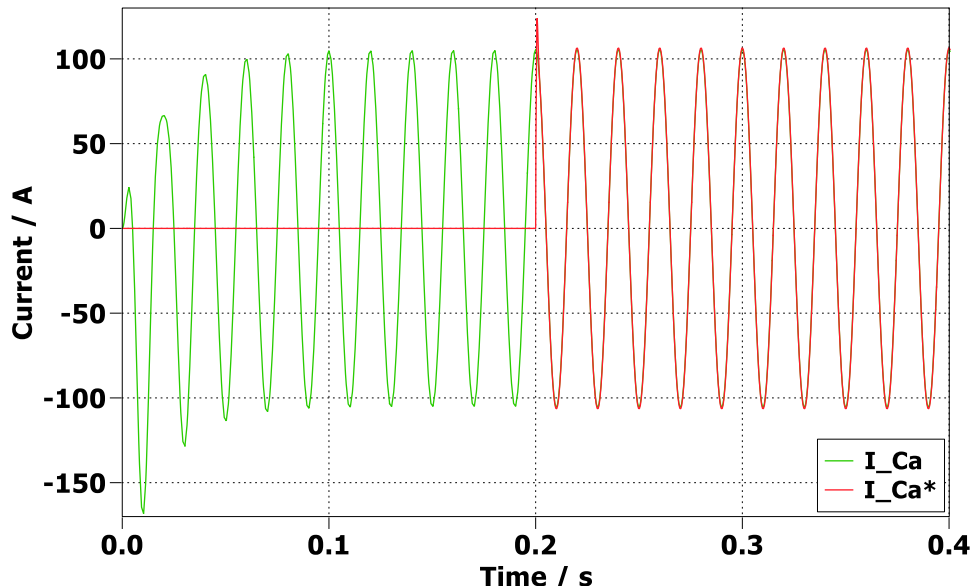
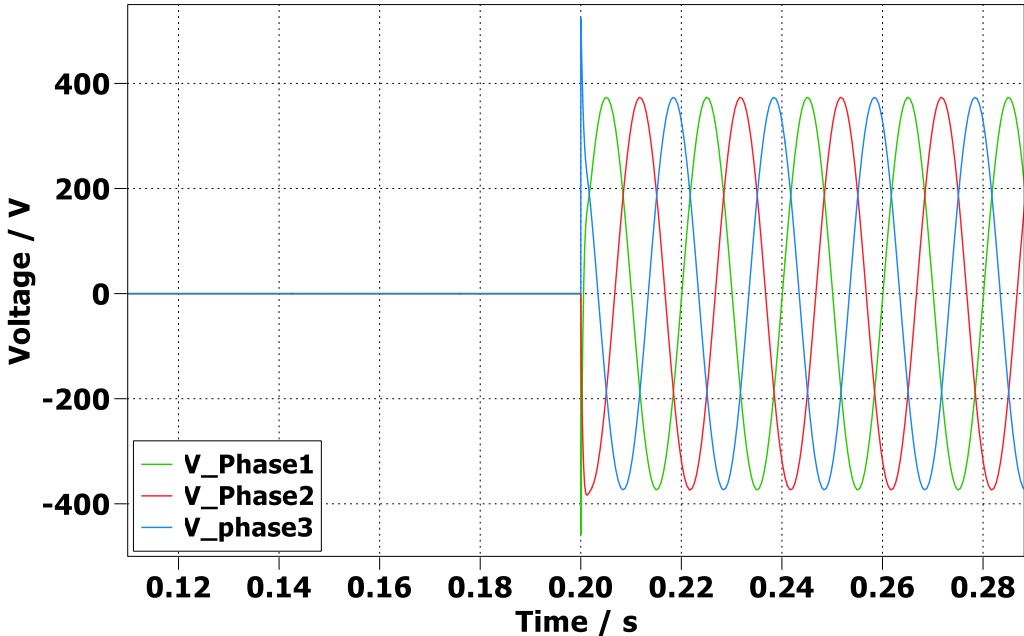


Figure 3.9 Current controller input comparison in a certain phase

In PWM modulation, the desired three-phase voltage analogue signal generated from current controller are compared as follows:



*Figure 3.10 Current controller input comparison in a certain phase*

It can be seen from *Figure 3.9* that, at a certain phase, after STATCOM is connected to the circuit, the current generated by STATCOM is basically consistent with the reference current obtained by Clark inverse conversion.

According to *Figure 3.10*, before STATCOM is connected to the circuit, the three-phase voltage generated by the current controller is equal to 0. After STATCOM is connected to the circuit, the magnitude and phase of the three-phase voltage generated by the current controller are changed to achieve the reactive power compensation for load., the above results prove that the current controller works as expected.

### 3.3 Fully controlled 3 phase STATCOM with linear load

In this section, the ideal voltage source in the STATCOM circuit is replaced with a full-bridge inverter. After applying the design of DC voltage controller and current controller in **Chapter 2 three-phase inverter**, a fully controllable three-phase STATCOM with linear load is successfully constructed. This section is roughly divided into two parts, the first part is to build and analyse the circuit in PLECS, the second part is to verify the circuit.

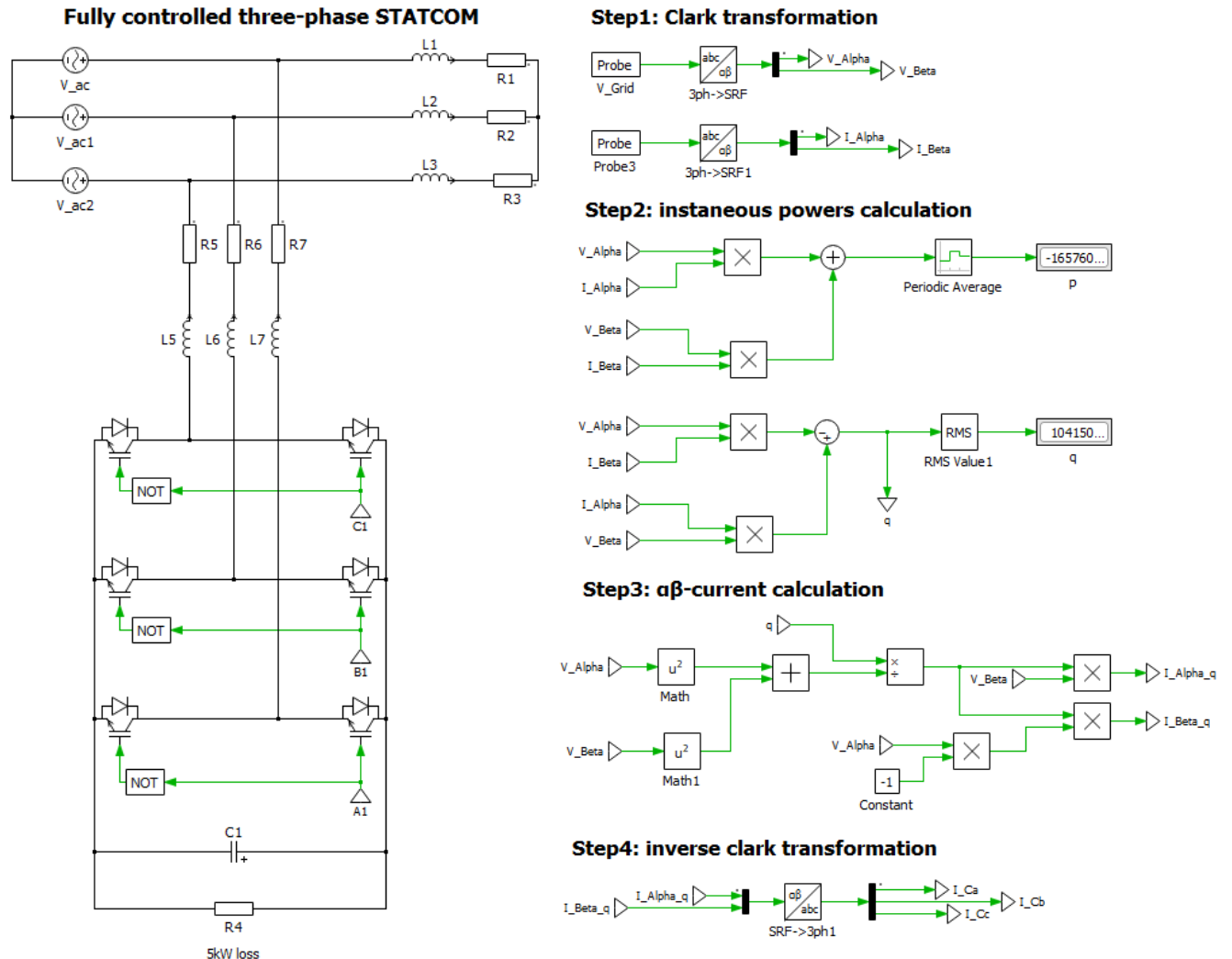
### 3.3.1 Specification

The system design specifications of fully controlled three-phase STATCOM are shown below:

Table 3.2. System design specifications

Term	Symbol	Value
Inductor in load	$L_1, L_2, L_3$	0.001H
Resistor in load	$R_1, R_2, R_3$	0.5Ω
Inductor in filter	$L_5, L_6, L_7$	0.001H
Resistor in filter	$R_5, R_6, R_7$	0.1 Ω
Capacitor in STATCOM	$C_1$	0.01F
Power loss in STATCOM	$R_4$	144.5Ω
Fundamental frequency	$f_B$	50Hz
Inverter Switching Frequency	$f_{sw}$	10KHz
DC voltage	$V_{DC}$	850V

### 3.3.2 Schematic



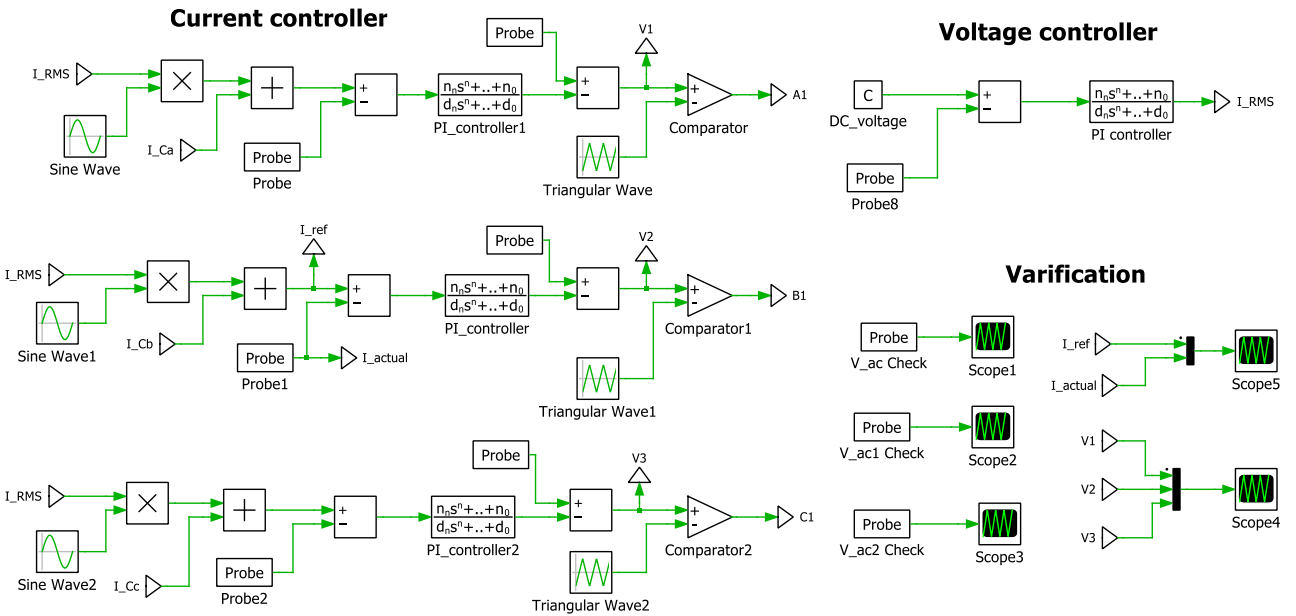


Figure 3.11 Fully controlled 3-phase STATCOM with linear load

In the main circuit, three-phase grid is connected in series with linear load, which is represented by resistance and inductance in series. A fully controlled 3-phase STATCOM in switching model is placed in parallel between three-phase grid and linear load.

STATCOM's reactive power compensation algorithm is divided into four steps: In the first step, the three-phase grid voltage and the three-phase load current are measured and converted into instantaneous  $\alpha$  and  $\beta$  components by Clark transformation. Secondly, the real power ( $p$ ) and imaginary power ( $q$ ) can be calculated through 'V\_Alpha', 'V\_Beta', which are obtained in step1. It worth noting that although the real power is calculated, it is not used in the reactive power compensation algorithm.

The third step is about  $\alpha\beta$ -current calculation. Based on the obtained imaginary power ( $q$ ), 'V\_Alpha' and 'V\_Beta', the instantaneous reactive current on the  $\alpha$  axis ( $I_{Alpha\_q}$ ) and on the  $\beta$  axis ( $I_{Beta\_q}$ ) can be calculated. In the last step, the ' $I_{Ca}$ ', ' $I_{Cb}$ ', ' $I_{Cc}$ ' can be calculated from ' $I_{Alpha\_q}$ ' and ' $I_{Beta\_q}$ ' through the inverse Clarke transformation. These three currents (' $I_{Ca}$ ', ' $I_{Cb}$ ', ' $I_{Cc}$ ') represent the reactive current of each phases in the current controller.

In addition, the voltage controller is applied to STATCOM to stabilize the DC voltage at 850V. The output of voltage controller is ( $I_{RMS}$ ), which is converted into AC current of different phases by multiplying the sin wave of magnitude  $\sqrt{2}$  with different phases. These AC currents are added to the reactive currents (' $I_{Ca}$ ', ' $I_{Cb}$ ', ' $I_{Cc}$ ') respectively to produce a reference current for the current controller in each phase. It worth noting that the design process of current controller and voltage controller included in **Chapter2: The three-phase inverter**.

### 3.3.3 Verification

In order to better verify the effect of STATCOM on the circuit, the switch blocks and an another load are added to the circuit. Therefore, the main circuit can be modified as follows:

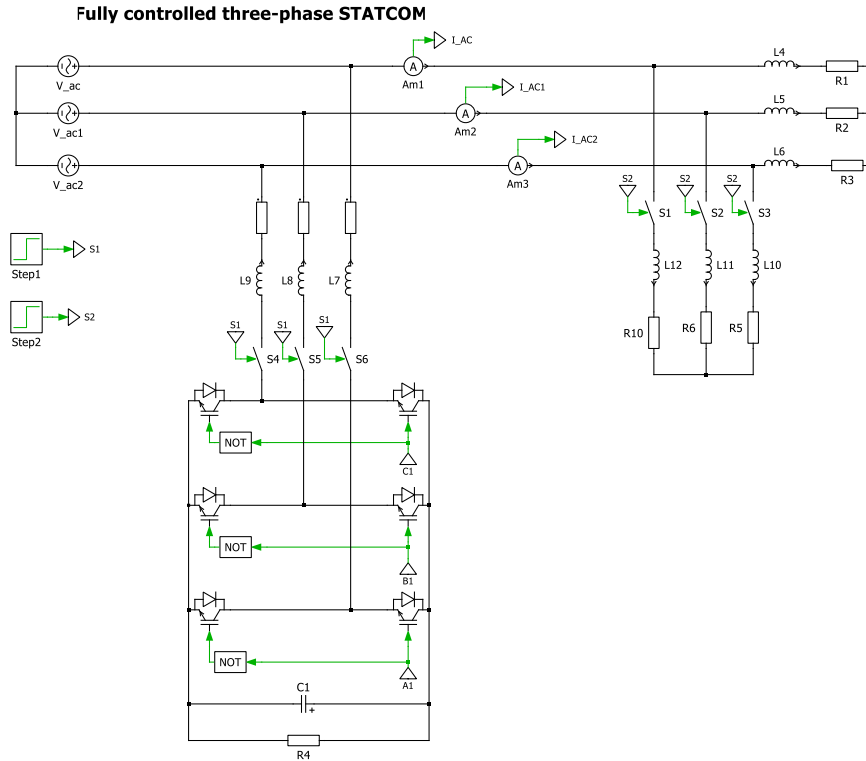


Figure 3.12 The main circuit containing the switch and two loads

In Figures 3.12, the step times of ‘Step 1’ and ‘Step 2’ are set to 0.2s and 0.4s respectively, which means that the STATCOM is connected to the circuit after 0.2 seconds, and another load is connected to the circuit after 0.4 seconds.

#### 3.3.3.1 Reactive power compensation verification

In each phase, the grid voltage and grid current are compared as follows:

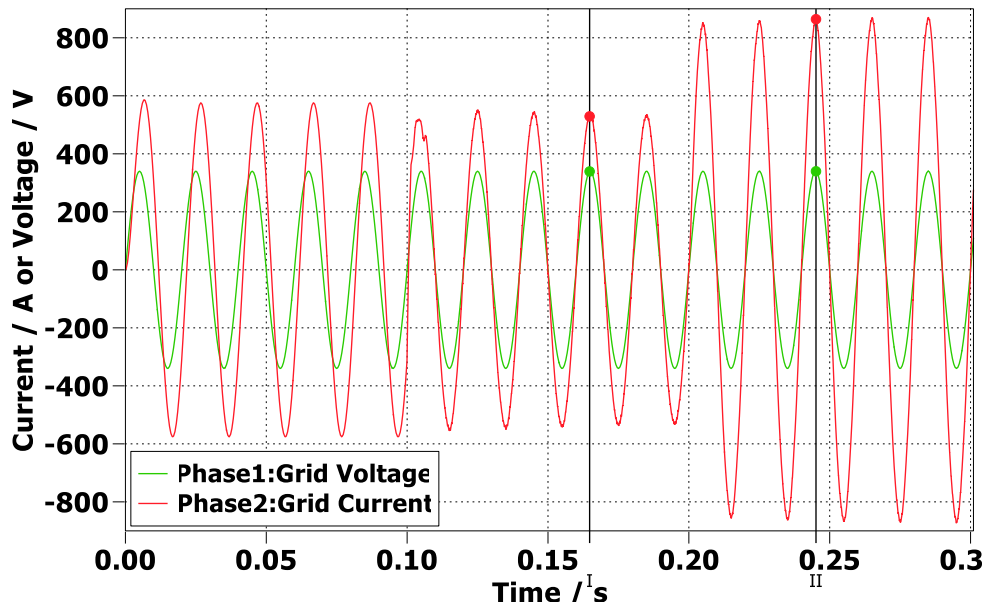


Figure 3.13 Comparison between grid voltage and grid current in phase 1.

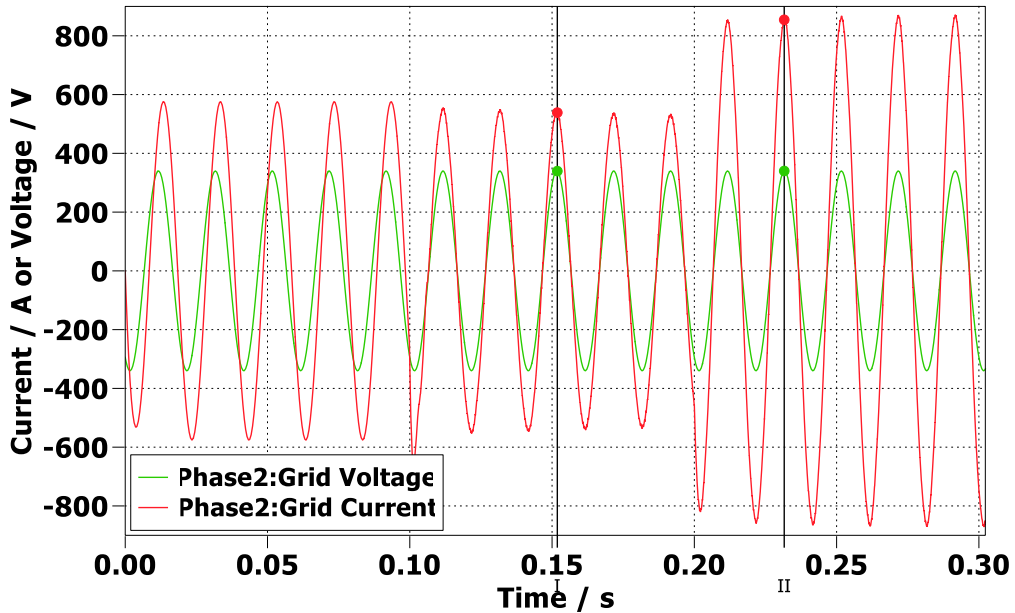


Figure 3.14 Comparison between grid voltage and grid current in phase 2.

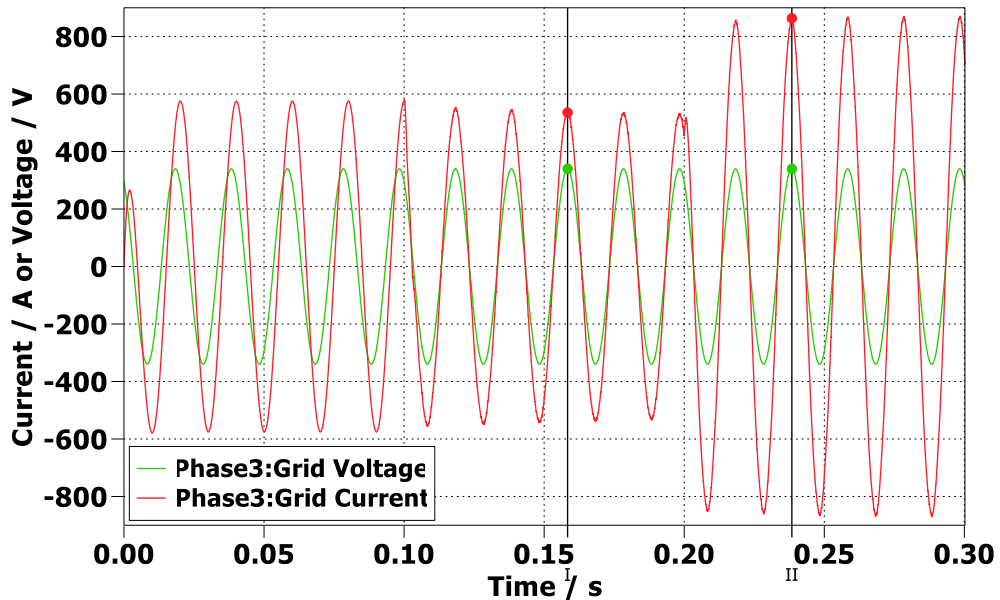


Figure 3.15 Comparison between grid voltage and grid current in phase 3.

As shown in Figures 3.13, 3.14, and 3.15, at each phase before STATCOM is connected to the circuit, there is a phase difference between the grid voltage and the grid current, which means that during this period, the grid provides both active and reactive power.

After STATCOM is connected to the circuit, as indicated by the cursor in the figure, the grid current and grid voltage reach the minimum and maximum values at the same time, which also means that the grid current and grid voltage are in the same phase state. After 0.2 seconds, another load is connected to the circuit, and the grid voltage and grid current remain in phase. Therefore, it can be proved that after STATCOM is connected to the circuit, the grid only provides active power, and the reactive power in the load is all provided by STATCOM.

### 3.3.3.2 Current controller verification

In order to better verify current controller on the circuit, the switch blocks are added to the current controller as well. The diagram is shown below:

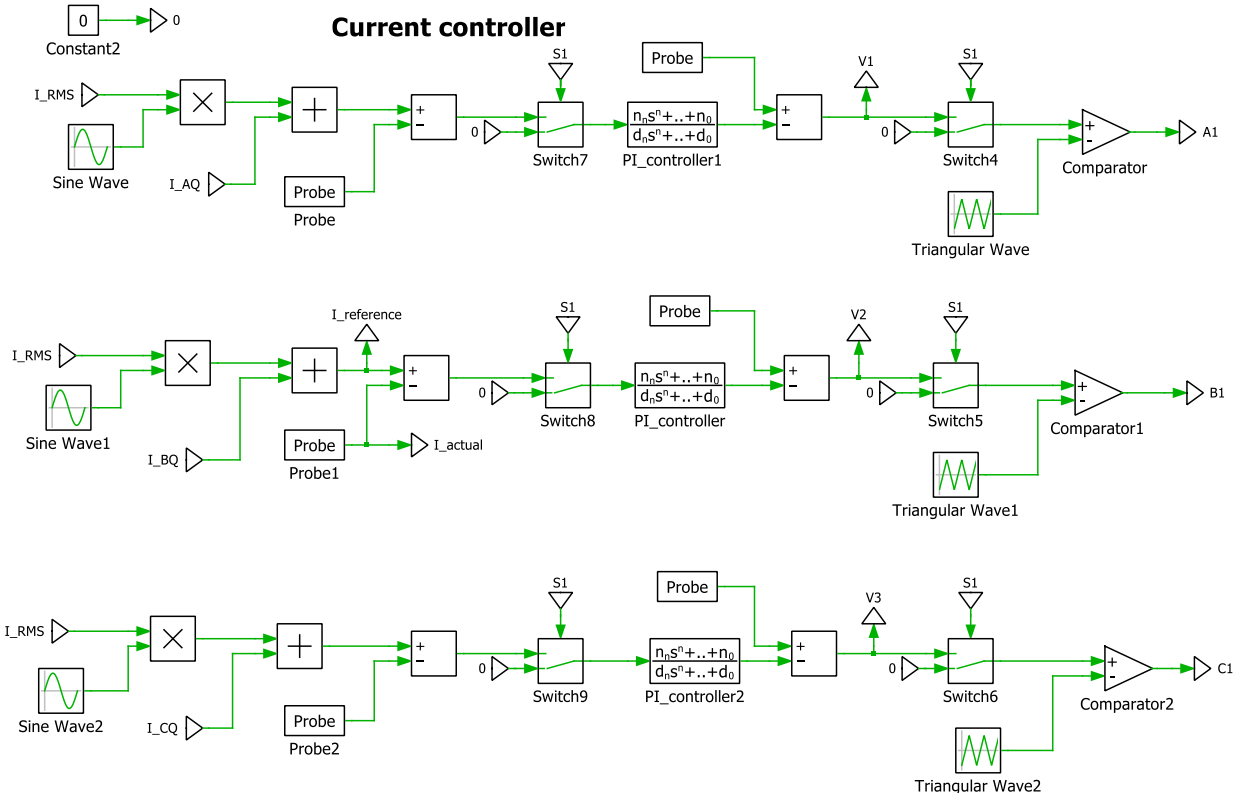


Figure 3.16 Current controller with switch blocks

In order to verify whether the current controller works properly, the connection time of the current controller to the circuit is also set to 0.1s. The current controller's inputs in a certain phase are compared as follows:

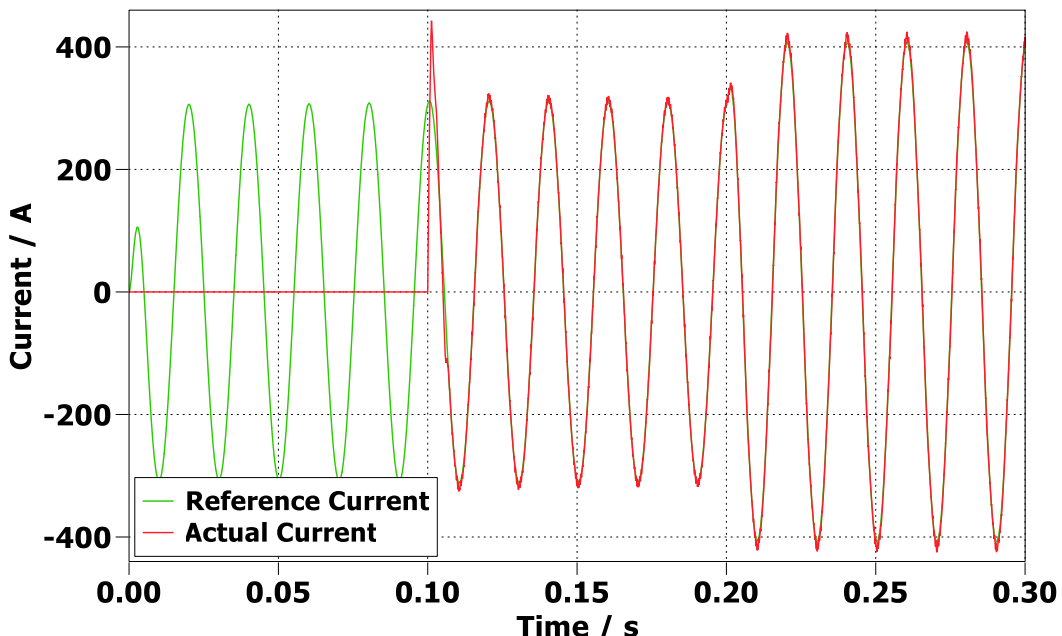


Figure 3.17 Current controller input comparison in a certain phase

In PWM modulation, the desired three-phase voltage analogue signal generated from current controller are compared as follows:

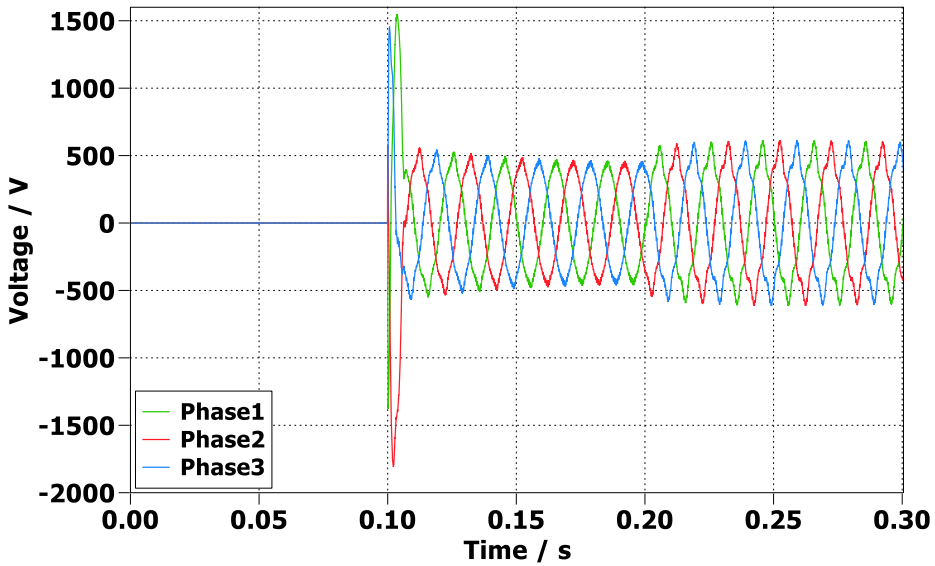


Figure 3.18 Current controller input comparison in a certain phase

It can be seen from Figure 3.17 that, at a certain phase, after STATCOM is connected to the circuit, the current generated by STATCOM is basically consistent with the reference current. After two seconds, another load is added to the circuit, but the actual current still matches the reference current. According to Figure 3.18, before STATCOM is connected to the circuit, the three-phase voltage generated by the current controller is equal to 0. After STATCOM is connected to the circuit, the magnitude and phase of the three-phase voltage generated by the current controller are changed to achieve the reactive power compensation for load. After two seconds later, another load is added to the circuit, and the magnitude of the three-phase voltage changes accordingly to achieve the reactive power compensation for both loads. Therefore, the above results prove that the current controller works as expected.

### 3.3.3.3 Voltage controller verification

To verify the voltage controller, the DC voltage and capacitor voltage is compared as follows:

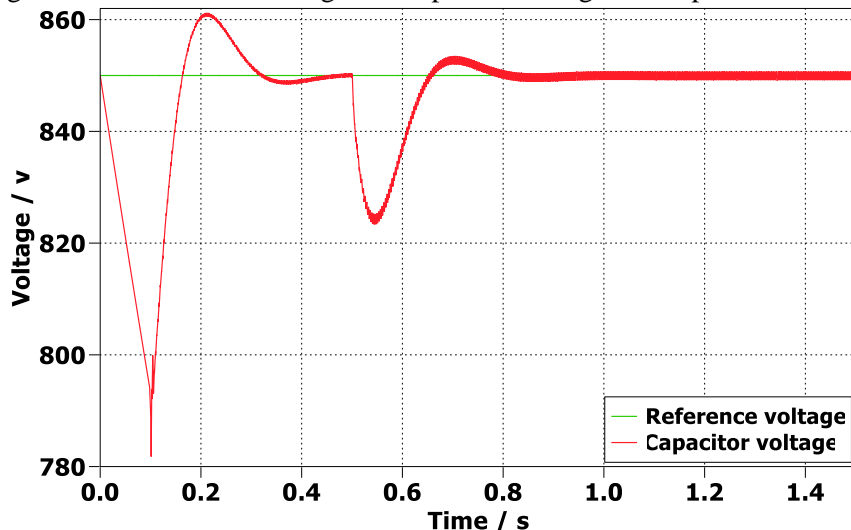


Figure 3.19 Comparison between DC voltage and capacitor voltage

As shown in 3.19, after STATCOM is connected, the voltage of the capacitor is almost consistent with the set DC voltage at steady state. After 0.8 seconds, when another load is attached, the capacitor voltage is still consistent with the DC voltage after a brief fluctuation. Therefore, the voltage controller works as expected.

## 4 CHAPTER4: STATCOM with non-linear load

In the previous chapter, a fully controlled 3 phase STATCOM with linear load was successfully built. In this chapter, linear load will be replaced by non-linear load, which means that the grid's current is chaotic and irregular in its original state. By updating the compensation algorithm and designing a fifth-order Butterworth filter, a more advanced STATCOM will be built in this chapter to implement reactive power and harmonics compensation. This chapter is basically divided into about three parts, updating the compensation algorithm, designing the filter and redesigning the controller, building and verifying the circuit in PLECS.

### 4.1 p-q theory for shunt current compensation

An essential use of the p-q theory is in compensating unwanted currents. *Figure4.1* depicts the fundamental concept of shunt current compensation. It presents a source that supplies power to a nonlinear load, which is compensated by a shunt compensator. For ease of understanding, it's assumed that the shunt compensator functions as a three-phase, controlled current source capable of drawing any predetermined set of current references ( $i_{Ca}^*, i_{Cb}^*, i_{Cc}^*$ ) [18]

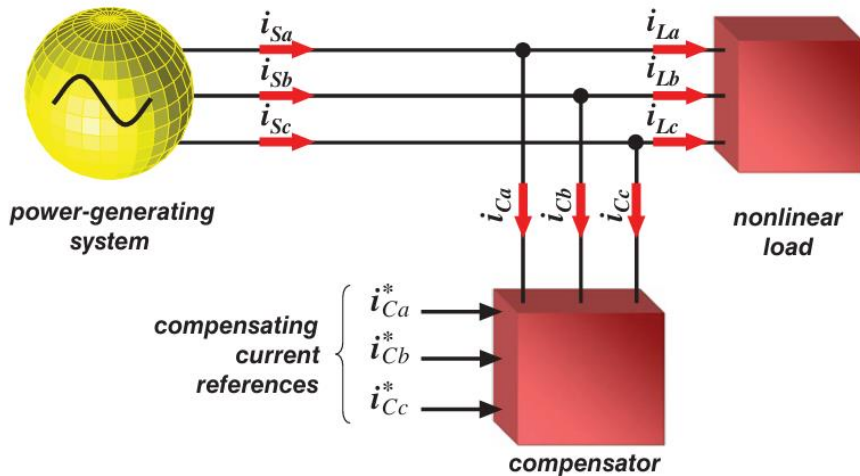


*Figure4.1 The Basic principle of shunt current compensation.* [18]

### 4.2 Active Filters for Constant Power Compensation

It worth noting that all the calculations in this section are derived from 'Shunt Active Filters' in the book 'Instantaneous Power Theory and Applications to Power Conditioning'. [18] The calculated active power ( $p$ ) of the load can be separated into its average ( $\bar{p}$ ) and oscillating ( $\tilde{p}$ ) parts. Likewise, the load imaginary power ( $q$ ) can be separated into its average ( $\bar{q}$ ) and oscillating ( $\tilde{q}$ ) parts. To maintain a constant instantaneous power

draw from the source, it is advisable to install the STATCOM as close as possible to the nonlinear load to compensate for its oscillating active power ( $\tilde{p}$ ). It is important to note that this setup is a three-phase system without a neutral wire, resulting in zero zero-sequence power. Therefore, the STATCOM's role is to provide the oscillating component of the instantaneous active current required by the load.

The oscillating part of the instantaneous active current on the  $\alpha$  axis  $i_{\alpha\tilde{p}}$ :

$$i_{\alpha\tilde{p}} = \frac{v_\alpha}{v_\alpha^2 + v_\beta^2} (-\tilde{p}) \quad \text{Eqn 4.1}$$

The oscillating part of the instantaneous active current on the  $\beta$  axis  $i_{\beta\tilde{p}}$ :

$$i_{\beta\tilde{p}} = \frac{v_\beta}{v_\alpha^2 + v_\beta^2} (-\tilde{p}) \quad \text{Eqn 4.2}$$

The inclusion of negative signs in the compensating powers highlights that the compensator is intended to generate a compensating current that exactly counteracts the undesirable powers drawn by the nonlinear load. If the current output by STATCOM produces exactly  $(-\tilde{p})$  of the load, the power system will only provide the average of the active power ( $\bar{p}$ ) of the load. The STATCOM should also compensate for the instantaneous reactive currents  $i_{\alpha q}$  and  $i_{\beta q}$ .

The instantaneous reactive current on the  $\alpha$  axis  $i_{\alpha q}$ :

$$i_{\alpha q} = \frac{v_\beta}{v_\alpha^2 + v_\beta^2} (-q) \quad \text{Eqn 4.3}$$

The instantaneous reactive current on the  $\beta$  axis  $i_{\beta q}$ :

$$i_{\beta q} = \frac{-v_\alpha}{v_\alpha^2 + v_\beta^2} (-q) \quad \text{Eqn 4.4}$$

The total imaginary power being compensated is represented as  $(-q = -\bar{q} - \tilde{p})$ , where the minus sign is used for the same reason as the active oscillating power compensation. By compensating both the oscillating active power ( $\tilde{p}$ ) and imaginary power ( $q$ ) of the load, the STATCOM ensures that the power system only supplies the average active power ( $\bar{p}$ ) of the load.

Therefore, from the point of view of ‘power transfer’, this strategy of constant instantaneous power control can achieve compensation even under non-sinusoidal or unbalanced system voltages. The concept is visualized in Figure 4.2, which illustrates the approach using “ $\alpha\beta$  wires” and the p-q theory framework.

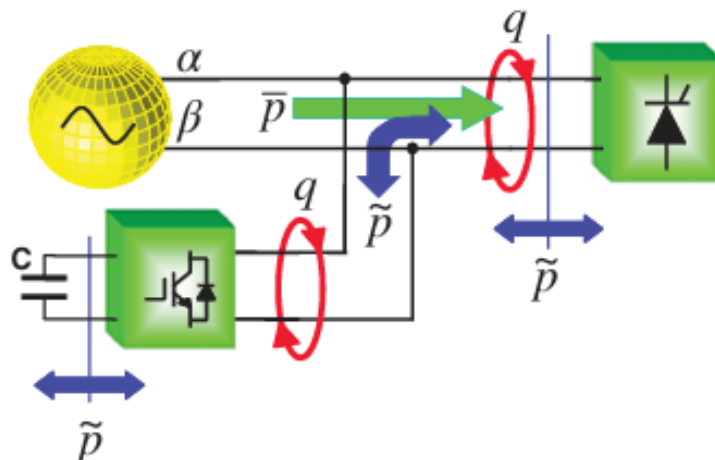


Figure 4.2 Power flow provided by STATCOM [18]

In practical implementations, the separation between the average active power ( $\bar{p}$ ) and the oscillating active power ( $\tilde{p}$ ) from the total active power ( $p$ ) is achieved using a low-pass filter. The selection of the low-pass filter and its cutoff frequency is important due to the dynamic characteristics that can cause compensation errors during transient states. However, the inherent time delay introduced by the low-pass filter can significantly impair the performance of a STATCOM during transients. This issue will be further clarified later in **4.4 Five-order Butterworth filter design**. In the project, a fifth-order Butterworth low-pass filter with a 150 Hz cutoff frequency has been designed to separate  $\bar{p}$  from  $p$ .

For digital implementations, the method of removing the average power ( $p$ ) is very straightforward. The oscillating active power can be simply calculated as the difference ( $\tilde{p} = p - \bar{p}$ ). Depending on the spectral components of  $\tilde{p}$  that need to be compensated, a lower cutoff frequency for the low-pass filter may be necessary. *Figure 4.3* illustrates the complete control algorithm for a three-phase STATCOM that compensates for both the oscillating active power and the imaginary power of the non-linear load.

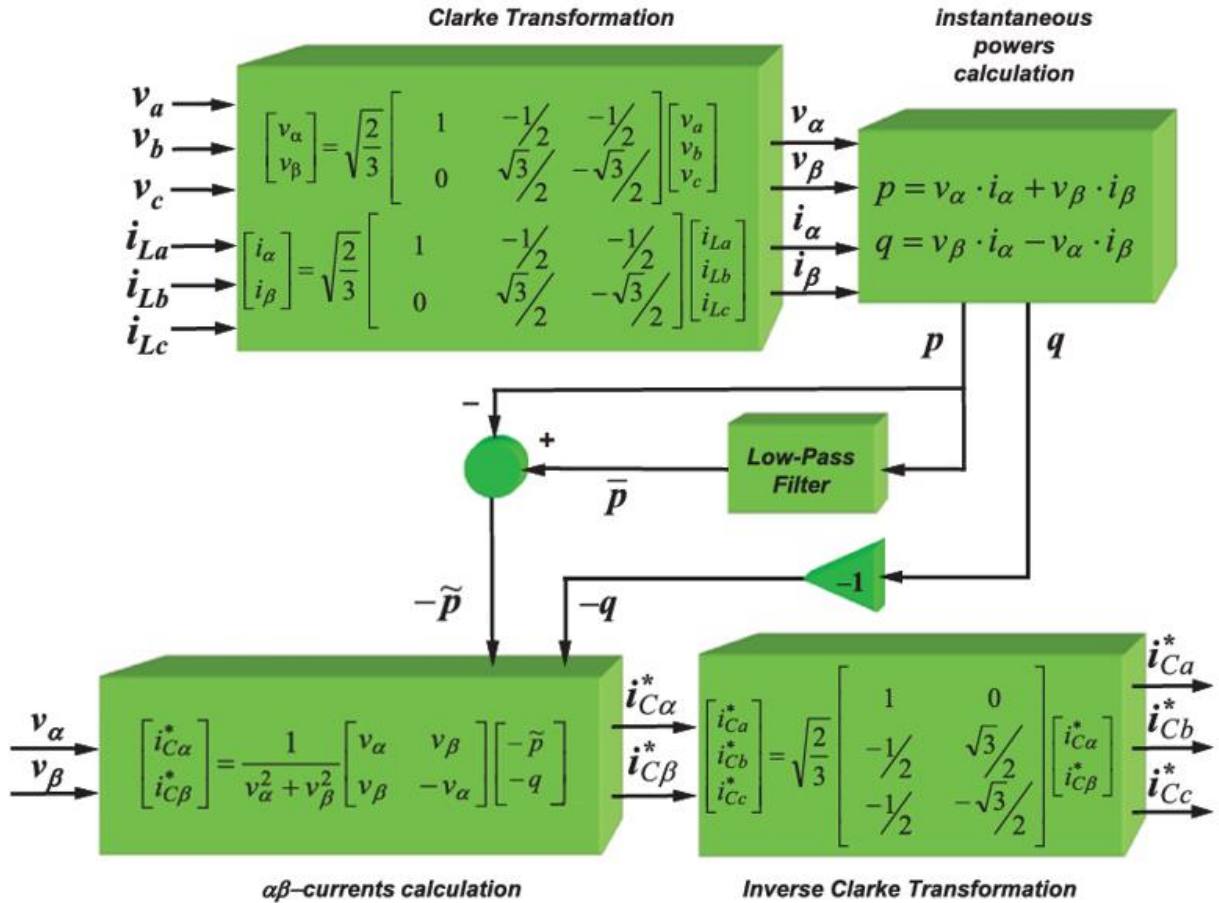


Figure 4.3 Compensation algorithm in STATCOM with nonlinear load [18]

Based on the oscillating active power ( $\tilde{p}$ ) and the load imaginary power ( $q$ ), the instantaneous reactive current on the  $\alpha$  axis ( $i_{C\alpha}^*$ ) and on the  $\beta$  axis ( $i_{C\beta}^*$ ) can be calculated through  $\alpha\beta$ -current calculation.

Finally, according to the inverse Clarke transformation, the  $i^*_{c\alpha}$ ,  $i^*_{c\beta}$ ,  $i^*_{c\gamma}$  can be calculated from  $i^*_{c\alpha}$  and  $i^*_{c\beta}$ . These three currents ( $i_{c\alpha}$ ,  $i_{c\beta}$ ,  $i_{c\gamma}$ ) represent the reactive current of the three phases in the current controller.

The voltage controller is also added to the control strategy in a real implementation. The purpose is to continuously extract switching loss and ohmic losses ( $\bar{p}_{loss}$ , not shown in *Figure 4.3*) of the PWM converters from the power system. Without voltage controller, the energy required would have to be supplied by the DC capacitor, which would result in its continuous discharge.

### 4.3 Five-order Butterworth filter design

In practical implementations, the separation between the average active power ( $\bar{p}$ ) and the oscillating active power ( $\tilde{p}$ ) from the total active power ( $p$ ) is achieved using a low-pass filter. In the project, a fifth-order Butterworth low-pass filter with a 150 Hz cutoff frequency is selected. Compared to lower order filters, fifth-order Butterworth low-pass filter can offer a sharper cutoff slope and better attenuation of unwanted frequencies. It provides a steeper attenuation beyond the cutoff frequency, improving the isolation of desired frequency ranges with minimal passband ripple. [19] This makes it particularly effective for STATCOM which requires precise frequency separation and minimal signal distortion.

In radians, the cutoff frequency can be expressed as follows:

$$\omega_c = 150 \text{Hz} * 2\pi = 9.42 * 10^2 \text{rad/s} \quad \text{Eqn 4.4}$$

The fifth-order Butterworth filter is composed of two second-order filters and one first-order filter in series.

In a first-order low pass filter, the ratio of output power to input power can be expressed as follows:

$$\frac{P_o}{P_{in}} = \frac{1}{\frac{s}{\omega_c} + 1} \quad \text{Eqn 4.5}$$

In a second-order low pass filter, the ratio of output power to input power can be expressed as follows:

$$\frac{P_o}{P_{in}} = \frac{1}{\frac{s^2}{\omega_c^2} + \frac{1}{Q\omega_c} + 1} \quad \text{Eqn 4.6}$$

In order to design higher order filters, the polynomials in *Figure 4.4* is generally used.

<b>n</b>	<b>Factors of Polynomial <math>B_n(s)</math></b>
1	$(s + 1)$
2	$(s^2 + 1.4142s + 1)$
3	$(s + 1)(s^2 + s + 1)$
4	$(s^2 + 0.7654s + 1)(s^2 + 1.8478s + 1)$
5	$(s + 1)(s^2 + 0.6180s + 1)(s^2 + 1.6180s + 1)$
6	$(s^2 + 0.5176s + 1)(s^2 + 1.4142s + 1)(s^2 + 1.9319s + 1)$
7	$(s + 1)(s^2 + 0.4450s + 1)(s^2 + 1.2470s + 1)(s^2 + 1.8019s + 1)$
8	$(s^2 + 0.3902s + 1)(s^2 + 1.1111s + 1)(s^2 + 1.6629s + 1)(s^2 + 1.9616s + 1)$

*Figure 4.4 Factor of polynomials in  $n^{th}$  order Butterworth filter [20]*

It worth noting that In the polynomials table, the cutoff frequency ( $\omega_c$ ) is assumed to be 1 rad/sec. [20] Therefore, when the order equal to five, the quality factor of these two second-order filters can be simply calculated as follows:

$$\begin{cases} s^2 + \frac{1}{Q_2}s + 1 = s^2 + 0.6180s + 1 \\ s^2 + \frac{1}{Q_2}s + 1 = s^2 + 1.6180s + 1 \end{cases} \rightarrow \begin{cases} Q_1 = \frac{1}{0.6180} = 1.6181 \\ Q_2 = \frac{1}{1.6180} = 0.6180 \end{cases} \quad \text{Eqn 4.7}$$

Based on the cut-off frequency and qualifiers, the transfer functions of the two second-order filters can be expressed as follows:

$$\begin{cases} H_1(s) = \frac{1}{\frac{s^2 + \frac{1}{Q_1} * \frac{s}{\omega_c} + 1}{\omega_c^2}} = \frac{1}{\frac{s^2}{\omega_c^2} + 1.6181 * \frac{s}{\omega_c} + 1} \\ H_2(s) = \frac{1}{\frac{s^2 + \frac{1}{Q_2} * \frac{s}{\omega_c} + 1}{\omega_c^2}} = \frac{1}{\frac{s^2}{\omega_c^2} + 0.6180 * \frac{s}{\omega_c} + 1} \end{cases} \quad (\omega_c = 9.42 * 10^2 \text{ rad/s}) \quad \text{Eqn 4.8}$$

Finally, the transfer functions of fifth-order Butterworth low pass filters can be calculated:

$$H(s) = \frac{1}{\frac{s}{\omega_c} + 1} * \frac{1}{\frac{s^2}{\omega_c^2} + 1.6181 * \frac{s}{\omega_c} + 1} * \frac{1}{\frac{s^2}{\omega_c^2} + 0.6180 * \frac{s}{\omega_c} + 1} \quad (\omega_c = 9.42 * 10^2 \text{ rad/s}) \quad \text{Eqn 4.9}$$

The step response of the five-order Butterworth filter can be plotted by MATLAB as follows:

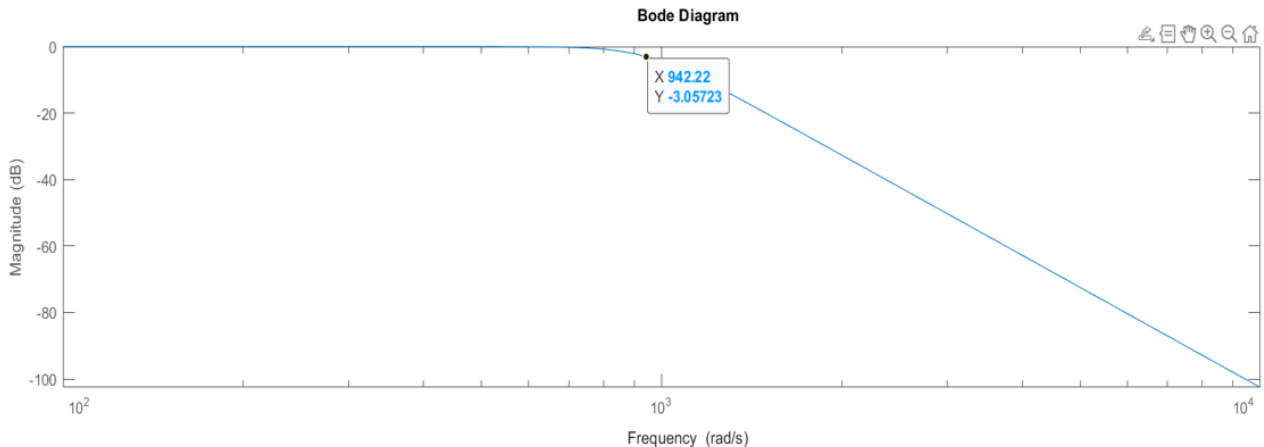


Figure 4.5 The step response of five-order Butterworth filter

According to label in Figure 4.5, when the frequency is the 942.22 rad/s, which is close to cut-off frequency ( $9.42 * 10^2 \text{ rad/s}$ ), the magnitude is -3.05723. As the frequency continues to increase, the magnitude gradually decreases. This shows that the five-order Butterworth filter can filter signals with frequencies higher than 942.22 rad/s, and retain signals less than that frequency. Therefore, the five-order Butterworth low pass filter is well designed.

## 4.4 Redesign of current controller

When linear load is replaced by non-linear load, there are more distortions in the grid current. To compensate for these distortions, current controllers with higher natural frequencies are designed in this chapter. This chapter is basically divided into two parts. The first part is an introduction to the distortions in linear load, and the second part is designing a new current controller with higher natural frequency.

### 4.4.1 Distortions caused by non-linear load

Different from linear loads, non-linear loads do not have a proportional relationship between voltage and current, resulting in many distortions in the electrical system. The most prominent issue is the generation of harmonic currents. Non-linear loads draw current in sudden pulses rather than in a smooth sinusoidal manner. These pulses create currents and voltages with frequencies that are multiples of the fundamental frequency (harmonics). These harmonic frequencies interfere with the fundamental frequency, leading to distorted waveforms. [21]

In addition to standard harmonics, non-linear loads also produce interharmonics, which are non-integer multiples of the fundamental frequency. These interharmonics can be produced by the interaction of different harmonic frequencies [21]. An example diagram comparing the current under linear load and nonlinear is shown below:

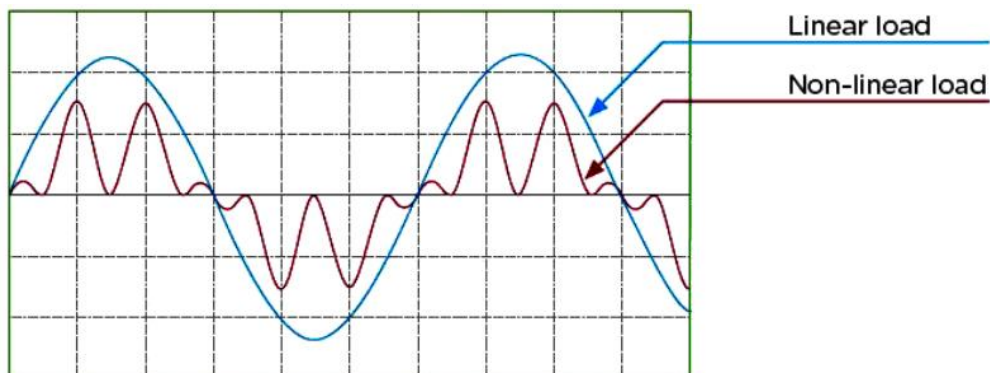


Figure 4.6 Current under linear and nonlinear loads [22]

### 4.4.2 Advantages of current controller with higher natural frequency

To compensate harmonics in grid current under non-linear load, a current controller with higher natural frequencies are designed in this section. The advantage of high natural frequency is shown below:

**Faster Response to Disturbances:** Increasing the natural frequency of the current controller in a STATCOM makes the controller more sensitive to changes or disturbances in the grid current, which means that any deviations from the desired current waveform caused by the non-linear load can be corrected more quickly, reducing the time that these disturbances affect the grid current.

**Improved Control Dynamics:** The natural frequency of a controller is typically related to how quickly the controller can react to errors and apply corrections. Higher natural frequency means higher controller bandwidth, which allows it to handle not only slowly changing changes, but also faster fluctuations in the grid current. This is crucial when dealing with nonlinear loads, which can cause rapid changes in current due to their switching action or harmonic generation.

**Reduced Phase Lag:** The higher natural frequency reduces the phase lag between the error detected in the current waveform and the compensatory action taken by STATCOM. Minimizing this lag is important for timely and accurate adjustments, which directly impacts the waveform quality.

**Reduce the impact of controller delay:** Any inherent delays within the control system can degrade STATCOM's performance in correcting current waveforms. The higher natural frequency minimizes the impact of these delays, ensuring that the control actions remain effective and timely, thereby maintaining the integrity of the grid current waveform. [23]

#### 4.4.3 Designing current controller with higher natural frequency in MATLAB

The transfer function of the new current controller could be obtained through sisotool in MATLAB. It worth noting that , the natural frequency was increased from  $1000\pi$  rad/s to  $2.33 * 10^4$ rad/s.

The whole process of deriving the transfer function is shown as follows: Firstly, the plant transfer function derived in **Eqn 2.5** in **CHAPTER2: Three phase inverter** is set as the controlled object. Secondly, an integrator and a real zero are added into compensator editor to represent the PI controller. Thirdly, the natural frequency and damping factor are set to  $2.33 * 10^4$  and 0.707 respectively in the editor. Accordingly, a black polyline and an arc appear on the figure. Finally, adjust the size of the ellipse by dragging real zero, then drag the pole on the ellipse to the intersection of the arc and the polyline. The final root locus diagram that meets all the requirements is shown below:

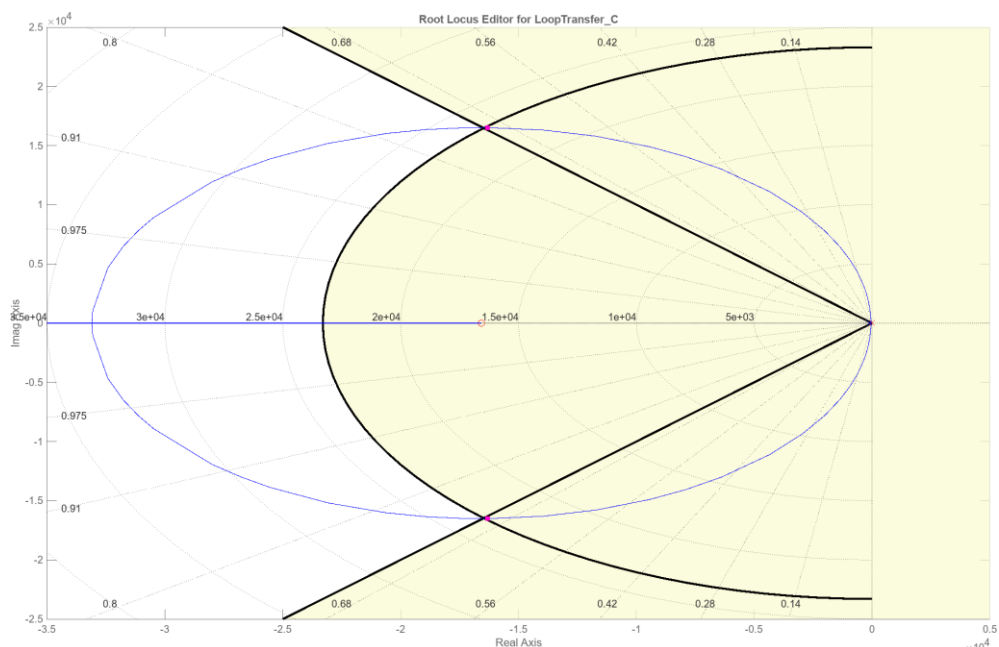
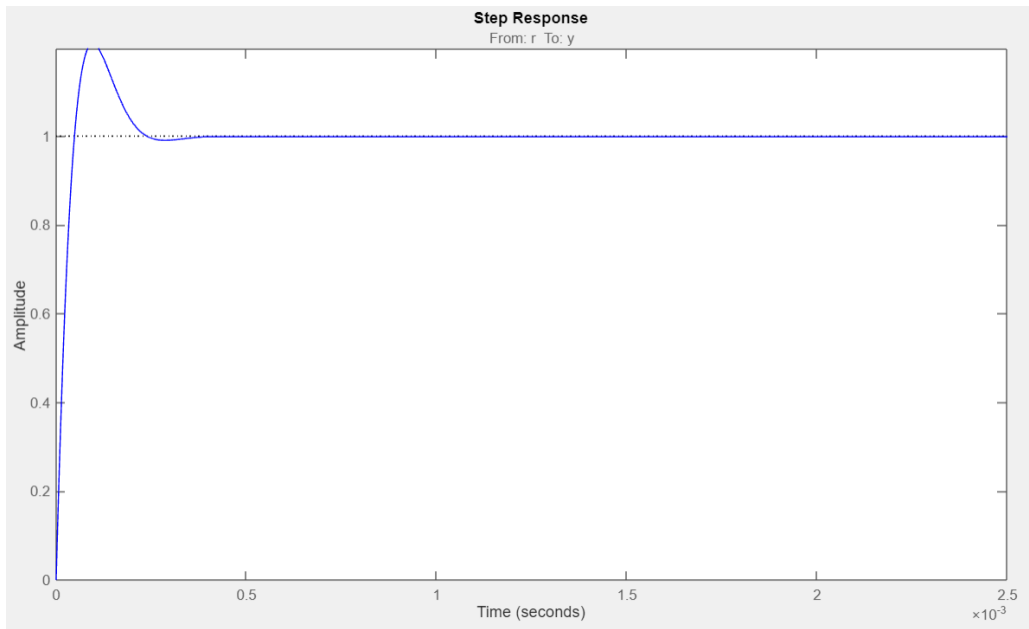


Figure 4.7 root locus diagram of new current controller

In ‘sisotool’, the step response also can be drawn as follows:



*Figure 4.8 step response of new current controller*

As shown in *Figure 4.8*, with the increase of time, the amplitude gradually stabilizes around 1, indicating that the entire system will eventually stabilize. The settling time is about 0.5 ms, which is also very short. The transfer function of the current controller obtained by sisotool is shown as follows:

$$G_c(s) = \frac{32.518(s+1.657*10^4)}{s} \quad \text{Eqn 4.10}$$

## 4.5 Fully controlled 3 phase STATCOM with non-linear load

In this section, a Fully controlled 3 phase STATCOM with nonlinear load is built in the PLECS. The function of 5-order Butterworth filter and compensation algorithm in circuit will be verified.

### 4.5.1 Specification

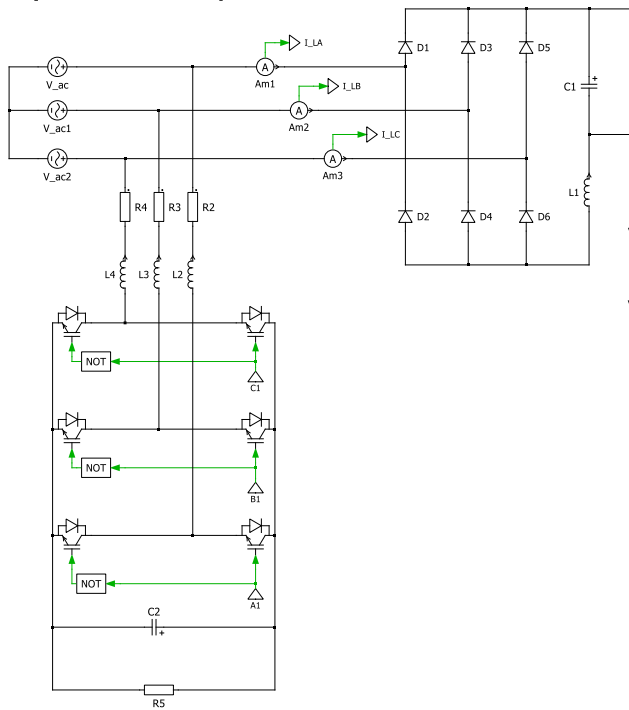
The system design specifications of fully controlled three-phase STATCOM are shown below:

*Table 4.1. System design specifications*

Term	Symbol	Value
Inductor in load	$L_1$	0.001H
Resistor in load	$R_1$	$0.5\Omega$
Capacitor in load	$C_1$	0.001F
Inductor in filter	$L_2, L_3, L_4$	0.001H
Resistor in filter	$R_2, R_3, R_4$	$0.1 \Omega$
Capacitor in STATCOM	$C_2$	0.01F
Fundamental frequency	$f_B$	50Hz
Inverter Switching Frequency	$f_{sw}$	10KHz
DC voltage	$V_{DC}$	850V

## 4.5.2 Schematic

Fully controlled three-phase STATCOM



Step1: Clark transformation

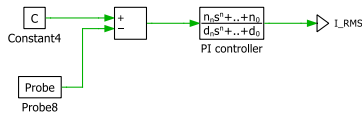
Step2: instantaneous powers calculation

Step3: Filtering

Step4:  $\alpha\beta$ -current calculation

Step5: inverse Clark transformation

Voltage controller



Current controller

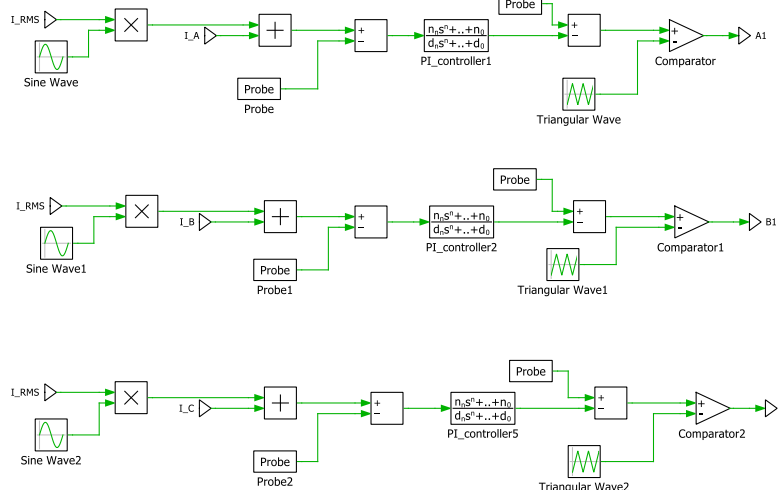


Figure 4.9 Fully controlled 3-phase STATCOM with non-linear load

In the main circuit, three-phase grid is connected in series with non-linear load. A fully controlled 3-phase STATCOM in switching model is placed in parallel between three-phase grid and load. After replacing linear load with nonlinear load, STATCOM's reactive power compensation algorithm is divided into five steps: In the first step, the three-phase grid voltage and the three-phase load current are measured and converted into instantaneous  $\alpha$  and  $\beta$  components by Clark transformation. Secondly, the active power ( $p$ ) and imaginary power ( $q$ ) can be calculated through 'V\_Alpha', 'V\_Beta', which are obtained in step1. As described in **4.2 Active Filters for Constant Power Compensation**, not only the load imaginary power ( $q$ ), but also the oscillating active power ( $\tilde{p}$ ) need to be compensated. So, the purpose of third step is to filter the oscillating active power ( $\tilde{p}$ ) from the active power ( $p$ ).

The fourth step is about  $\alpha\beta$ -current calculation. Based on the oscillating active power ( $\tilde{p}$ ), imaginary power ( $q$ ), ‘V\_Alpha’ and ‘V\_Beta’, the instantaneous reactive current on the  $\alpha$  axis ( $I_{Alpha\_q}$ ) and on the  $\beta$  axis ( $I_{Beta\_q}$ ) can be calculated. In the last step, the ‘ $I_{Ca}$ ’, ‘ $I_{Cb}$ ’, ‘ $I_{Cc}$ ’ can be calculated from ‘ $I_{Alpha\_q}$ ’ and ‘ $I_{Beta\_q}$ ’ through the inverse Clarke transformation. These three currents (‘ $I_{Ca}$ ’, ‘ $I_{Cb}$ ’, ‘ $I_{Cc}$ ’) represent the reactive current of each phases in the current controller.

In addition, the voltage controller is applied to STATCOM to stabilize the DC voltage at 850V and continuously extract switching loss and ohmic losses of the PWM converters from the power system. The output of voltage controller is ( $I_{RMS}$ ), which is converted into AC current by multiplying the sin wave of magnitude  $\sqrt{2}$ . These AC currents are added to the reactive currents (‘ $I_{Ca}$ ’, ‘ $I_{Cb}$ ’, ‘ $I_{Cc}$ ’) respectively to produce a reference current for the current controller in each phase. It worth noting that the design process of current controller and voltage controller included in **Chapter2: The three-phase inverter**. It worth noting that in order to compensate oscillating real power, the PWM converter's DC capacitor needs to be sufficiently large (0.01F in the specification) to act as an energy storage unit, preventing significant voltage changes. It's important that if the DC voltage falls below the AC voltage amplitude, this type of PWM converter would become uncontrollable. Different from compensation of ( $-\tilde{p}$ ), compensating for the reactive power ( $-q$ ) does not necessitate any energy storage elements.

## 4.6 Verification

In order to better verify the effect of STATCOM on the circuit, the switch blocks and an another load are added to the circuit. Therefore, the main circuit can be modified as follows:

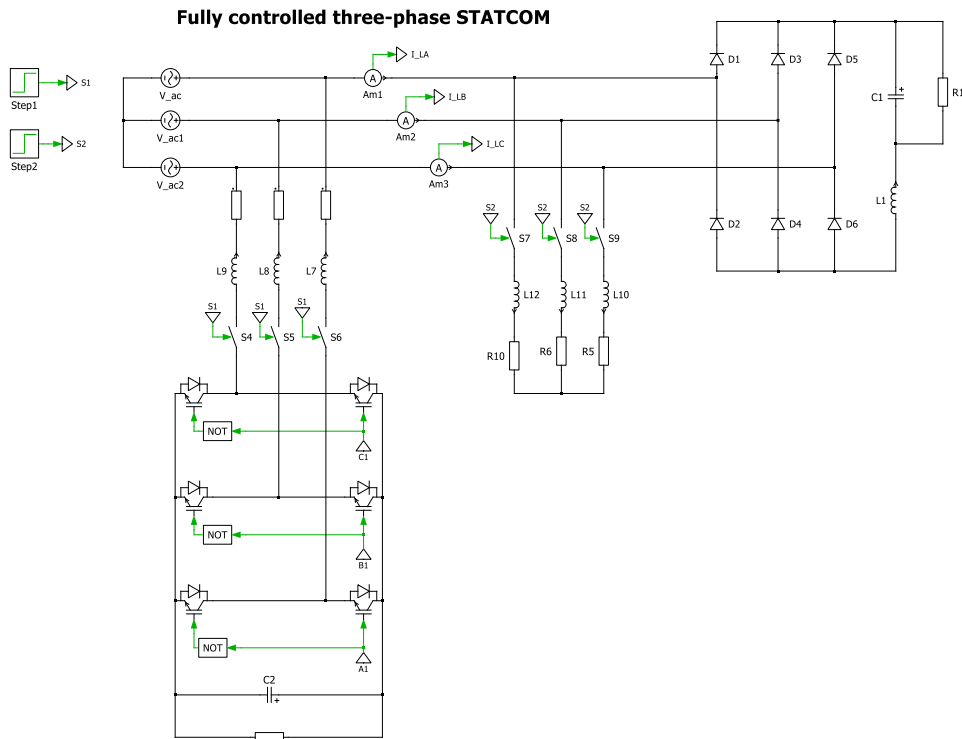


Figure 4.10 The main circuit containing the switch and two loads

In Figures 4.10, the step times of ‘Step 1’ and ‘Step 2’ are set to 0.2s and 0.8s respectively, which means that the STATCOM and current controller are connected to the circuit after 0.2 seconds, and another load is connected to the circuit after 0.8 seconds.

#### 4.6.1 Filter verification

In the circuit, a fifth-order Butterworth low-pass filter is designed to separate the average active power ( $\bar{p}$ ) and the oscillating active power ( $\tilde{p}$ ) from the total active power ( $p$ ). The comparison between the active power ( $\bar{p}$ ) and total active power ( $p$ ) is shown below:

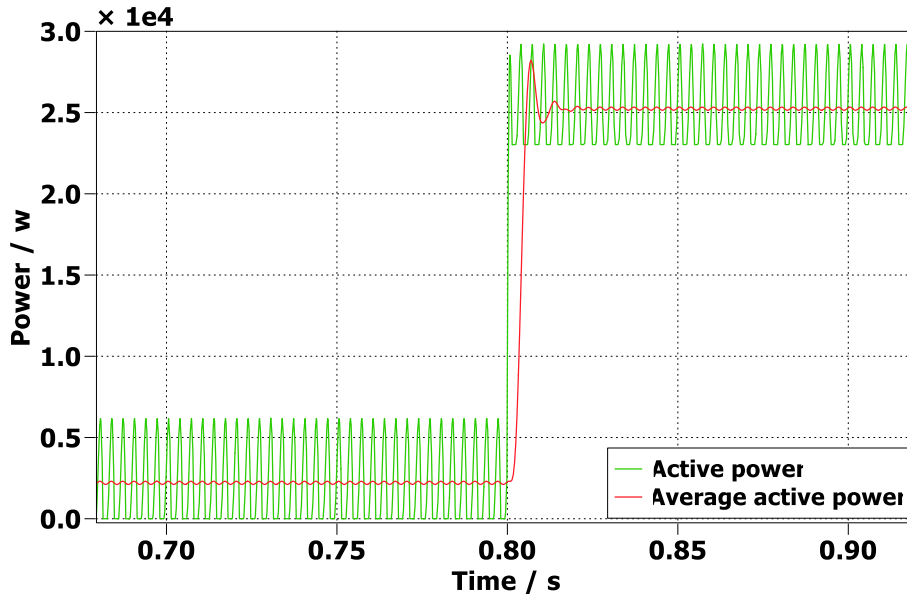


Figure 4.11 The comparison between the average active power ( $\bar{p}$ ) and total active power ( $p$ )

The oscillating active power ( $\tilde{p}$ ) is measured below:

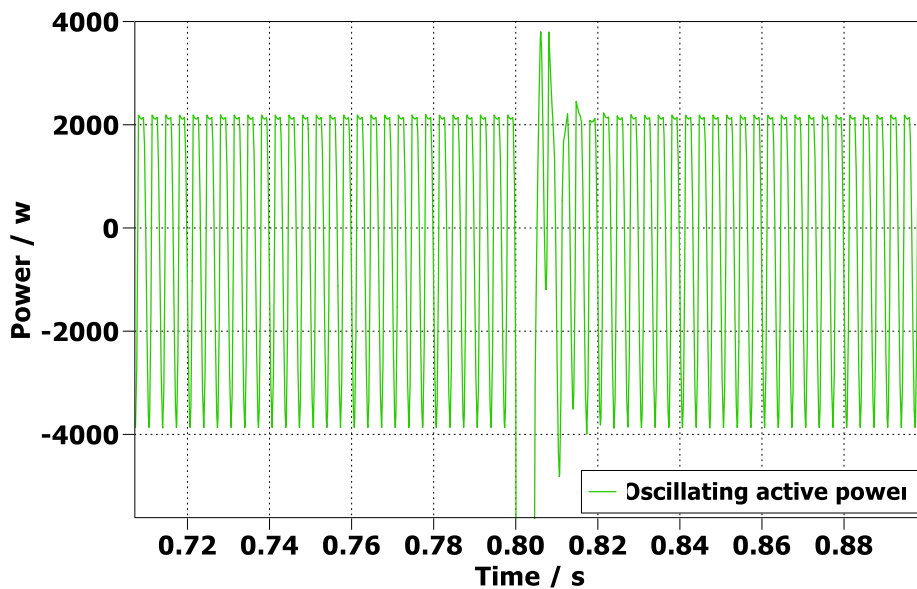


Figure 4.12 The oscillating active power ( $\tilde{p}$ ) power

As shown in Figure 4.11, the average active power obtained after the five-order Butterworth filtering is in the middle of the total active power. The average active power is almost constant at steady state, and the ripple is small. After connecting to another load, the average active power can still be located in the middle

of the total active power, and the adjustment time is very short. *Figure 4.12* shows the waveform of the oscillating active power, where the oscillating power ( $\tilde{p}$ ) fluctuates around 0 watts. The maximum value is about 2000w while the minimum value is about -4000w, because the oscillating active power is positive for a longer time. The integral of the entire image is about 0. As a result, the five-level Butterworth designed works as expected.

#### 4.6.2 Current controller verification

In order to better verify current controller on the circuit, the switch blocks are added to the current controller as well. The diagram is shown below:

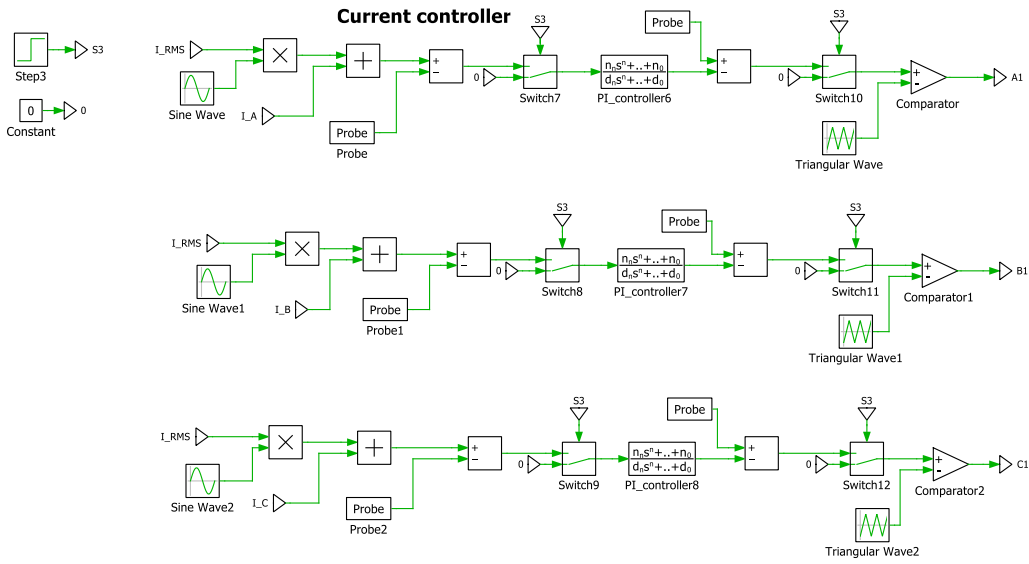


*Figure 4.13 Current controller with switch blocks*

In order to better show the role of the current controller, the connection time of the STATCOM and current controller to the circuit is reset to 0.5s. The reference current and actual current in a certain phase are compared as follows:

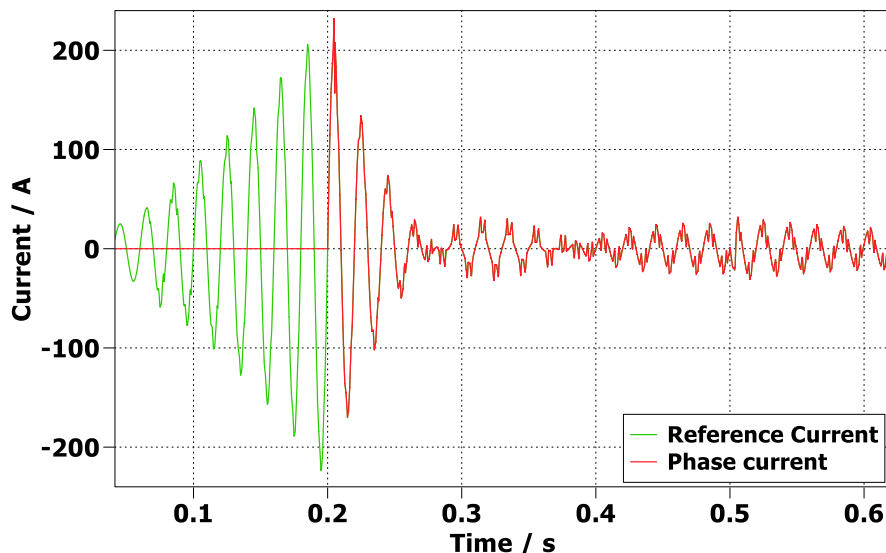


*Figure 4.14 Current controller input comparison in a certain phase*

In PWM modulation, the desired three-phase voltage analogue signal generated from current controller are compared as follows:

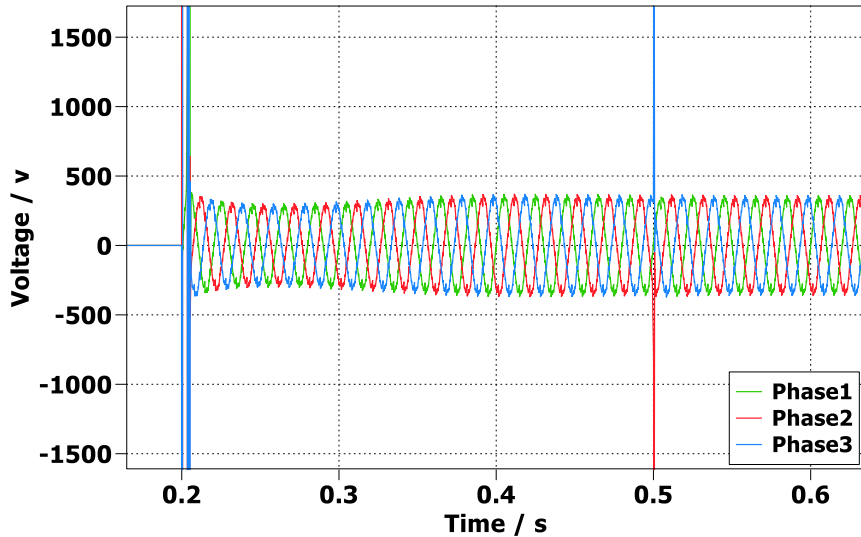


Figure 4.15 Current controller output comparison in a certain phase

It can be seen from Figure 4.14 that, at a certain phase, after STATCOM is connected to the circuit, the current generated by STATCOM is basically consistent with the reference current. After 0.5 seconds, another load is added to the circuit, but the actual current still matches the reference current. According to Figure 4.15, before STATCOM is connected to the circuit, the three-phase voltage generated by the current controller is equal to 0. After STATCOM is connected to the circuit, the magnitude and phase of the three-phase voltage generated by the current controller are changed to achieve the reactive power compensation for load. After two seconds later, another load is added to the circuit, and the magnitude of the three-phase voltage changes accordingly to achieve the reactive power compensation for both loads. Therefore, the above results prove that the current controller works as expected.

#### 4.6.3 Voltage controller verification

To verify the voltage controller, the DC voltage and capacitor voltage is compared as follows:

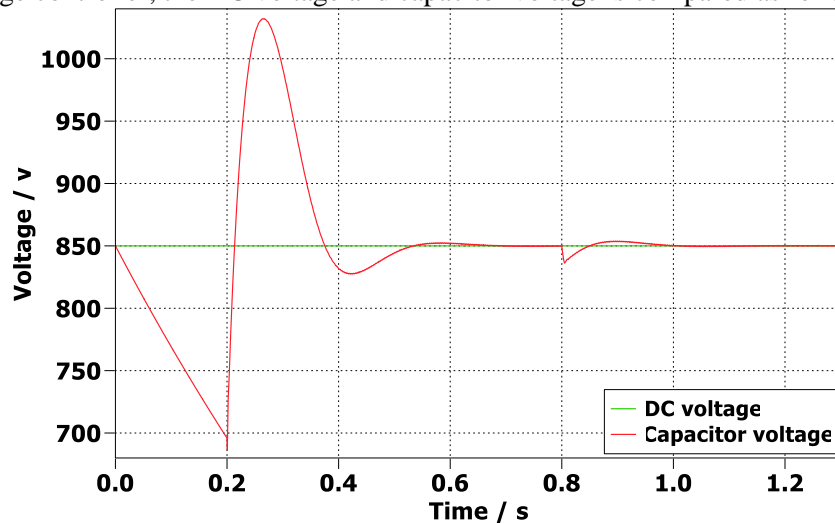


Figure 4.16 Comparison between DC voltage and capacitor voltage

As shown in Figure 4.16, after STATCOM is connected, the voltage of the capacitor is almost consistent with the set DC voltage at steady state. After 0.8 seconds, when another load is attached, the capacitor voltage is

still consistent with the DC voltage after a brief fluctuation. Therefore, the voltage controller works as expected.

#### 4.6.4 Reactive power compensation verification

At each phase, before STATCOM is connected to the circuit, the grid voltage and grid current are compared:

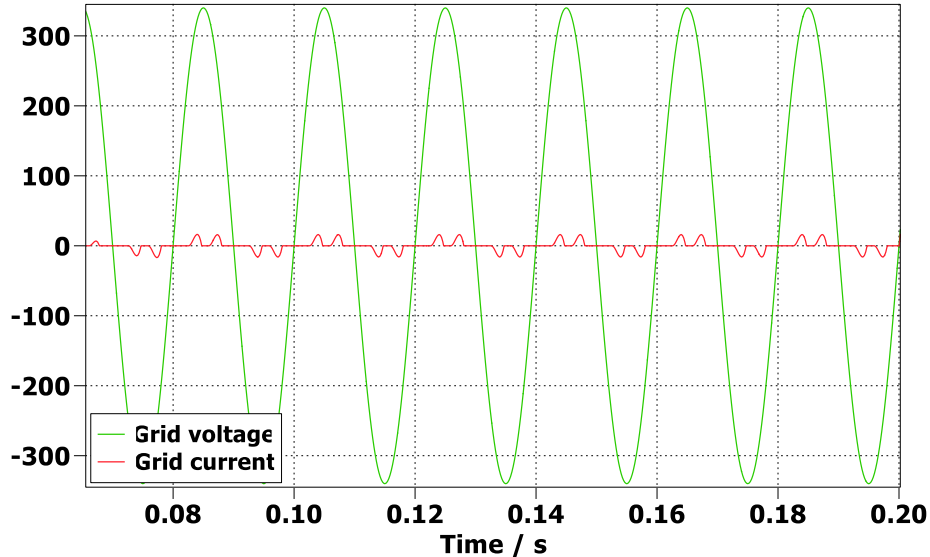


Figure 4.17 Grid voltage vs grid current before STATCOM is connected to circuit

After STATCOM connects the circuit, the comparison of grid voltage and grid current is as follows:

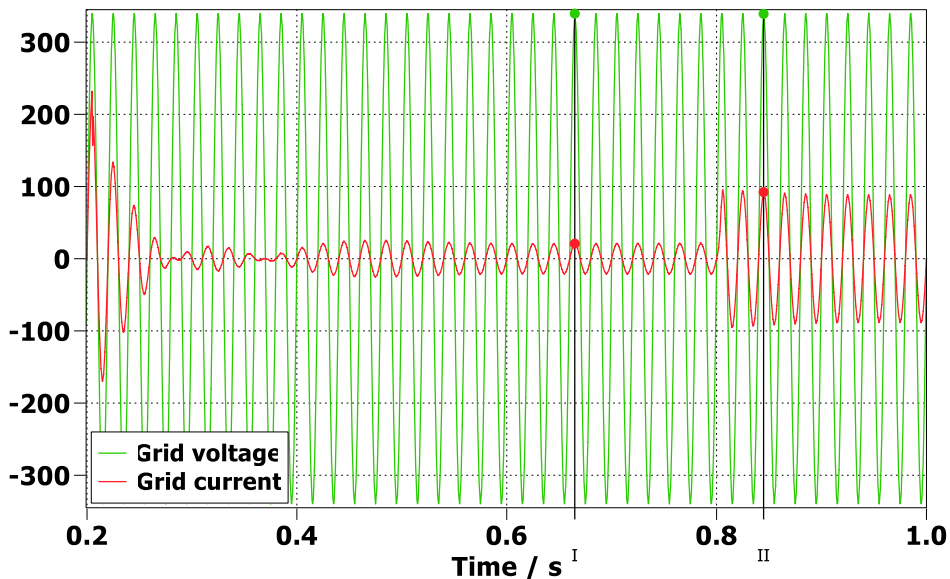


Figure 4.18 Grid voltage vs grid current after STATCOM is connected to circuit

As shown in *Figure 4.17*, at each phase before STATCOM is connected to the circuit, the waveform of the grid current is not a standard sine wave, which is very irregular and difficult to judge whether it is in phase with the grid voltage. After STATCOM is connected to the circuit, the system reaches steady state at about 0.5s. As indicated by the cursor in the *Figure 4.18*, the grid current and grid voltage reach the minimum and maximum values at the same time, which also means that the grid current and grid voltage are in the same

phase state. After 0.8 seconds, another load is connected to the circuit, and the grid voltage and grid current remain in phase. Therefore, it can be proved that after STATCOM is connected to the circuit, in the steady state, the grid only provides active power, and all the reactive power in the load is provided by STATCOM.

#### 4.6.5 Harmonics compensation verification

Before STATCOM is connected to the main circuit, when the load consists of only one nonlinear load, the grid three-phase current spectrum is measured as follows:

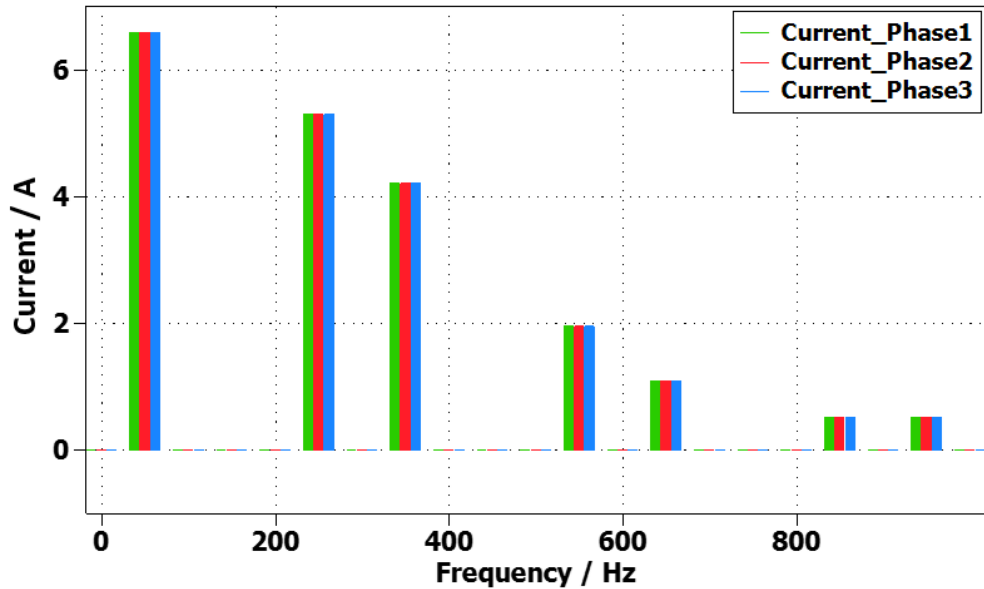


Figure 4.19 The frequency spectrum of three phase AC current before STATCOM is connected.

After STATCOM is connected to the main circuit, the grid three-phase current spectrum is measured below:

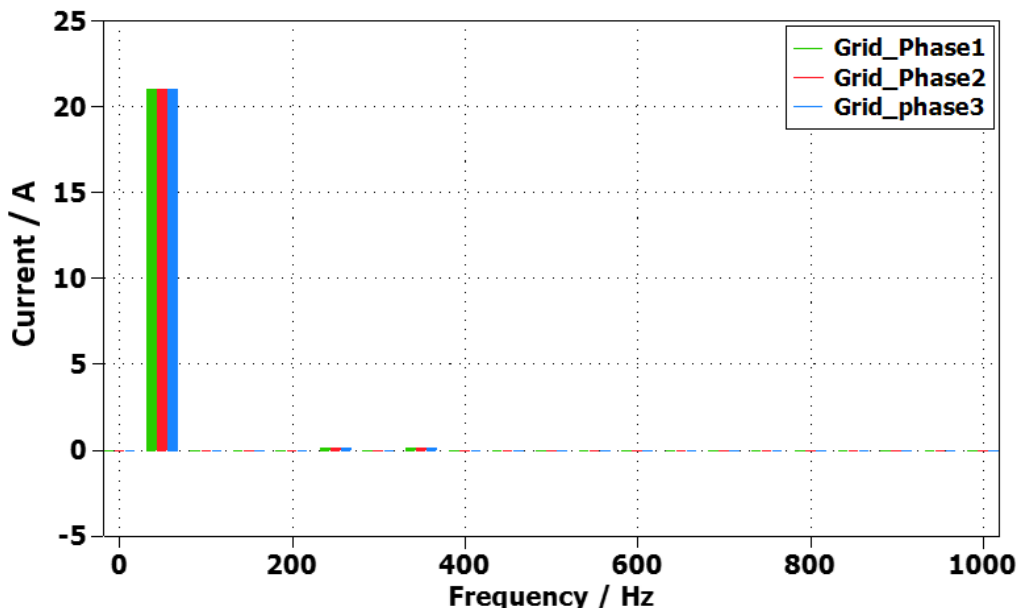
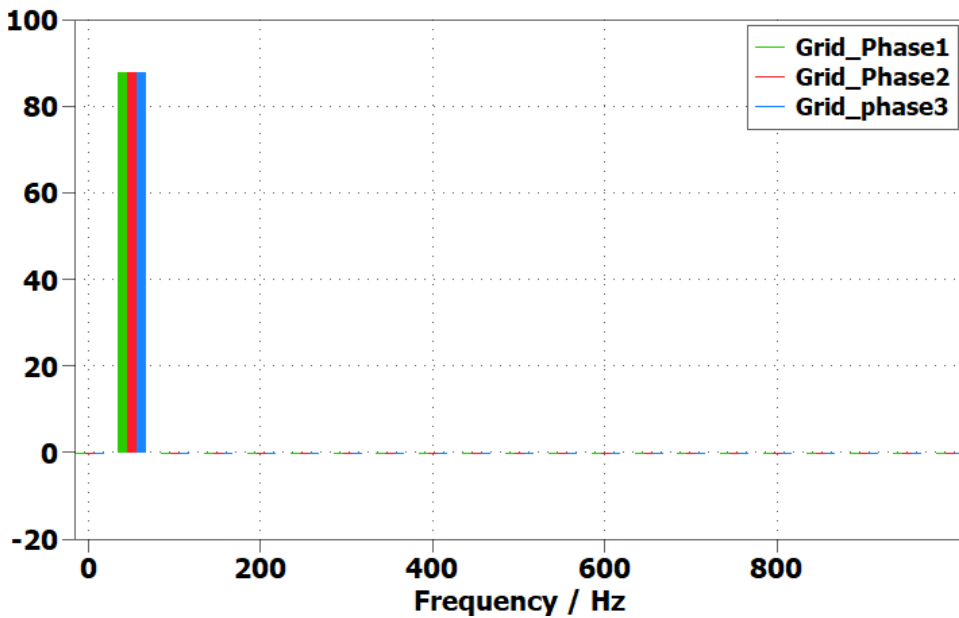


Figure 4.20 The frequency spectrum of three phase AC current after STATCOM is connected.

After another load is added to the circuit, the grid three-phase current spectrum is measured below:



*Figure 4.21 The frequency spectrum of three phase AC current after STATCOM is connected.*

It is worth noting that when analysing the frequency spectrum of grid current, the base frequency is set to 50Hz (consistent with the fundamental frequency in the **4.5.1 specification**). *Figure 4.19* shows that there are a lot of currents of different frequencies before STATCOM is connected to the circuit, which means there are a lot of harmonics in the three-phase grid current. As shown in *Figure 4.20*, after the STATCOM is connected to the circuit, the grid current of the three phases is concentrated at 50HZ with very few harmonics. According to *Figure 4.21*, when another load is added to the circuit, the three-phase grid current is still concentrated at 50hz, and harmonics are still very few. Therefore, STATCOM circuit effectively eliminates a lot of harmonics in nonlinear loads.

## 5 CHAPTER5: Conclusion

In the project ‘Simulation Study of a STATCOM for Reactive Power and Harmonics Compensation’, The main goal is to build a fully controlled 3 phase STATCOM with linear load to achieve reactive power compensation. The Stretch goal is to compensate the reactive power and harmonics in nonlinear loads. In general, both goals were largely achieved.

In **CHAPTER2: Three phase inverter**, Through the in-depth investigation of PWM modulation, the design of current controller and voltage controller, a three inverter successfully built in PLCS and the conversion from DC current to three-phase AC current is achieved. In **CHAPTER3: STATCOM with linear load**, firstly, the P-Q theory is introduced in detail, and then the reactive power compensation algorithm is derived. In PLECS, on the basis of three inverters, STATCOM is modelled as an ideal voltage source to implement the compensation algorithm, and finally a fully controlled three-phase STATCOM with linear load is successfully constructed. In **CHAPTER4: STATCOM with non-linear load**, On the basis of p-q theory introduced in CHAPTER3, it continues to implement the compensation algorithm of reactive power and

harmonics for nonlinear loads. In PLCES, a fully controlled three-phase STATCOM with non-linear load was successfully constructed and verified. In the future, the immediate development should be to further refine STATCOM simulations, including positive sequence detectors and 4-wire systems, which takes a lot of research and experimentation. The long-term development is to optimize the use of STATCOM in industry based on simulation.

STATCOM benefit society primarily by improving the stability and efficiency of power systems. It plays a crucial role in reducing the power factor of the grid, improving voltage stability, and avoiding the risk of power outages. This is especially valuable in grids with variable power sources such as wind or solar energy, where power supply can be unpredictable. By dynamically adjusting voltage levels and compensating for fluctuations, a STATCOM helps maintain consistent power quality and reliability. This reduces interruptions and increases energy efficiency, not only maintaining industrial productivity, but also ensuring that households have a stable, uninterrupted supply of electricity. [24]

STATCOM is considered a mature technology in the field of power electronics and electrical engineering. Developed in the 1980s and 1990s as part of advancements in voltage source converter (VSC) technologies, STATCOMs have been widely implemented in electricity networks around the world. [24] Although this project is limited to the simulation of STATCOM on PLECS, which is not very helpful to industrial STATCOM, it can contribute to the current projects within the PEMC group. As a key component in this field, it could contribute to results that may be published in the future.

## 5.1 Reflection on management

The biggest difference between the actual project process and the expected process, as compared to the Gantt chart and Progress review pro-forma's in appendix, is that the single-phase inverters are expected to be explored first, while the actual project development begins directly with the three inverters. The reason is that building the single-phase inverter has been included in the coursework of Power Electronic applications and control (EEE3083 UNUK). And according to further research, it was found that the study of single-phase inverters does not help the understanding of three-phase inverters. Therefore, in future projects, it is necessary to flexibly plan goals and grasp the core content. In many cases, the more content done does not mean the deeper understanding, efficiency is the key.

The second obvious difference between actual project process and the expected process is that the phase lock loop is not built as expected. Because the core of this project is to implement STATCOM's compensation algorithm for reactive power and harmonics. PLL is mainly used to synchronize the phase and frequency of the signal with the phase of the reference signal, so this is not a necessary part. Therefore, when doing future projects, it is necessary to grasp the core issues, understand the main objectives of the project, and improve efficiency.

During the process of the project, I would sometimes encounter problems that could not be solved independently. At this time, I would further study the literature (usually the book ‘Instantaneous Power Theory and Applications to Power Conditioning’) or seek the supervisor’s help to keep the project on track. In future projects, it is also a good idea to seek the help of experienced people and study the literature more deeply when encountering problems beyond my capacity.

Since the project consists only of simulations, the risk is minimal. The biggest potential risk is data loss. In fact, during the course of the project, I sometimes forget to save data during the project, such as forgetting to save the established circuit in PLECS, forgetting to save the transfer function derived from MATLAB sisotool. This causes me to sometimes waste time on things I’ve already done. If the data is well saved at each step, the project process will go smoothly and writing reports will be much easier.

## 6 Reference

- [1] N. Hingorani, L. Gyugi, "Understanding FACTS: Concepts and technology of Flexible AC Transmission Systems", IEEE Press, 2000
- [2] R. Strzelecki, G. Benysek, "Power Electronics in Smart Electrical Energy Networks", Springer, 2008
- [3] H. Akagi, E. H. Watanabe, M. Aredes, "Instantaneous Power Theory and Applications to Power Conditioning", IEEE Wiley, 2007
- [4] J. L. Alfonso, M. J. S. Freitas, J. S. Martins "P-Q Theory power components calculations", IEEE international Symposium on Industrial Electronics, 2003
- [5] A. Yazdani, R. Iravani, "Voltage Sourced Converters in Power Systems: Modelling, Control and Applications", Wiley IEEE, 2010
- [6] Power Electronic applications and control (EEEEE3083 UNUK) L8\_INVERTER\_PART3 23\_24
- [7] M. Jafari, Z. Malekjamshidi, Li Li and Jian Guo Zhu, "Performance analysis of full bridge, boost half bridge and half bridge topologies for application in phase shift converters," 2013 International Conference on Electrical Machines and Systems (ICEMS), Busan, 2013, pp. 1589-1595.
- [8] C. -S. Shieh, "Quick implementation of Pule Wise Modulation(PWM), Pulse Frequency Modulation(PFM) and mixed PWM/PFM on FPGA chip," 2020 International Symposium on Computer, Consumer and Control (IS3C), Taichung City, Taiwan, 2020, pp. 444-447
- [9] Power Electronic applications and control (EEEEE3083 UNUK) L7\_INVERTER\_PART2 23\_24
- [10] Bu Ruofei, Zhao Rongxiang, Yang Huan and Zeng Zhiyong, "Inductor minimum calculation based on analysis of AC current ripple for PWM converter with dead-time effect," 2013 IEEE Industry Applications Society Annual Meeting, Lake Buena Vista, FL, USA, 2013, pp. 1-6.
- [11] N. S. Yusof and A. Z. Ahmad, "Single-Phase grid-connected of PV inverter using PR current controller," 2017 IEEE Conference on Systems, Process and Control (ICSPC), Meleka, Malaysia, 2017, pp. 117-121.
- [12] B. Yang and Y. Sun, "Damping Factor Based Delay Margin for Wide Area Signals in Power System Damping Control," in IEEE Transactions on Power Systems, vol. 28, no. 3, pp. 3501-3502, Aug. 2013.
- [13] T. Bhattacharjee, M. Jamil and A. Jana, "Designing a Controller Circuit for Three Phase Inverter in PV application," 2018 International Conference on Electrical, Electronics, Communication, Computer, and Optimization Techniques (ICEECCOT), Mysuru, India, 2018, pp. 882-886.
- [14] Y. Zhang and X. Xu, "Robust controller design for three-phase medium frequency power supply," IECON 2017 - 43rd Annual Conference of the IEEE Industrial Electronics Society, Beijing, China, 2017, pp. 1511-1518.

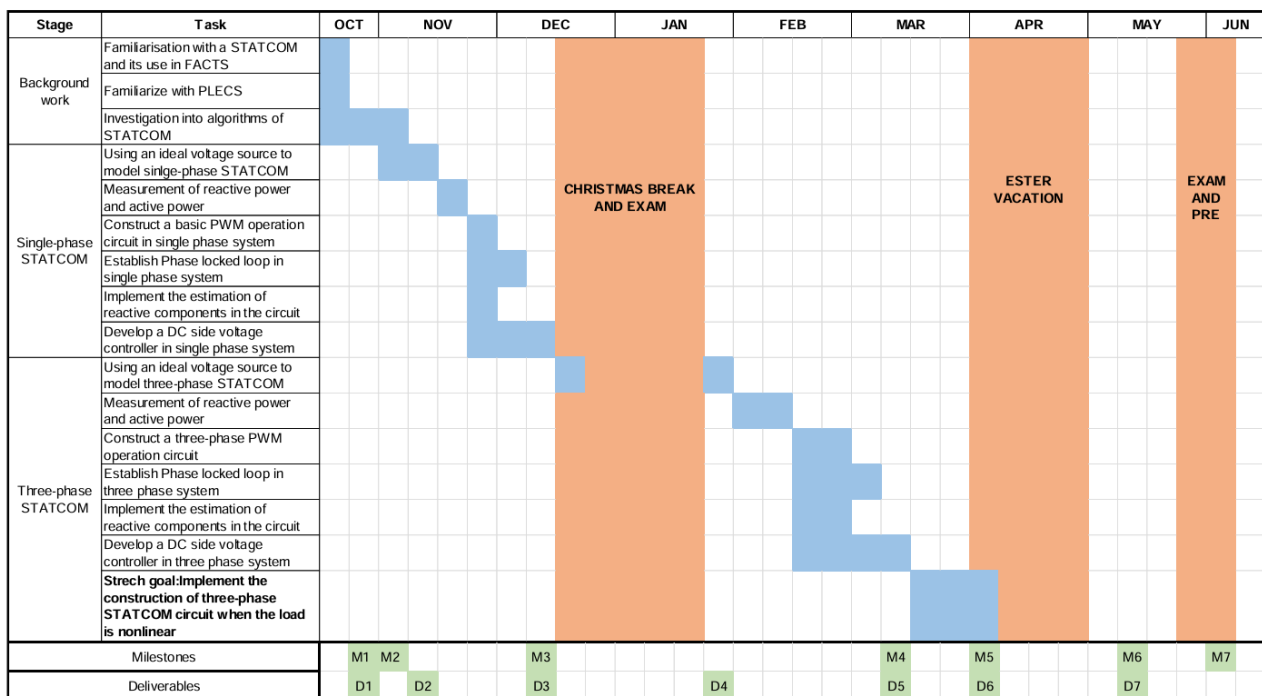
- [15] H. Li, Z. Chen, J. Li and Z. Zhang, "Current ripple reduction of aircraft start generators in the starting mode with variable switching frequency method," IECON 2017 - 43rd Annual Conference of the IEEE Industrial Electronics Society, Beijing, China, 2017, pp. 4124-4129.
- [16] T. Tanaka, H. Wang and F. Blaabjerg, "A DC-Link Capacitor Voltage Ripple Reduction Method for a Modular Multilevel Cascade Converter With Single Delta Bridge Cells," in IEEE Transactions on Industry Applications, vol. 55, no. 6, pp. 6115-6126, Nov.-Dec. 2019.
- [17] Hirofumi Akagi; Edson Hirokazu Watanabe; Mauricio Aredes, "The Instantaneous Power Theory," in Instantaneous Power Theory and Applications to Power Conditioning , IEEE, 2017, pp.37-109.
- [18] Hirofumi Akagi; Edson Hirokazu Watanabe; Mauricio Aredes, "Shunt Active Filters," in Instantaneous Power Theory and Applications to Power Conditioning , IEEE, 2017, pp.111-236.
- [19] N. Aupithak, U. Tortechai, B. Burapattanasiri, S. Lerkvaranyu, F. Khateb and M. Kumngern, "Extremely Low-Power Fifth-Order Low-Pass Butterworth Filter," 2021 7th International Conference on Engineering, Applied Sciences and Technology (ICEAST), Pattaya, Thailand, 2021, pp. 253-256.
- [20] "Butterworth filter," Wikipedia, [https://en.wikipedia.org/wiki/Butterworth\\_filter](https://en.wikipedia.org/wiki/Butterworth_filter) (accessed May 7, 2024).
- [21] W. Su, Z. Li and Z. Shao, "The harmonic calculation model of non-linear load," 2014 China International Conference on Electricity Distribution (CICED), Shenzhen, China, 2014, pp. 866-872.
- [22] "Butterworth filter," Wikipedia, [https://en.wikipedia.org/wiki/Butterworth\\_filter](https://en.wikipedia.org/wiki/Butterworth_filter) (accessed May 7, 2024). V. J. K, "Harmonics : A silent killer in your electrical systems !!," LinkedIn, <https://www.linkedin.com/pulse/harmonics-silent-killer-your-electrical-systems-venkatesh-j-k> (accessed May 7, 2024).
- [23] PID control,  
[https://www.maplesoft.com/content/EngineeringFundamentals/12/MapleDocument\\_12/PID%20Control.pdf](https://www.maplesoft.com/content/EngineeringFundamentals/12/MapleDocument_12/PID%20Control.pdf) (accessed May 7, 2024).
- [24]N. Kumar, P. Wagh, D. Kolhe, P. Arane and P. Kadlag, "Power quality improvement in distributed energy resources for EV charging using STATCOM," 2022 1st International Conference on Sustainable Technology for Power and Energy Systems (STPES), SRINAGAR, India, 2022, pp. 1-4.

## 7 Appendix

*Table 7.1 Milestones and Deliverables*

Milestones	Deliverables
M1. Completing proposal and defence	D1. Project proposal report
M2. Understanding the algorithm of a STATCOM for reactive power compensation	D2. PLECS file for single-phase STATCOM (model STATCOM as an ideal voltage source)
M3. Complete simulation of fully controlled single phase STATCOM	D3. PLECS file for fully controlled single-phase STATCOM
M4. Complete simulation of fully controlled three phase STATCOM	D4. PLECS file for three-phase STATCOM (model STATCOM as an ideal voltage source)
M5. Complete simulation of fully controlled three phase STATCOM with non-linear load	D5. PLECS file for fully controlled three-phase STATCOM
M6. Completing project Thesis and defence	D6. PLECS file for fully controlled three-phase STATCOM with non-linear load
M7. Attending project presentation	D7. Project Thesis

*Table 7.2 Gantt chart*



<b>Summarised Planned State of Project:</b> Complete the design of the current controller according to the notes provided by the supervisor	<b>Actual Progress Since Last Review</b> The current controllers are well designed by MATLAB and built in the PLECS.
<b>Next Steps and Supervisor Feedback</b> Next step: Try to design the voltage controller, and then complete the design of the whole three-phase inverter  Supervisor feedback: Well done.	

*Figure7.1 Progress review pro-forma's 1*

<b>Summarised Planned State of Project:</b> Complete the design of the voltage controller, and then complete the design of the whole three-phase inverter	<b>Actual Progress Since Last Review</b> The voltage controllers are well designed by MATLAB and built in the PLECS.  However, when combined with current controllers to form a complete three-phase inverter, the output three-phase current is in a mess.
<b>Next Steps and Supervisor Feedback</b> Next step: Redesign the voltage controller and complete the construction of the three-phase inverter  Supervisor feedback: For very strange and stupid reasons, after the voltage controller is connected to the three-phase inverter, the output current is strange. Supervisor then gave me a well-designed PLECS file for three-phase inverter to adjust my own design.	

*Figure7.2 Progress review pro-forma's 2*

<b>Summarised Planned State of Project:</b> According to the three-phase inverter PLECS file provided by the supervisor, adjust my own three-phase inverter is not working properly.	<b>Actual Progress Since Last Review</b> In PLECS, a three-phase inverter is successfully built.
<b>Next Steps and Supervisor Feedback</b> Next step: investigate the reactive power compensation algorithm for linear load. Try to build the fully controlled 3 phase STATCOM with linear load.  Supervisor feedback: Well done.	

Figure7.3 Progress review pro-forma's 3

<b>Summarised Planned State of Project:</b> 1. Implement compensation algorithm in PLECS, modelling the STATCOM as an ideal voltage source.  2. Replace the ideal voltage source with a power converter and develop a DC side voltage controller  3. Complete simulation of fully controlled 3 phase STATCOM with linear load.	<b>Actual Progress Since Last Review</b> 1.Create a PLECS file called STATCOM_PWM. Implement compensation algorithm in this file, modelling the STATCOM as an ideal voltage source.  2.Create a PLECS file called STATCOM_Linearload. Complete simulation of fully controlled 3 phase STATCOM with linear load in this file. A DC side voltage controller is also built.
<b>Next Steps and Supervisor Feedback</b> Next step: investigate the reactive power and harmonics compensation algorithm for non-linear load. Try to build the fully controlled 3 phase STATCOM with non-linear load.  Supervisor feedback: Both files are well done. More switches can be added to the circuit to verify the results	

Figure7.4 Progress review pro-forma's 4

<b>Summarised Planned State of Project:</b> Building a fully controlled 3 phase STATCOM with non-linear load. The verification circuit should be also built.	<b>Actual Progress Since Last Review</b> A fully controllable three-phase STATCOM with nonlinear load and a verification circuit are successfully constructed.
<b>Next Steps and Supervisor Feedback</b> The main goal and the stretch goal of the project have been fully achieved. The supervisor suggested that I start my Dissertation	

*Figure 7.5 Progress review pro-forma's 5*